



Technical Support Working Group

PIPELINE BLAST MITIGATION TECHNOLOGIES

Contract Number: 09-C-4602; TSWG T-2950

Final Technical Report

May 2011

DISTRIBUTION STATEMENT: Products and information developed under this effort are authorized for distribution to U.S. Government agencies, U.S. state and local government agencies, and U.S. DoD contractors (with approval of a government sponsor). Release to allied governments will be made with approval of the Director, CTTSO. This distribution restriction is based on authority cited in TSWG Classification Guide, December 2000. Other requests for these products and information shall be referred to CTTSO via e-mail to pssubgroup@tswg.gov and/or techtrans@tswg.gov.

WARNING – This document contains technical data whose export is restricted by the Arms Export Control Act (Title 22, U.S.C., Sec 2751 et seq.) or Executive Order 12470. Violation of these export laws are subject to severe criminal penalties.

DESTRUCTION NOTICE – For classified documents, follow the procedures in DOD 5200.22-M, Industrial Security Manual, Section 11-19 or DOD 5200.1-R, Information Security Program Regulation, Chapter IX. For unclassified, limited documents, destroy by any method that will prevent disclosure of contents or reconstruction of the document.

THIS DOCUMENT HAS BEEN MODIFIED FOR PUBLIC RELEASE.
THE SSI/RESTRICTED VERSION CAN OBTAINED BY CONTACTING
CTTSO AS DIRECTED IN THE DISTRIBUTION STATEMENT ABOVE.

EXECUTIVE SUMMARY

Pipeline Blast Mitigation Technologies: Project Report

Introduction

Pipelines are an extensive and critical part of the nation's infrastructure. Nationwide, there are 320,500 miles of natural gas transmission line and 168,900 miles of hazardous liquid line. Lines for local distribution of natural gas total 2.2 million miles.¹ Nearly all natural gas and 65% of hazardous liquids are transported by pipelines. Natural gas provides over 25% of residential and industrial energy needs, while oil products provide 97% of the energy used for transportation. In total, 62% of the energy used in the US is derived from these two sources.²

Despite the importance of pipeline systems, there are few technologies for mitigating their vulnerabilities to explosive attack. To address this need, the Technical Support Working Group (TSWG) contracted Protection Engineering Consultants (PEC) to perform the following three tasks (Contract no. N41756-09-C-4602) as part of Phase 1:

1. Survey of existing research and technology proposed specifically for blast protection of pipelines (*Survey of Existing Technology and Research*, submitted October 15, 2009);
2. Identification and assessment of the vulnerability of pipeline systems and infrastructure (*Pipeline Vulnerability Assessment* submitted December 3, 2009);
3. Assessment of blast mitigation technologies for pipeline protection using analytical and numerical simulations (*Assessment of Blast Mitigation Technologies* submitted January 28, 2010).

Full scale testing was performed in Phase 2, which was initiated upon completion of Tasks 1 through 3 of Phase 1. The results of the Task 3 report were used to develop the Phase 2 *Test Plan*, which was executed as Task 5 (Task 4 was project management). The Phase 2 explosive tests included source characterization and pipe, valve, and protective structure tests. The source characterization tests verified the repeatability of explosive yield for charge configuration used in pipeline component tests. The pipe, valve, and protective structure tests determined the resistance of pipeline components to explosive threats, whether protected by blast mitigation technologies or unprotected.

Phase 1, Task 1 - Survey of Existing Technology and Research

¹*Pipeline Modal Annex to the Transportation Sector Specific Plan*, Department of Homeland Security, 2010 (Draft Only), Washington, DC, www.dhs.gov

²*Transportation Systems: Critical Infrastructure and Key Resources Sector-Specific Plan as input to the National Infrastructure Protection Plan*, Department of Homeland Security, May 2007, Washington, DC, www.dhs.gov

In the Task 1 survey of existing technology and research, eight distinct blast mitigation technologies were identified, as discussed in the following sections and summarized in Table E-1. These technologies were organized into five broad groups, based on the method by which blast protection was provided:

- Stiff reinforcement
- Independent barrier
- Dependent barrier
- Crushable layer
- Ductile layer

Stiff Reinforcement

Stiff reinforcement includes fiber-reinforced polymer (FRP) and steel-reinforced thermoplastic (SRT). FRP is a composite material of glass, carbon, or Kevlar™ fibers within a resin matrix. FRP vendors include QuakeWrap™, Sika, and Fyfe, among others. SRT is a high-strength steel mesh embedded in a thermoplastic resin, as proposed by Hardwire® LLC.

Independent Barriers

Barriers may be structurally independent of the pipeline component. These barriers shield the pipeline from the blast but likely sustain significant damage while doing so. The shielded pipeline component is intended to remain in its pre-blast condition. Infrastructure Defense Technologies (IDT) has proposed a steel-clad earthen barrier called Metalith™ to protect the pipeline. The steel panels and soil are intended to prevent significant blast impulse, fragments, and projectiles from reaching the pipeline.

Armor Designs markets a system as a general barrier that could be used for any structure, including pipes, valve stations, manifolds, etc. to protect against blast and ballistic attack.

Dependent Barriers

Like an independent barrier, the primary function of a dependent barrier is to shield the pipeline component from threats, including blast, ballistic, or physical attack. Unlike the independent barrier, a dependent barrier is structurally dependent on the pipeline; it is not free-standing. Composite Technologies has developed a pipeline cover system consisting of outer and inner steel layers, separated by a very high-strength concrete core. The cover is designed for a specific diameter of pipe and installed in a “clam-shell” method. The cover is then fixed in place with concealed tamper-resistant fasteners.

WinTec Security has advertised development of a protective jacket designed to defeat ballistic and portable drill threats. Tightening of the jacket fastener is intended to release a bonding agent that joins the sleeve to the pipe, providing self-sealing capabilities. The bonding agent is also intended to provide structural reinforcement.

Crushable Layer

In the crushable layer approach, a layer of deformable material is installed on the surface of the pipeline component. Failure of the material during a blast event is intended to reduce the peak pressures applied to the component and thereby reduce the likelihood of rupture.

BlastGard® has proposed its crushable material BlastWrap™ for pipeline blast mitigation. BlastWrap™ is heat-treated perlite (a volcanic glass) contained within 3-in compartments.

Ductile Layer

In the ductile layer approach, a ductile material is applied to the exterior surface of the pipeline component. Specialty Products Inc., BASF, DefensTech International Inc, Mid-American Group, and Berry Plastics™ propose a ductile cover for the pipeline. The ductile layer is intended to resist localized penetration and perforation and to self-seal, thereby preventing loss of liquid material in the event of perforation.

TableE-1. Summary of Blast Mitigation Technologies

Category	Subcategory	Vendor	Product Name
Stiff Reinforcement	Fiber-Reinforced Polymer	QuakeWrap™, Sika, Fyfe	
	Steel-Reinforced Thermoplastic	Hardwire™	
Independent Barrier	Steel-Clad Earthen Barrier	Infrastructure Defense Tech.	Metalith™
	Light-Weight Blast-Resistant Panels	Armor Designs, Inc.	
Dependent Barrier	Fiber-Reinforced Concrete	Composite Technologies	
	Protective Jacket	WinTec Security	Pipe Jacket
Crushable Layer	Compartmentalized Heat-Treated Perlite	BlastGard®	BlastWrap™
Ductile Layer	Polyurea Coating	Specialty Products Inc.	Dragonshield BC™
	Polyurethane Coating	BASF	
	Polymer Coating	DefensTech Int. Inc.	
		Mid-American Group	Line-X

Phase 1, Task 2 - Pipeline Vulnerability Assessment

In Task 2, the vulnerabilities of pipeline systems to explosive attack were assessed. For that assessment, the basic components of the pipeline system were identified and described generically, both for natural gas and liquid lines. The general vulnerability and resistance of pipeline components to explosive threats were assessed. Specific explosive threats that could be applied to a pipeline were then characterized. Finally, the consequences of pipeline failure were examined, both by component type and by line type (liquid and natural gas), to establish priorities for protecting the components.

Pipeline System Components

Natural Gas Lines

Natural gas pipelines are composed of line pipe, valves, manifolds, and compressors. Line pipe contains the product and valves provide control of the flow. Manifolds are the combinations of pipes, valves, flanges, and fittings assembled for a specific application. Compressors maintain flow by pressurizing the line at regular intervals along its length.

These components are present in gas pipeline stations, which include the components as well as any instrumentation specific to the station type. There are four types of stations: compressor, metering, block valve, and maintenance. Compressor stations are equipped with a number of compressors of sufficient size to sustain flow. Metering stations measure the volume of gas that passes through the pipeline. Block valve stations stop flow during emergencies and scheduled maintenance. One type of maintenance station is a pig station, which permits ingress and egress of diagnostic devices known as pigs.

Gas storage facilities are another part of the gas pipeline system. To meet peak winter demand, the industry maintains an auxiliary source of gas near markets, stored as liquefied natural gas or liquefied petroleum gas, and operates pipelines below capacity for the rest of the year. This approach allows the gas industry to maintain a relatively small flow capacity compared with peak demand without service interruption to consumers.

The industry also maintains pipeline control centers that can be distributed or consolidated. If distributed, there are several control centers, each for a segment of pipeline. A consolidated control center directs the entire pipeline from a single location.

Liquid Lines

As with gas lines, the components of liquid lines include line pipe, valves, and manifolds. In most cases, pipeline head is maintained using electric pumps. The physical characteristics of the pump depend upon the line operating pressure, flow rate, and the specific gravity of the liquid.

These components are assembled into pump, metering, block valve, and maintenance stations. Booster pump stations maintain the head and thus flow rate of the line. An originating pump station is located at the head of a line and can also include metering equipment, supervisory control, and data acquisition equipment. Liquid block valves are required on both sides of pump stations and at major waterways.

Liquid storage facilities, also known as storage fields or tank farms, reduce flow fluctuation in a pipeline by providing a buffer supply. They are commonly used for petroleum products.

Access to Critical Pipeline Components

The sheer size of the United States liquid and natural gas pipeline system makes it vulnerable to numerous threats, including explosive, ballistic, sabotage, vandalism, and accidents. Explosive threats include improvised explosive devices (IEDs) and vehicle borne IEDs (VBIEDs). The proximity of pipelines to vehicular infrastructure (roads, parking areas, and bridges) contributes to the vulnerability, allowing easy access for VBIED and other IED threats.

General hardening of pipeline infrastructure against these threats would be exorbitantly expensive. The vast size of the infrastructure is simply too great. The size of the pipeline system has also prevented broad surveillance because of the cost of security personnel and instrumentation for monitoring such a large area.³

Resistance to Explosive Threats

Standoff

Although pipeline systems are very accessible to explosive attack, they also exhibit some inherent resistance. Nearly all pipelines in the continental US are belowground, as required by federal regulations⁴, and the typical soil cover is 30-in to 36-in. In cases where it is aboveground, the pipeline is often covered with insulation. Both the soil and insulation prevent explosive charge from being placed directly on the pipe, a condition that enforces standoff (the distance from the center of the charge to the surface of the pipe). An increased standoff reduces the damage to the pipe.

Internal Pressure

In general, both liquid and natural gas lines have significant internal pressure, and this fact also enhances their resistance to attack. Explosive testing has shown that a larger charge weight is required to fail a pressurized line than an unpressurized line⁵. The mass of fluid in a liquid pipeline, pump, or valve also increases the inertial resistance to blast loading. Finally, the circular shape of the pipe can reduce the applied load, by as much as 20% compared to a square configuration where the width is equal to the diameter of the circular pipe.⁶

Redundancy

The consequence of an explosive attack on a pipeline system may be reduced due to the redundancy that is designed into systems to minimize supply disruption when repairs must be made. For example, many pipelines include a built-in looped line to bypass critical segments, such as compressor or pump stations. In cases where this looped line has not already been installed, pipeline operators can install an aboveground bypass for a damaged segment of the line in a matter of hours.

Control systems are also typically redundant. In many cases, Supervisory Control and Data Acquisition (SCADA) systems have double or even triple redundancies. Manual backups that bypass SCADA are also available.

³*Characteristics and Common Vulnerabilities Infrastructure Category: Petroleum Pipelines*, Department of Homeland Security, 22 April 2005, Washington DC, <http://www.dhs.gov/index.shtm>, p. 12

⁴*Pipeline Threat Assessment*, Transportation Security Administration, Office of Intelligence, 23 October 2008, Washington DC, <http://www.tsa.gov/>

⁵*Vulnerability of Large Diameter Natural Gas Pipelines to Attack with Commercial Explosives*, Bert von Rosen, Canadian Explosives Research Laboratory, presented at the International Pipeline Security Forum, 23-25 October 2007

⁶*Blast-Resistant Design of Highway Bridge Columns*, Holland, Carrie, U Texas-Austin, August 2008

Vulnerability to Specific Explosive Threats

The specific vulnerability of a pipeline to an explosive threat depends on the threat itself. In this project, four explosive threats to pipelines were identified: bulk explosive, contact charge, shaped charge, and flyer plate.

Bulk Explosive Threat

The bulk explosive threat is defined as a relatively large charge weight, such as 50-lb TNT or greater, detonated at some distance from the pipeline. The explosion generates a high-pressure shock wave that propagates through the air before striking the target.

To assess the vulnerability of an aboveground pipeline to a bulk explosive threat, eight finite element analysis (FEA) simulations were developed, and the results are summarized in Table E-2. For all eight FEA simulations, the bulk explosive was TNT, spherical in shape and the segment of pipeline was 100-ft long with a diameter of 24-in and a wall thickness of 0.25-in, as shown in Figure E-1. Symmetry was used such that the model itself was 50-ft long. A valve, compressor, or pump was approximately modeled as a 4-ft long segment of pipe with 1.0-in wall thickness, illustrated by the green part in Figure E-1.

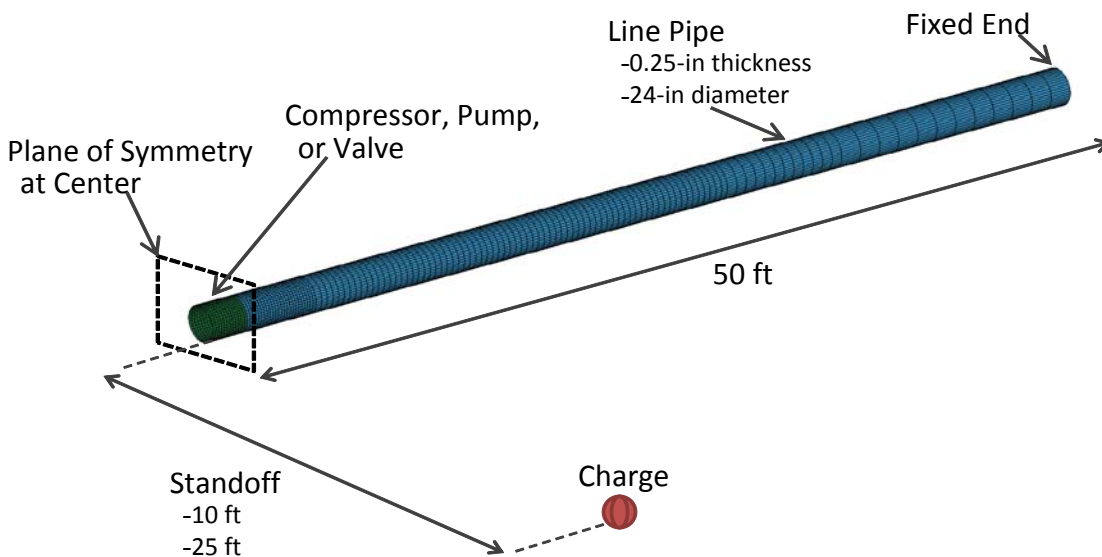


Figure E-1. Layout of FEA Model for Bulk Explosive Simulations

Two standoffs (10-ft and 25-ft) were considered; the pipe contents were either gas or liquid and the center component was a valve, pump or compressor.

The results of the eight analyses are summarized in Table E-2. As shown, a large volume of bulk explosives is required to fail line pipe at standoffs greater than 10 ft. It is unlikely that an aggressor would actually attack the pipeline with such a large volume of explosive. Rather, an aggressor with such a weapon would more likely target a site where a large number of human casualties could be caused. Therefore, bulk explosives were concluded to be an inappropriate threat against pipeline infrastructure.

Table E-2. Summary of Results from Bulk Explosive FEA Simulations

Sim. No.	Pipeline Contents	Charge Standoff [ft]	Component at Center	Charge Weight (TNT) [lb]
1	Gas	25	Valve	SSI ^A
2	Gas	25	Compressor	SSI
3	Gas	10	Valve	SSI
4	Gas	10	Compressor	SSI
5	Liquid	25	Valve	SSI
6	Liquid	25	Pump	SSI
7	Liquid	10	Valve	SSI
8	Liquid	10	Pump	SSI

^A SSI = Sensitive Security Information

Contact Charge Threat

Contact charge threats were also considered. A contact charge consists of a relatively small explosive weight placed in direct contact with a target. This threat is distinct from a charge with standoff because the blast energy does not propagate through air to the target.

An FEA model was developed to simulate contact charges detonated on a pipeline. The pipe had a diameter of 24-in and a wall thickness of 0.25-in. The model is shown in Figure E-2.

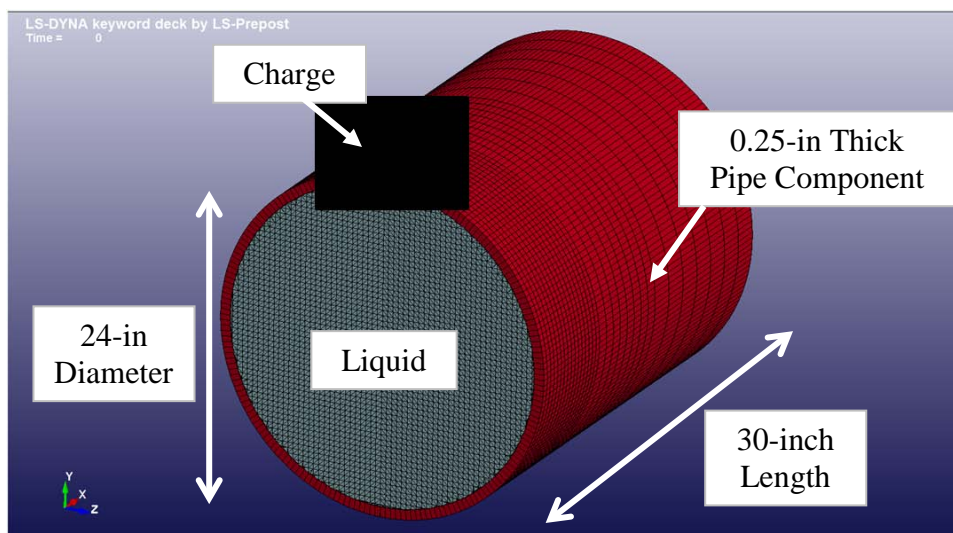


Figure E-2. Bare Pipe Component Model

Three cases were examined in the FEA contact charge simulations:

1. Empty pipe
2. Gas-filled pipe at 800-psi
3. Liquid-filled pipe at 800-psi

In each of the three cases, the initial charge size was w -lbs TNT (w -lbs C4), which was found to breach the pipeline. The charge size was progressively decreased to find the threshold for pipe failure. It was found that charges as small as w -lb TNT (w -lbs C4) produced holes in this particular pipe configuration for all three cases. While pipelines with larger wall thicknesses will require more explosive, these analyses illustrate that typical pipeline components are vulnerable to small contact charges, with weights as low as w -lb TNT (w -lb C4).

Shaped Charge Threat

Shaped charges are common in military ordnance but are also used for drilling activities, instantaneous release of sections of rockets, and engineered demolition charges. Types of shaped charge include conical and linear, shown respectively in Figure E-3 and Figure E-4. A conical charge is composed of a copper-lined cone embedded in high explosive (HE). At ignition, the copper cone collapses and forms a metal jet which is ejected from the casing along with a lower velocity slug. The jet makes a deep and narrow penetration in the target material. Given the significant penetration capability, all pipeline components were considered vulnerable to a shaped charge threat.

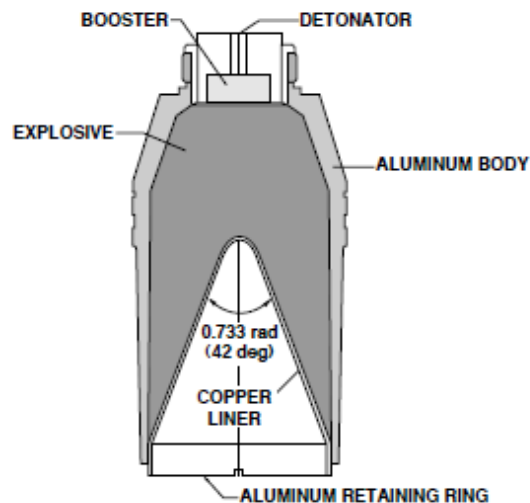


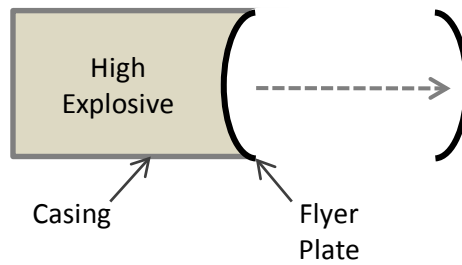
Figure E-3. Section of Conical Shaped Charge⁷

⁷UFC3-340-01 *Design and Analysis of Hardened Structures to Conventional Weapons Effects*, Department of Defense, 1 June 2002, Washington DC, p. 6-17

Figure E-4. Linear Shaped Charge⁸

Flyer Plate Threat

Flyer plates were the last explosive threat to be considered. A flyer plate consists of a circular, concave plate, usually copper, backed by high explosive. Detonation of the explosive ejects the flyer plate with sufficient force that it deforms, becoming a convex highvelocity projectile, as shown in Figure E-5, with considerable penetration capacity.



FigureE-5. Flyer Plate Configuration

Preliminary analysis performed showed that a 9-in diameter plate can form an 11-in diameter hole in xx-in of standard steel. This result was obtained by comparing the energy required to fail the target plate to the energy applied by the flyer plate. Therefore, all aboveground pipeline components are vulnerable to flyer plate threats of any reasonable size.

Consequences of Pipeline Failure

The consequences of pipeline failure depend on the type of component that fails and on the product. Seven possible consequences for pipeline failure were identified:

- Product loss
- Replacement/repair costs
- Environmental damage
- Property damage
- Human evacuation
- Human injury and fatality
- Interruption of service

⁸http://www.dynawell.de/products_specialty_products.html, www.mcselph.com/lfe.htm

Consequences by Component Failure

The consequences of failure for a particular component were used to prioritize the components in terms of blast mitigation protection requirements. A prioritized list of pipeline components is provided in Table E-3. The logic behind these rankings is discussed in the following paragraphs.

Pumps and compressors were assigned the highest priority. These are expensive items and the lead times for replacement can be 6 months or longer. In many cases, loop lines that bypass pump or compressor stations will permit continued operation if the station is damaged, but loss of multiple stations may be sufficient to shut down a line. While the amount of lost product may be small due to the presence of block valves, the importance of pumps and compressors to line operation and the difficulty of replacing them give them the highest priority for protection.

Destruction of a valve, particularly a block valve, can result in considerable product loss and reduce an operator's control of the line. Furthermore, depending on the type, valves can be costly to replace and require long lead times for delivery. As a result, valves have the second highest priority for protection.

The volume of leaked product due to manifold failure can be greater than for pipe because manifolds can include the intersection of multiple lines. In addition, replacing manifolds is generally more costly and time-consuming because significant welding is typically required, and installation tolerances are tighter due to the need to join several lines. For these reasons, manifolds have higher priority for protection than line pipe, but because they require less lead time for installation, they are below pumps, compressors, and valves.

Rupture of a storage tank would result in loss of a large volume of product. In the case of gas, that product would be dissipated into the atmosphere, as long there is no location where the gas can collect near an ignition source and be ignited. For a liquid product, spill control measures are typically in place at tank farms. Therefore, in the absence of ignition of the lost product, the consequences to the event site would be relatively manageable. Loss of a gas tank would reduce the buffer capacity of gas lines, which permits peak shaving, and liquid tank loss would reduce spare capacity. However, for much of the year, neither a gas tank loss nor liquid tank loss would significantly impair line service. Therefore, the protection priority of storage tanks is below pumps, valves, compressors, and manifolds but above line pipe.

Protection of line pipe has the lowest priority. Failure of line pipe does result in product leakage, but uncontrolled leakage is prevented by intermittently spaced block valves. Operators are able to replace line pipe quickly, often within 24 hours of leak detection.

The control center was not included in this ranking of priority. It is a critical asset, but its protection is generally considered separate from physical hardening, which is the subject of this research effort.

TableE-3. Summary of Protection Priority for Pipeline Components

Protection Priority	Component	Reason for Priority
1	Compressor or Pump	Long replacement time, large cost, line service impairment
2	Valve	Large-volume product loss, intermediate replacement time, line service impairment, cost
3	Manifold	Intermediate-volume product loss, intermediate replacement time
4	Storage Facility	Controlled, large-volume product loss
5	Line Pipe	Intermediate-volume product loss, easily repaired or replaced
Not considered	SCADA	Protection typically distinguished from physical hardening and therefore outside the scope of this effort

Consequences by Product Type

The contents of a pipeline system influence the consequences of its failure. If a leak develops in a natural gas line, the gas will dissipate into the environment; there are no remediation costs, but there are costs associated with product loss. Also, pipeline contents are potentially harmful to humans and certain products are susceptible to ignition if allowed to collect. If the product is ignited, it can cause immediate environmental damage, property damage, human evacuation, and human injury and fatality.

Interruption of gas service can impair industries that rely on the service, and one example is power generation. Historically, the natural gas pipelines have been independent of the electrical grid. However, in recent years, electric compressors have been installed on lines, and power generation from natural gas has increased such that a significant number of electrical plants are gas-fired. The interdependence of natural gas lines with the electrical grid could therefore have cascading effects.

Any discussion of service interruption should note that the gas pipeline system rarely operates at peak capacity. Therefore, though the effects of interrupting service could cascade, actually interrupting service with an explosive attack would likely require considerable planning and coordination. An unsophisticated attack could cause loss of redundant capacity and place strains on the gas system, but the attack would need to target critical nodes at specific times to actually interrupt service.

The potential consequences of a liquid line incident can be costly depending on the specifics of the incident. The type of product in a liquid line clearly has a large impact on the costs of product loss, environmental damage, property damage, and human injury and fatality. Loss of finished product is generally more costly than loss of raw product because the finished product has undergone a refining process. In addition, finished products can be toxic, which increases the hazard they pose to the environment, property, and humans.

As with gas lines, interruption of liquid service can economically impair industries that rely on the service. For example, interruption of jet fuel service could also have national consequences for the US airport system. US airports almost solely rely on a dedicated line for direct delivery of jet fuel.⁹ Loss of this line at a single airport could disrupt air travel nationally, given the interdependence of US airports.

Phase 1, Task 3 - Assessment of Blast Mitigation Technologies

The identified blast mitigation products from Task 1 were evaluated with numerical simulations to determine their ability to reduce the vulnerabilities that were assessed in Task 2.

Three of the explosive threats were removed from consideration for the following reasons: bulk charges are inefficient and unlikely to be used; to defeat shaped charges, a large amount of material (soil, steel, concrete, etc) must be employed; protection against flyer plates likewise requires large amounts of protective material. It is noted that some existing blast protection devices, such as Metalith™, do employ large amounts of material that are capable of defeating shaped charges and flyer plates. Given these exclusions, Task 3 was focused on contact charges.

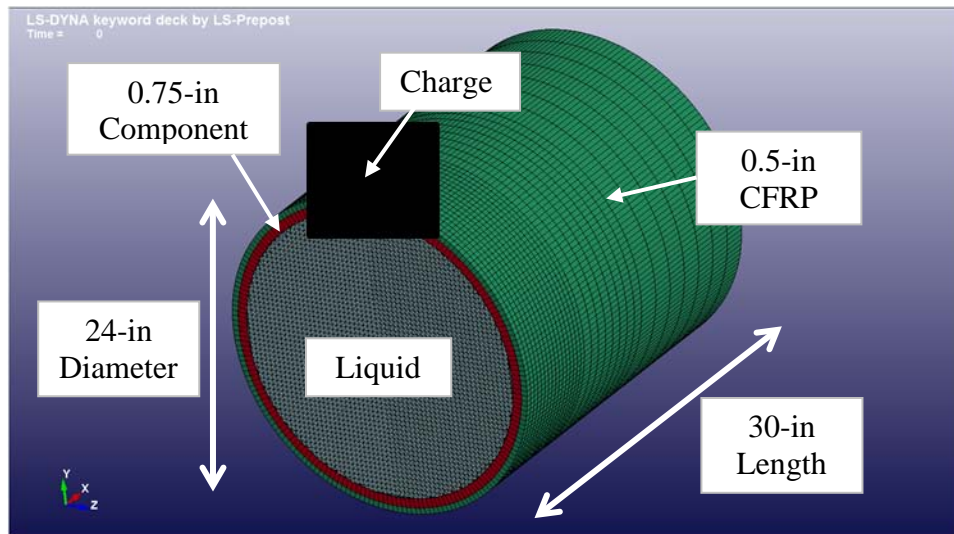
Three of the technologies identified in Task 1 were not numerically evaluated in Task 3. Two of the vendors from the survey did not provide the data required for a numerical simulation. The third technology that was not evaluated was Metalith™, the steel-clad, earth-filled barrier. Because the thickness of the Metalith™ barrier can be chosen to defeat a given contact charge threat, numerical modeling was not required to prove its ability.

Therefore, the five simulations shown in Table E-4 were performed for five distinct blast mitigation technologies. The five simulations were similar to the FEA models performed for the contact charge threat in the vulnerability assessment in Task 2. The technologies listed in Table E-4 were added to the model shown in Figure E-2. To illustrate this approach, a pipeline component with the carbon fiber-reinforced polymer (CFRP) product is shown in Figure E-6. The geometry of the other simulations was similar.

⁹*Characteristics and Common Vulnerabilities Infrastructure Category: Petroleum Pipelines*, Department of Homeland Security, 22 April 2005, Washington DC, <http://www.dhs.gov/index.shtm>, p. 4

TableE-4. Simulations for Contact Charge Threat

Sim. No.	Category	Subcategory
1	Stiff Reinforcement	Fiber-Reinforced Polymer (FRP)
2		Steel-Reinforced Thermoplastic (SRT)
3	Ductile Layer	Polyurea Coating
		Polyurethane Coating
		Polymer Coating
		Fiber-Reinforced Polyurethane
4	Crushable Layer	Compartmentalized Heat-Treated Perlite
5	Dependent Barrier	Steel-Encased Fiber-Reinforced Concrete (SEFRC)



FigureE-6. Carbon Fiber-Reinforced Polymer on Pipe Segment

Contact Charge Simulations

For each combination of charge weight and blast mitigation technology, both liquid and gas pipe contents were modeled. For the gas-filled pipe, the gas itself was not explicitly modeled; instead, an empty pipe was used with a pressure load applied to the interior face to model the gas effect.

Bare Pipe

As a basis for comparison, a 0.75-in thick bare steel pipeline component was modeled to determine its resistance to a contact charge. A thickness of 0.75-in was used to roughly replicate the wall thickness of a compressor or pump. The charge was positioned directly in contact with

the component, as shown in Figure E-2. The analyses showed that a charge size of ww-lb C4 was sufficient to breach both the gas-filled and liquid-filled pipes.

Stiff Reinforcement

For the fiber-reinforced polymer simulations, the fiber was assumed to be carbon. Based on correspondence with vendors, the thickness of the carbon fiber-reinforced polymer (CFRP) was modeled as 0.50-in because that is the maximum practical thickness for a field installation. The details of applying steel-reinforced thermoplastic (SRT) was assumed to be qualitatively similar to CFRP with the main difference being the strength and density of the fibers. Therefore, a thickness of 0.50-in was used for the SRT as well. The model showed that a charge size of ww-lb C4 was sufficient to breach both the gas-filled and liquid-filled pipes, retrofitted with the CFRP and SRT.

Ductile Layer

The ductile polymer was assumed to have the properties of a spray-on polyurea and a 0.50-in thickness of the polyurea was modeled. The model showed that a charge size of ww-lb C4 was sufficient to breach both the gas-filled and liquid-filled pipes, retrofitted with the polyurea.

Crushable Layer

Since the compartmentalized, crushable perlite provides standoff due to its thickness, two simulations were performed to determine the benefits of just standoff and of standoff with the crushable perlite. In the first simulation, a ww-lb charge was placed at a 3-in standoff from the pipeline component with only air in the intervening space. In the second case, a 3-in layer of perlite was placed between the charge and the pipeline component. A thickness of 3-in was used because it is a thickness manufactured by one crushable layer vendor. The condition of the perlite at the end of the C4 detonation is shown in Figure E-8. The hole diameters in the two cases were essentially equivalent, and it appears that the perlite adds minimal structural resistance.

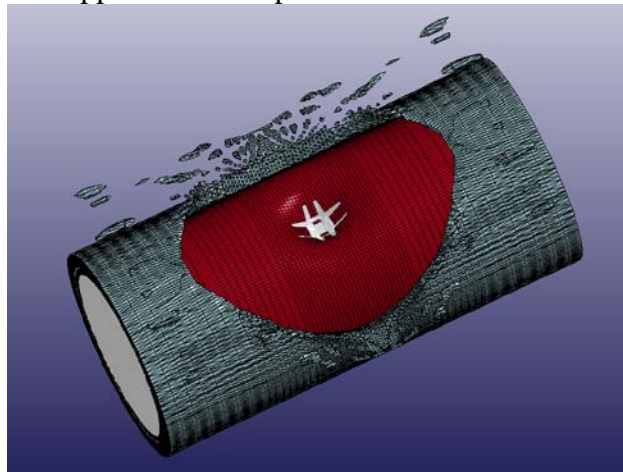


Figure E-8. Condition of Perlite after Detonation

Dependent Barrier

The steel-encased fiber-reinforced concrete (SEFRC) product is available in a variety of thicknesses and geometries. For the simulation, a thickness of 5-in was selected for the high-performance concrete (HPC) core, based on information provided by the vendor. The inner and outer layers of steel were assumed to be 0.25-in thick, again based on vendor information. The overall geometry is presented in Figure E-9.

In contrast to the other products, SEFRC increased the protection level significantly. In the simulation, the SEFRC product resisted greater than a ww-lb C4 charge without breach.

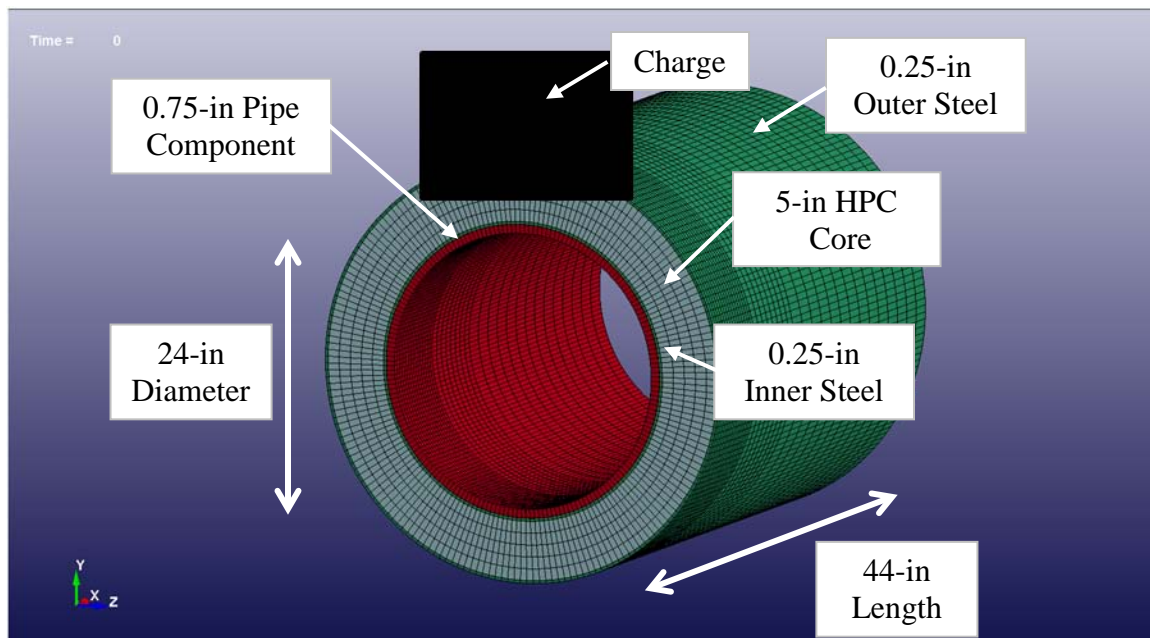


Figure E-9. Steel-Encased Fiber-Reinforced Concrete (SEFRC) Model

Conclusions from Phase 1

Based on the results of the numerical analysis, only the steel-encased fiber-reinforced concrete (SEFRC) barrier system appears capable of providing significant protection for the contact charge threat. The SEFRC vendor has stated that the cost of installing its product depends on the particular design threat and the geometry of the structure to be hardened. Maintenance costs are likely low, given that the technology is a combination of steel and concrete, both of which can be readily weatherized. The barrier system can be removed for inspection and maintenance of the pipe but given the likely weight of the system, mechanical assistance (forklift, crane, block and tackle, etc) would be required.

The other technology that is expected to increase protection level significantly is the Metalith™ barrier system. As with the SEFRC, the installation costs for Metalith™ are highly dependent on threat and the geometry of the pipeline components to be protected. Maintenance may be an issue, since much of the Metalith™ barrier would need to be removed to perform inspections and repairs.

For this assessment of pipeline blast mitigation technologies, PEC employed a combination of engineering judgment, analysis approaches, and numerical methods. Very little experimental data and essentially no engineering evaluations prior to this effort were found in regards to the vulnerability of unprotected and protected pipeline components from explosive threats. Any available data was incorporated into this assessment, but it was insufficient to validate the analyses performed. Therefore, to confirm the conclusions of this assessment, it was recommended that blast field tests be performed, and these were conducted as part of Phase 2, Task 5, as discussed below.

Phase 2, Task 5 –Blast Tests

The Task 5 blast tests included source characterization and pipe, valve, and protective structure tests. The source characterization tests verified the repeatability of explosive yield for charge configuration used in pipeline component tests. The pipe, valve, and protective structure tests determined the resistance of pipeline components to explosive threats, either unprotected or with blast mitigation technologies applied. The resistance of certain blast mitigation technologies to removal by an aggressor was also tested in a series of anti-tamper tests.

Source Characterization Tests

The goal of the source characterization tests was to verify the repeatability of explosive yield of the charge configuration used in subsequent tests. The explosive threat was a block-shaped xx-lb C4 charge (base to height ratio nominally 2:1). Each pipe specimen was a 4-ft long segment of 24-in diameter API 5L X52 pipe with a wall thickness of 0.375-in. The segments were uncapped and unpressurized. The 4-ft pipe segments were supported at the ends by reinforced-concrete blocks, as shown in Figure E-10.



Figure E-10. Typical Source Characterization Specimen Supported by Reinforced-Concrete Blocks

Five identical tests were performed to verify repeatability of explosive yield, using the impulse measured by free-field pressure gauges. The average impulses for each test were divided by the corresponding averages across all tests, for each standoff. The resulting ratio of average by test to total average (average for all tests) provided a measure of variability on a per-test basis. This

ratio is shown for each of the five tests in Figure E-11. From the figure, the average impulse per test ranged from 93% to 105% of the total average, and this variability was deemed acceptable.

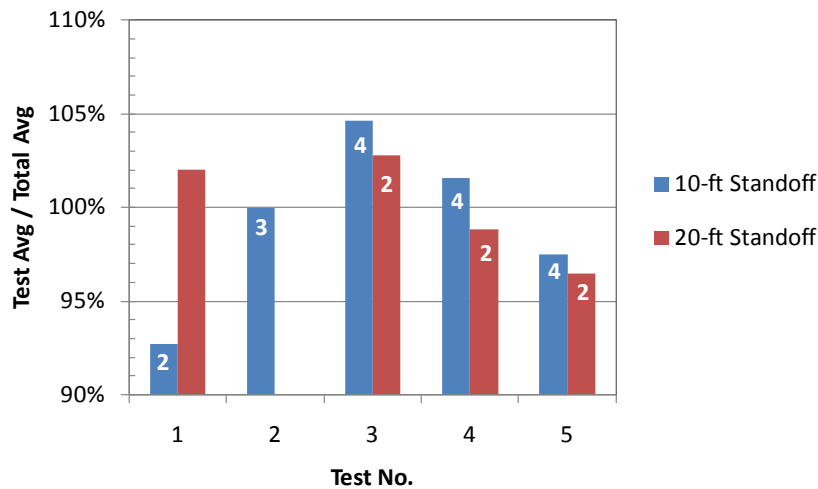


Figure E-11. Ratio of Test Average Impulse to Total Average Impulse
(Missing or corrupt data not included)

Pipe Tests

The goal of the pipe tests was to determine the resistance of bare (unprotected) and protected pipes to C4 charges, in contact or at a standoff. For the pipe specimens, any breach or cracking of the pipe was defined as a failure. Figure E-12 is an illustration of a typical pipe specimen.

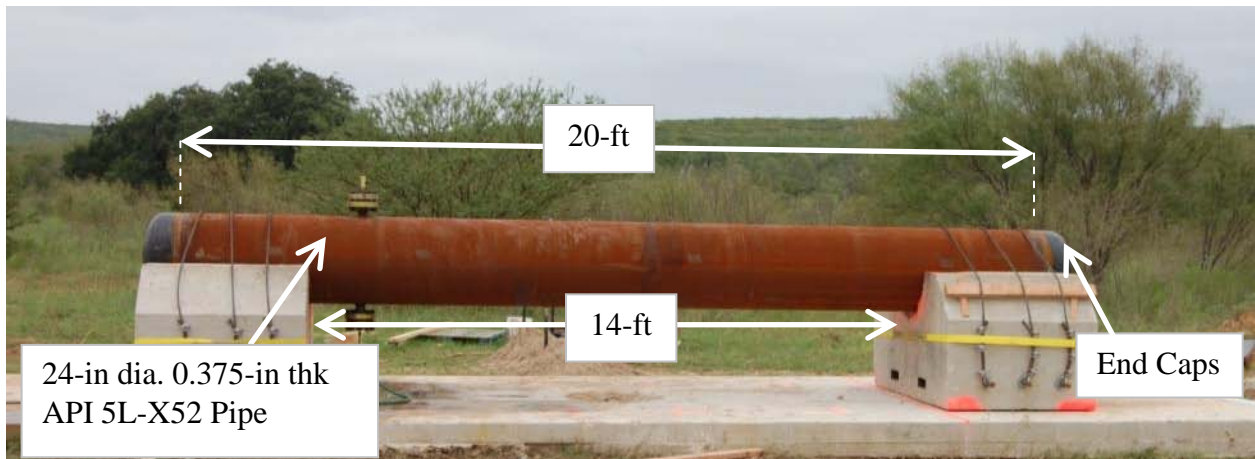


Figure E-12. Typical Capped Pipe Specimen

The explosive threat was anxx-lb C4 charge, identical to the one used in the source characterization tests. The charge was placed mid-span, at the apex of the pipe section for all tests except two, where the charge was placed at 12-standoff.

Ten pressurized pipe tests were performed, and the results are summarized in Table E-5. Both water and nitrogen-filled specimens with a 12-in standoff (Tests 11 and 17) remained intact. However, with the exception of the SEFRC covered specimens, all pipe specimens failed when the xx-lb charge was placed in contact with the bare pipe or blast mitigation technology (BMT). The SEFRC covers were breached during the tests, but the pipes remained intact and retained their pre-detonation internal pressures.

Table E-5. Summary of Pipe Contact Charge Tests

Test	Component	Fill	Blast Protection	Charge Weight [lb]	Standoff [in]	Post-Test Pipe Condition
11	24-in pipe, 0.375-in wall, X52	Water	None	xx	12	Intact
12	24-in pipe, 0.375-in wall, X52	Water	None	xx	0	Failed
13	24-in pipe, 0.375-in wall, X52	Water	Steel encased FRC	xx	0	Intact
14	24-in pipe, 0.375-in wall, X52	Water	Protective sleeve	xx	0	Failed
15	24-in pipe, 0.375-in wall, X52	Water	Composite wrap	xx	0	Failed
16	24-in pipe, 0.375-in wall, X52	Water	Polymer coating	xx	0	Failed
17	24-in pipe, 0.375-in wall, X52	Nitrogen	None	xx	12	Intact
18	24-in pipe, 0.375-in wall, X52	Nitrogen	None	xx	0	Failed
19	24-in pipe, 0.375-in wall, X52	Nitrogen	Steel encased FRC	xx	0	Intact
20	24-in pipe, 0.375-in wall, X52	Nitrogen	Protective sleeve	xx	0	Failed

Valve Tests

The goal of the valve tests was to determine the resistance of bare (unprotected) and protected valves to a xx-lb C4 contact charge. Failure was defined as inoperability of the valve mechanism. A typical valve specimen is shown in Figure E-13. With the exception of one test, the explosive threat for the valve tests was xx-lb C4 in contact with the valve or BMT, nominally identical to the threat in the source characterization tests.

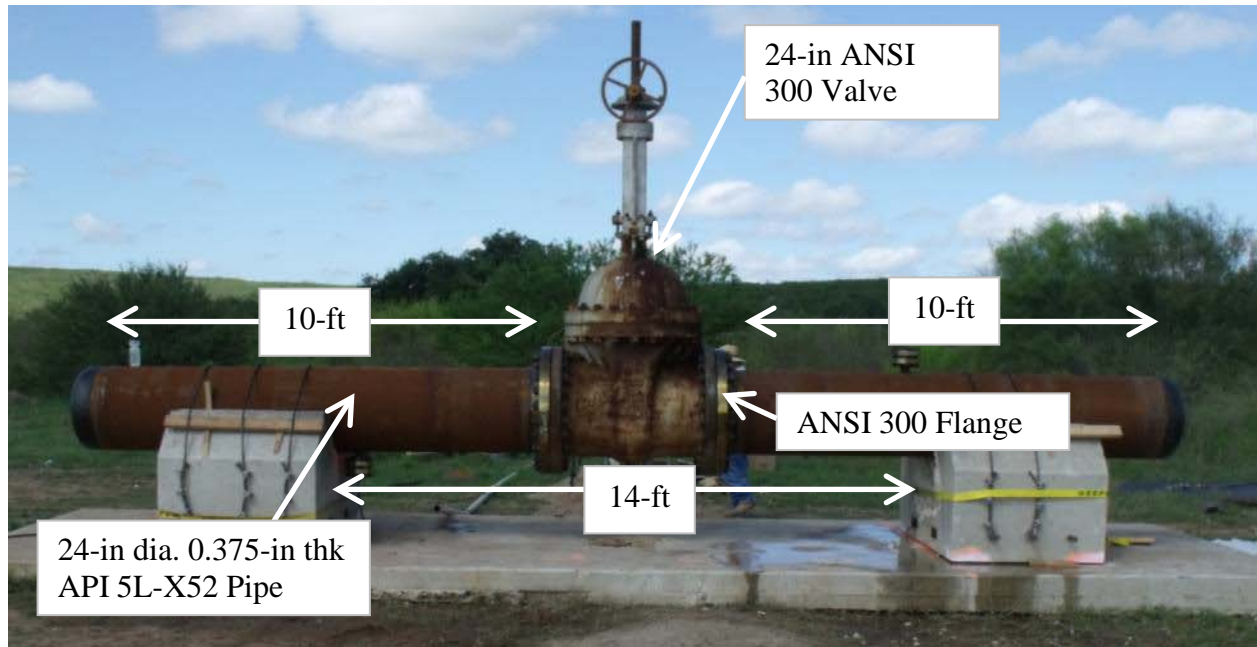


Figure E-13. Typical Valve Specimen

The results from the valve tests are summarized in Table E-6. Only the SEFRC BMT prevented breach of the valve for the xx-lb C4 contact threat; it was further able to resist the ww-lb C4 threat. As in the pipe tests, the wall of the SEFRC BMT was breached, but this breaching did not result in damage to the valve.

Table E-6. Summary of Valve Contact Charge Tests

Test	Component	Blast Mitigation Technology	Charge Weight [lb]	Valve Condition
21	24-in valve, 24-in pipe, 0.375-in wall, X52	None	ww	Failed
22	24-in valve, 24-in pipe, 0.375-in wall, X52	SEFRC Cover	ww	Intact
22B	24-in valve, 24-in pipe, 0.375-in wall, X52	SEFRC Cover	ww	Intact
23	24-in valve, 24-in pipe, 0.375-in wall, X52	Protective Structure	ww	Failed

Protective Structure Contact Charge Tests

The purpose of the protective structure is to prevent damage to critical pipeline components such as pumps or compressors. The threats were yy-lb and zz-lb C4 contact charges. The goal was to determine the resistance of two distinct protective structure concept to these threats. Ideally, for the yy-lb charge, the protective structures would not breach, and if there were breach for the zz-lb charge, the secondary debris would not be hazardous to the main mechanical components of a pump or compressor.

A witness element, shown in Figure E-14, was placed behind each protective structure prior to detonation. The element was a decommissioned compressor cylinder from a transmission line

for natural gas, selected to represent a critical pipeline component. For the test, breach of any structural component of that witness element was defined as failure.



Figure E-14. Decommissioned Compressor Cylinder as Witness Element

The results from the protective structure test are summarized in Table E-7. The two types of barriers were the Metalith™ and ICB, shown respectively in Figure E-15 and Figure E-16. For the Metalith™ barriers, the witness element was intact for the yy-lb and zz-lb threats. In the case of the ICB panel structure, the debris from the yy-lb threat failed the witness element, and the zz-lb test was not performed due to concern with the material’s performance.

Table E-7. Summary of Protective Structure Contact Charge Tests

Test	Blast Mitigation Technology	C4 Charge Weight [lb]	Post-Test Witness Element Condition
31	Metalith™	yy	Intact
32	Metalith™	zz	Intact
33	ICB Panel Structure	yy	Failed
34	ICB Panel Structure	zz	Not Tested



Figure E-15. Pre-Test Metalith™, Blast-Loaded Side



Figure E-16. ICB Panel Structure, Blast-Loaded Side

Anti-Tamper Tests

The goal of the anti-tamper tests was to determine the resistance of BMTs to tampering and removal by an aggressor.

A modified version of the test procedure in ASTM Standard WK10816 *Standard Test Method for Time Evaluation of Forced Entry Resistant Assemblies* (currently in draft form) was used. For the pipe specimens, the goal was to create a minimum 6-in x 6-in clear space on the surface of the pipe. For the protective structure specimens, the goal was to create a man-passable opening such that a 12-in x 12-in x 8-in object could be passed through the opening. The tools used in this assessment were those listed for the Very Low threat level in the draft ASTM standard WK10816 but with the addition of three battery-powered tools, an extra shovel, an oxyacetylene torch, and the removal of the two fire axes.

The results from the anti-tamper tests are summarized in Table E-8. As shown in the table, the SEFRC cover and Metalith™ with red oak had the highest forced entry resistance rating of VLww. The polyurea coating and Metalith™ with no red oak had a lower rating of VLww. Finally, the FRP had the lowest rating of VLww. The protective jacket was not tested because they were destroyed in the blast tests; the ICB protective structures were not tested because their material was not representative.

Table E-8. Summary of Protective Structure Tests

Blast Mitigation Technology	Test No.	Forced Entry Resistance Rating
Steel-Encased Fiber-Reinforced Concrete (SEFRC) Cover	41	VLww
Protective Jacket	42	Not performed
Fiber-Reinforced Polymer	43	VLww
Polyurea Coating	44	VLww
Metalith™ Protective Structure: w/ Red Oak	45	VLww
Metalith™ Protective Structure: no Red Oak	45B	VLww
ICB Protective Structure	46	Not performed

Conclusions from Phase 2

A summary of the tests for the pipe contact charge, valve contact charge, protective structure, and anti-tamper evaluation is provided in Table E-9. As demonstrated in these test series, there are two viable BMTs for protecting pipeline components: SEFRC covers and Metalith™ barriers. SEFRC covers are particularly appropriate for installations where there is minimal clearance around the component to be protected. Metalith™ barriers are more appropriate for hardening the perimeter around large pipeline components.

Table E-9. Summary of Test Results

Blast Mitigation Technology	Test No.	Installation	Protected Component	Component Contents	Post-Test Component Condition	Forced Entry Resistance Rating
Steel-Encased Fiber-Reinforced Concrete (SEFRC)	13, 41	Pipe Cover	Pipe	Nitrogen	Intact	VLww
	19, 41	Pipe Cover	Pipe	Water	Intact	VLww
	22, 22B	Valve Structure	Valve	Water	Intact	No test planned
Protective Jacket/Structure	14	Pipe Jacket	Pipe	Nitrogen	Failed	Jacket destroyed in blast test
	20	Pipe Jacket	Pipe	Water	Failed	Jacket destroyed in blast test
	23	Valve Structure	Valve	Water	Failed	No test planned
Fiber-Reinforced Polymer	15, 43	Reinforcing Layer	Pipe	Water	Failed	VLww
Polyurea	16, 44	Protective Coating	Pipe	Water	Failed	VLww
IDT Metalith™	31, 32, 45	Steel-Clad Earthen Barrier	Compressor Cylinder	NA	Intact	VLww*
ICB Panel Structure	33	Panel Barrier	Compressor Cylinder	NA	Failed	Unrep. material

*Forced-entry resistance rating based on Metalith™ without red oak layer.

Table of Contents

Table of Contents	i
List of Figures	vii
List of Tables	xiii
1 Phase 1 Introduction	2
2 Task 1: Survey of Existing Technology and Research	2
2.1 Stiff Reinforcement.....	3
2.1.1 Fiber-Reinforced Polymer	3
2.1.2 Steel-Reinforced Thermoplastic	4
2.2 Independent Barrier	5
2.2.1 Steel-Clad Earthen Barrier	5
2.2.2 Lightweight Blast-Resistant Panels	6
2.3 Dependent Barrier	7
2.3.1 Fiber-Reinforced Concrete.....	7
2.3.2 Protective Jacket	8
2.4 Crushable Layer	8
2.5 Ductile Layer	9
2.5.1 Polyurea Coating.....	10
2.5.2 Polyurethane Coating.....	10
2.5.3 General Polymer Coating.....	10
2.5.4 Fiber-Reinforced Polyurethane	10
2.6 Summary Table.....	11
3 Task 2: Pipeline Vulnerability Assessment	13
3.1 Natural Gas Pipeline	13
3.1.1 Basic Components	13
3.1.1.1 Line Pipe.....	13
3.1.1.2 Valve	13
3.1.1.3 Manifold	15
3.1.1.4 Compressor.....	16
3.1.2 Stations.....	17
3.1.2.1 Compressor Station	17
3.1.2.2 Metering Station	18
3.1.2.3 Block Valve Station.....	19
3.1.2.4 Maintenance Station	19
3.1.3 Storage Facilities.....	19
3.1.4 Control Centers	20
3.2 Liquid Pipeline.....	20
3.2.1 Basic Components	20

3.2.1.1	Line Pipe.....	20
3.2.1.2	Pumps	21
3.2.2	Pump Stations	22
3.2.3	Storage Facilities.....	23
3.2.4	Control Centers	24
3.3	Vulnerabilities to Explosive Threats.....	24
3.3.1	Access to Critical Pipeline Components.....	24
3.3.2	Resistance to Explosive Threats	24
3.3.2.1	Enforced Standoff.....	24
3.3.2.2	Structural Resistance	26
3.3.2.3	Redundancy	26
3.3.3	Vulnerability to Specific Explosive Threats	26
3.3.3.1	Bulk Explosive	27
3.3.3.2	Contact Charge	32
3.3.3.3	Shaped Charge.....	36
3.3.3.4	Flyer Plate.....	37
3.4	Consequences of Pipeline Failure.....	38
3.4.1	Consequences by Component Failure.....	38
3.4.1.1	Line Pipe.....	38
3.4.1.2	Manifold	39
3.4.1.3	Valve	39
3.4.1.4	Compressor or Pump	39
3.4.1.5	Storage Tank.....	39
3.4.1.6	Control Center	40
3.4.1.7	Priority for Component Protection	40
3.4.2	Consequences by Line Product Type.....	41
3.4.2.1	Natural Gas Pipeline.....	41
3.4.2.2	Liquid Pipeline	42
3.5	Conclusions from Pipeline Vulnerability Assessment.....	42
4	Task 3: Assessment of Blast Mitigation Technologies	44
4.1	Development of Numerical Simulation Matrix	44
4.2	Contact Charge FEA Model.....	49
4.2.1	Modeling Approach	49
4.2.2	Modeling Issues	52
4.2.2.1	Constitutive Models	52
4.2.2.2	Mesh Refinement	52
4.2.2.3	Sliding Energy	53
4.3	Contact Charge Simulation Results	53
4.3.1	Bare Pipeline Component	53
4.3.2	Stiff Reinforcement.....	58
4.3.2.1	Fiber-Reinforced Polymer	58
4.3.2.2	Steel-Reinforced Thermoplastic.....	60
4.3.3	Steel-Encased Fiber-Reinforced Concrete	61
4.3.4	Compartmentalized Heat-Treated Perlite	64

4.3.5	Ductile Polymer	67
4.4	Assessment by Criteria	69
4.5	Conclusions from Assessment of Blast Mitigation Technologies	70
5	Phase 2 Introduction	73
6	Source Characterization Tests.....	73
6.1	Test Overview	73
6.1.1	Test Objective	73
6.1.2	Test Subcontractor	73
6.1.3	Typical Test Specimen.....	73
6.1.4	Explosive Threat	74
6.1.5	Test Matrix	76
6.1.6	Instrumentation	76
6.2	Test Results.....	78
6.2.1	Post-Test Specimen Condition.....	78
6.2.2	Repeatability	80
7	Pipe Tests	82
7.1	Test Overview	82
7.1.1	Test Objectives.....	82
7.1.2	Failure Criterion.....	82
7.1.3	Typical Pipe Specimen	82
7.1.4	Explosive Threat	84
7.1.5	Test Matrix.....	84
7.1.6	Instrumentation	85
7.2	Test 11: Water-Filled Pipe, xx-lb C4 Charge at 12-in Standoff	87
7.2.1	Test Details	87
7.2.2	Post-Test Condition	87
7.2.3	Pressure-Time Histories.....	88
7.3	Test 12: Water-Filled Pipe, xx-lb C4 Contact Charge.....	89
7.3.1	Test Details	89
7.3.2	Post-Test Condition	89
7.3.3	Pressure-Time Histories.....	91
7.4	Test 13: Water-Filled Pipe with SEFRC Cover, xx-lb C4 Contact Charge.....	92
7.4.1	Test Details	92
7.4.2	Post-Test Condition	94
7.4.3	Pressure-Time Histories.....	94
7.5	Test 14: Water-Filled Pipe with Pipe Jacket, xx-lb C4 Contact Charge.....	95
7.5.1	Test Details	95
7.5.2	Post-Test Condition	96
7.5.3	Pressure-Time Histories.....	98
7.6	Test 15: Water-Filled Pipe with FRP Layer, xx-lb C4 Contact Charge	99
7.6.1	Test Details	99

7.6.2	Post-Test Condition	100
7.6.3	Pressure-Time Histories	100
7.7	Test 16: Water-Filled Pipe with Polyurea Coating, xx-lb C4 Contact Charge	101
7.7.1	Test Details	101
7.7.2	Post-Test Condition	102
7.7.3	Pressure-Time Histories	103
7.8	Test 17: Nitrogen-Filled Pipe, xx-lb C4 Charge at 12-in Standoff	103
7.8.1	Test Details	103
7.8.2	Post-Test Condition	104
7.8.3	Pressure-Time Histories	104
7.9	Test 18: Nitrogen-Filled Pipe, xx-lb C4 Contact Charge	105
7.9.1	Test Details	105
7.9.2	Post-Test Condition	105
7.9.3	Pressure-Time Histories	107
7.10	Test 19: Nitrogen-Filled Pipe with SEFRC Cover, xx-lb C4 Contact Charge	108
7.10.1	Test Details	108
7.10.2	Post-Test Condition	108
7.10.3	Pressure-Time Histories	109
7.11	Test 20: Nitrogen-Filled Pipe with Pipe Jacket, xx-lb C4 Contact Charge	110
7.11.1	Test Details	110
7.11.2	Post-Test Condition	110
7.11.3	Pressure-Time Histories	111
7.12	Pipe Tests: Summary of Results	112
8	Valve Tests	113
8.1	Test Overview	113
8.1.1	Test Objectives	113
8.1.2	Failure Criterion	113
8.1.3	Typical Valve Specimen	113
8.1.4	Explosive Threat	115
8.1.5	Test Matrix	115
8.2	Test 21: Bare Valve, xx-lb C4 Contact Charge	115
8.2.1	Test Details	115
8.2.2	Instrumentation	116
8.2.3	Post-Test Condition	117
8.2.4	Pressure-Time Histories	119
8.3	Test 22: SEFRC-Covered Valve, xx-lb C4 Contact Charge	120
8.3.1	Test Details	120
8.3.2	Instrumentation	121
8.3.3	Post-Test Condition	121
8.3.4	Pressure-Time Histories	123
8.4	Test 22B: SEFRC-Covered Valve, ww-lb C4 Contact Charge	123
8.4.1	Test Details	123

8.4.2	Instrumentation	124
8.4.3	Post-Test Condition	124
8.4.4	Pressure-Time Histories.....	126
8.5	Test 23: Steel Protective Structure, xx-lb C4 Contact Charge.....	126
8.5.1	Test Details	126
8.5.2	Instrumentation	127
8.5.3	Post-Test Condition	128
8.5.4	Pressure-Time Histories.....	129
8.6	Valve Tests: Summary of Results.....	130
9	Protective Structure Contact Charge Tests	131
9.1	Test Overview.....	131
9.1.1	Test Objectives.....	131
9.1.2	Failure Criterion.....	131
9.1.3	Explosive Threat.....	131
9.1.4	Test Matrix.....	133
9.2	Test 31: Metalith™, yy-lb C4 Contact Charge.....	133
9.2.1	Test Details	133
9.2.2	Instrumentation	136
9.2.3	Post-Test Condition	137
9.2.4	Pressure-Time Histories.....	138
9.3	Test 32: Metalith™, zz-lb C4 Contact Charge	139
9.3.1	Test Details	139
9.3.2	Instrumentation	139
9.3.3	Post-Test Condition	140
9.3.4	Pressure-Time Histories.....	142
9.4	Test 33: ICB, yy-lb C4 Contact Charge.....	142
9.4.1	Test Details	142
9.4.2	Instrumentation	144
9.4.3	Post-Test Condition	145
9.4.4	Pressure-Time Histories.....	146
9.5	Test 34: ICB, zz-lb C4 Contact Charge	146
9.6	Protective Structure Tests: Summary of Results	147
10	Anti-Tamper Tests	147
10.1	Test Overview.....	147
10.1.1	Test Objective	147
10.1.2	Test Matrix.....	147
10.1.3	Test Procedure	148
10.1.4	Test Documentation	149
10.2	Test 41: Steel-Encased Fiber-Reinforced Concrete (SEFRC) Cover	150
10.2.1	Test Details	150
10.2.2	Test Results.....	150

10.3 Test 42: Protective Jacket 153

10.4 Test 43: Fiber-Reinforced Polymer (FRP) Cover 153

 10.4.1 Test Details 153

 10.4.2 Test Results 153

10.5 Test 44: Polyurea Coating 156

 10.5.1 Test Details 156

 10.5.2 Test Results 156

10.6 Test 45: Metalith™ Protective Structure, with Red Oak 158

 10.6.1 Test Details 158

 10.6.2 Test Results 159

10.7 Test 45B: Metalith™ Protective Structure, No Red Oak 162

 10.7.1 Test Details 162

 10.7.2 Test Results 162

10.8 Test 46: ICB Protective Structure 165

10.9 Anti-Tamper Tests: Summary of Results 165

11 Conclusions 165

List of Figures

Figure 1. Effect of Adding Stiff Reinforcement on Ultimate Strength.....	3
Figure 2. Installation of FRP on Reinforced Concrete Column.....	4
Figure 3. Example of Hardwire® Steel Mesh.....	4
Figure 4. Proposed Metalith™ Barrier for Pipeline Protection	5
Figure 5. Corrugated-Steel Compartments for Earth.....	5
Figure 6. Explosive Tests Conducted on Metalith™ Barriers	6
Figure 7. Clam-Shell Installation of SEFRC Pipe Cover Frame	7
Figure 8. Protective Jacket Concept proposed by WinTec Security.....	8
Figure 9. BlastWrap™ Sample	9
Figure 10. X-Flex™ Installation Process.....	11
Figure 11. X-Flex™ Floor Anchoring	11
Figure 12. Ball Valve Mechanism	14
Figure 13. Side Elevation View of Ball Valve	14
Figure 14. Plug Valve	15
Figure 15. Check Valve	15
Figure 16. Pipeline Manifold	16
Figure 17. Centrifugal Compressor: Gas Turbine.....	16
Figure 18. Centrifugal Compressor: Electric Motor	17
Figure 19. Reciprocating Compressor: Reciprocating Gas Engine	17
Figure 20. Location of Cross Head Guide Assembly	17
Figure 21. Large Natural Gas Compressor Station.....	18
Figure 22. Small Metering Station.....	18
Figure 23. Large Metering Station.....	19
Figure 24. Pig Launcher Station	19
Figure 25. Plan View of Pump for 20-in Crude Oil Line	21
Figure 26. Side Elevation View Pump for 20-in Crude Line	21
Figure 27. Photograph of Pump for 20-in Crude Line.....	22
Figure 28. Typical Pump Station	22
Figure 29. Typical Block Valve Station	23
Figure 30. Petroleum Tank Farm.....	23
Figure 31. Peak Reflected Impulse versus Standoff for xx-lb TNT Charge.....	25
Figure 32. Heavy Insulation on the Trans Alaska Pipeline System (TAPS)	25
Figure 33. Shock Pressure Accumulation for (a) Square Cross Section and (b) Circular Cross Section.....	26
Figure 34. Layout of FEA Model for Bulk Explosive Simulations.....	28
Figure 35. Longitudinal Pipeline Loading Considerations	29
Figure 36. Circumferential Pipeline Loading Considerations	29
Figure 37. Typical Deformed Shape for Valve Case (Valve Section with Density of Steel).....	30
Figure 38. Typical Deformed Shape for Pump or Compressor Case (Pump or Compressor with Mass 100 times that of Valve)	31
Figure 39. Conceptual Scheme of Contact-Charge Analysis.....	33
Figure 40. Hole diameter versus Spherical Charge Weight TNT: 0.35-in and 1.00-in	33
Figure 41. C4 Contact Charge ALE Model Before Fluid Fill	34

Figure 42. Contact Charge ALE Model After Fluid Fill (air outside pipe omitted for clarity) ...	34
Figure 43. Detail of Box-Shaped C4 Charge on Bare Pipe (Half Shown by Symmetry).....	35
Figure 44. Contact Charge ALE Model Validation Case	35
Figure 45. Section of Conical Shaped Charge	36
Figure 46. Linear Shaped Charge	37
Figure 47. Flyer Plate Configuration	37
Figure 48. Assumed Explosive Distribution for Analytical Model	38
Figure 49. Quarter-Symmetry Model	51
Figure 50. Hole diameter: Bare Pipe ww-lb Gas Content at 260-usec (Reflections about XY and YZ Planes)	52
Figure 51. Bare Pipe Component Model (Reflection about XY Plane)	53
Figure 52. Bare Pipe ww-lb C4 Charge Liquid Content, Initial Condition (Reflections about XY and YZ Planes).....	55
Figure 53. Bare Pipe ww-lb C4 Charge Liquid Content, 40-usec after Detonation (Reflections about XY and YZ Planes).....	55
Figure 54. Bare Pipe ww-lb C4 Charge Liquid Content, 140-usec after Detonation (Reflections about XY and YZ Planes).....	56
Figure 55. Bare Pipe ww-lb C4 Charge Liquid Content, 140-usec after Detonation Eulerian Mesh Rendered (Reflections about XY and YZ Planes)	56
Figure 56. Bare Pipe ww-lb C4 Charge Liquid Content, Initial Condition, Von Mises Stress (Reflections about XY and YZ Planes)	56
Figure 57. Bare Pipe ww-lb C4 Charge Liquid Content, 40-usec after Detonation, Von Mises Stress (Reflections about XY and YZ Planes).....	57
Figure 58. Bare Pipe ww-lb C4 Charge Liquid Content, 140-usec after Detonation, Von Mises Stress (Reflections about XY and YZ Planes).....	57
Figure 59. Hole Diameter: Bare Pipe ww-lb C4 Charge Liquid Content at 1000-usec (Reflections about XY and YZ Planes)	57
Figure 60. CFRP Model (Reflection about XY Plane).....	58
Figure 61. Hole Diameter: CFRP ww-lb C4 Charge Liquid Content at 1000-usec (Reflections about XY and YZ Planes).....	59
Figure 62. Hole diameter: SRT ww-lb C4 Charge Liquid Content at 1000-usec (Reflections about XY and YZ Planes).....	61
Figure 63. SEFRC Model, Gas-Filled Case (Reflection about XY Plane).....	63
Figure 64. Von Mises Stresses in the Composite Technologies System 110-usec after Detonation (Front View, Reflection about XY Plane)	64
Figure 65. Pipeline Component with 3-in Charge Standoff (Reflection about XY Plane).....	64
Figure 66. Pipeline Component with 3-in Perlite Layer (Reflection about XY Plane)	65
Figure 67. Assumed Pressure versus Volumetric Strain for Perlite.....	66
Figure 68. Condition of Perlite 100-usec after C4 Detonation (Reflections about XY and YZ Planes).....	66
Figure 69. (a) Pipe Component with Perlite (1000-usec) (b) Pipe Component without Perlite (1000-usec)	67
Figure 70. Hole diameter for ww-lb C4 Charge Liquid Contents (Reflections about XY and YZ Planes).....	68
Figure 71. Hole Diameter by Charge Weight, Contents, and Blast Mitigation Technology	69
Figure 72. Source Characterization Specimen Supported by Reinforced-Concrete Blocks.....	74

Figure 73. Supported Length of Source Characterization Specimen..... 74

Figure 74. C4 Charge and Plywood Mold 75

Figure 75. EBW Placed in Top Center of C4 Block..... 75

Figure 76. Detail of EBW and Placement Guide..... 75

Figure 77. Charge Placed on Source Characterization Specimen..... 76

Figure 78. Location of Instrumentation in Source Characterization Tests (Plan View)..... 77

Figure 79. Location of Instrumentation in Source Characterization Tests (Elevation View)..... 77

Figure 80. Top of Unfilled Pipe Segment, Post-Detonation Condition (Test 1) 78

Figure 81. Width of Top Hole in Unfilled Pipe Segment (Test 1) 78

Figure 82. Length of Top Hole in Unfilled Pipe Segment (Test 1) 79

Figure 83. Bottom Interior of Unfilled Pipe Segment, Post-Detonation Condition (Test 1)..... 79

Figure 84. Width of Bottom Hole in Unfilled Pipe Segment (Test 1)..... 79

Figure 85. Length of Bottom Hole in Unfilled Pipe Segment (Test 1)..... 80

Figure 86. Example Pressure-Time Histories for Source Characterization Tests (Test 5)..... 80

Figure 87. Integrated Pressure-Time Histories to Obtain Impulse (Test 5)..... 81

Figure 88. Ratio of Test Average Impulse to Total Average Impulse (*Missing or corrupt data not included*) 82

Figure 89. Typical Capped Pipe Segment..... 83

Figure 90. Fitting Used for Pipe Pressurization..... 83

Figure 91. Typical xx-lb C4 Charge Location 84

Figure 92. Location of Instrumentation for Pipe Tests (Plan View)..... 86

Figure 93. Location of Instrumentation for Pipe Tests (Elevation View) 86

Figure 94. C4 Charge on Foam Support for 12-in Standoff (Test 11)..... 87

Figure 95. Hole in Top of Foam Support (Test 11) 87

Figure 96. Depth of Dent in Pipe (Test 11) 88

Figure 97. Length of Dent in Pipe (Test 11)..... 88

Figure 98. Pressure-Time Histories, xx-lb C4 Charge at 12-in Standoff from Water-Filled Bare Pipe (Test 11)..... 89

Figure 99. C4 Charge in Contact with Bare Pipe (Test 12)..... 89

Figure 100. Length of Hole in Pipe (Test 12)..... 90

Figure 101. Width of Hole in Pipe (Test 12) 90

Figure 102. Detail of Hole in Pipe (Test 12) 90

Figure 103. Water-Filled Pipe, xx-lb C4 Contact Charge (Test 12), at Time = 0 s..... 91

Figure 104. Water-Filled Pipe, xx-lb C4 Contact Charge (Test 12) at Time = 0.4369 s..... 91

Figure 105. Pressure-Time Histories, xx-lb C4 Contact Charge on Water-Filled Bare Pipe (Test 12)..... 92

Figure 106. Clam-Shell Installation of SEFRC Cover System..... 93

Figure 107. SEFRC Pipe Cover System, Installed on Pipe Specimen (Test 13)..... 93

Figure 108. C4 Charge Placed at Hinge-Cover Joint (Test 13) 94

Figure 109. Width of Hole in SEFRC Cover, No Breach of Pipe (Test 13)..... 94

Figure 110. Depth of Hole in SEFRC Cover, No Breach of Pipe (Test 13)..... 94

Figure 111. Pressure-Time Histories, xx-lb C4 Contact Charge on SEFRC Pipe Cover (Test 13) 95

Figure 112. Protective Jacket Concept Proposed by WinTec Security 95

Figure 113. Pre-Detonation Condition of Pipe Jacket (Test 14)..... 96

Figure 114. Charge Placed on Pipe Jacket (Test 14) 96

Figure 115. Post-Detonation Condition of Pipe Jacket (Test 14)	97
Figure 116. Length of Hole in Jacket-Covered Pipe (Test 14)	97
Figure 117. Width of Hole in Jacket-Covered Pipe (Test 14)	97
Figure 118. Depth of Hole in Jacket-Covered Pipe (Test 14).....	98
Figure 119. Steel Plug from Jacket-Covered Pipe (Test 14)	98
Figure 120. Pressure-Time Histories, xx-lb C4 Contact Charge on Pipe Jacket (Test 14).....	98
Figure 121. FRP Installation on Pipe (Test 15)	99
Figure 122. FRP Installed on Pipe Specimen (Test 15).....	99
Figure 123. C4 Charge in Contact with FRP BMT (Test 15).....	99
Figure 124. Length of Hole in FRP-Covered Pipe (Test 15).....	100
Figure 125. Width of Hole in FRP-Covered Pipe (Test 15)	100
Figure 126. Depth of Hole in FRP-Covered Pipe (Test 15)	100
Figure 127. Pressure-Time Histories, xx-lb C4 Charge on FRP Layer (Test 15).....	101
Figure 128. Polyurea Coating Installation (Test 16).....	101
Figure 129. Ductile Coating with Placed Charge (Test 16).....	102
Figure 130. Length of Hole in Polyurea-Coated Pipe (Test 16).....	102
Figure 131. Width of Hole in Polyurea-Coated Pipe (Test 16)	102
Figure 132. Depth of Hole in Polyurea-Coated Pipe (Test 16).....	103
Figure 133. Pressure-Time Histories, xx-lb C4 Contact Charge on Polyurea Coating (Test 16).....	103
Figure 134. Depth of Dent Pipe (Test 17).....	104
Figure 135. Length of Dent in Pipe (Test 17).....	104
Figure 136. Pressure-Time Histories, xx-lb C4 Charge at 12-in Standoff from Nitrogen-Filled Bare Pipe (Test 17)	105
Figure 137. Top Hole in Pipe (Test 18)	106
Figure 138. Bottom Hole in Pipe (Test 18).....	106
Figure 139. Detail of Bottom Hole in Pipe (Test 18)	106
Figure 140. Nitrogen-Filled Pipe, xx-lb C4 Contact Charge (Test 18) at Time = 0 s	107
Figure 141. Nitrogen-Filled Pipe, xx-lb C4 Contact Charge (Test 18) at Time = 0.2150 s	107
Figure 142. Pressure-Time Histories, xx-lb C4 Contact Charge on Nitrogen-Filled Bare Pipe (Test 18).....	108
Figure 143. Width of Hole in SEFRC Cover, No Breach of Pipe (Test 19).....	109
Figure 144. Depth of Hole in SEFRC Cover, No Breach of Pipe (Test 19).....	109
Figure 145. Pressure-Time Histories, xx-lb C4 Contact Charge on SEFRC Pipe Cover (Test 19)	110
Figure 146. Length of Hole in Jacket-Covered Pipe (Test 20)	110
Figure 147. Width of Hole in Jacket-Covered Pipe (Test 20)	111
Figure 148. Bottom of Hole in Jacket-Covered Pipe (Test 20)	111
Figure 149. Post-Detonation Condition and Location of Pipe Jacket (Test 20).....	111
Figure 150. Pressure-Time Histories, xx-lb C4 Contact Charge on Pipe Jacket (Test 20).....	112
Figure 151. Typical Valve Specimen (Side Elevation View).....	114
Figure 152. Location of C4 Charge for Bare Valve Test (Test 21)	116
Figure 153. Detail of Location of C4 Charge for Bare Valve Test (Test 21).....	116
Figure 154. Location of Instrumentation in Valve Test 21 (Plan View)	117
Figure 155. Holes in Bare Valve (Test 21).....	118
Figure 156. Hole Detail in Bare Valve (Test 21).....	118
Figure 157. Hole Detail in Bare Valve (Test 21).....	118

Figure 158. Water-Filled Bare Valve, xx-lb C4 Contact Charge (Test 21) at Time = 0 s.....	119
Figure 159. Water-Filled Bare Valve, xx-lb C4 Contact Charge (Test 21) at Time = 0.123 s...	119
Figure 160. Pressure-Time Histories, xx-lb C4 Contact Charge on Bare Valve (Test 21).....	120
Figure 161. Pre-Test Condition of Valve SEFRC BMT, xx-lb Charge (Test 22)	120
Figure 162. Location of Instrumentation in Valve Test 22 (Plan View)	121
Figure 163. Post-Detonation Condition of Valve SEFRC BMT (Test 22).....	122
Figure 164. Width of Hole in SEFRC BMT, No Breach of Valve (Test 22)	122
Figure 165. Height of Hole in SEFRC BMT, No Breach of Valve (Test 22)	122
Figure 166. Post-Detonation Mark on Face of Valve, No Breach (Test 22)	123
Figure 167. Pre-Test Condition of Valve SEFRC BMT, ww-lb Charge (Test 22B).....	123
Figure 168. Location of Instrumentation in Valve Test 22B (Plan View).....	124
Figure 169. Post-Detonation Condition of Valve SEFRC BMT (Test 22B)	125
Figure 170. Width of Hole in SEFRC BMT, No Breach of Valve (Test 22B).....	125
Figure 171. Height of Hole in SEFRC BMT, No Breach of Valve (Test 22B).....	125
Figure 172. Post-Detonation Mark on Face of Valve, No Breach (Test 22B).....	126
Figure 173. Pressure-Time Histories, ww-lb C4 Charge in Contact with SEFRC Valve Cover (Test 22B)	126
Figure 174. Pre-Test Condition of Valve BMT (Test 23)	127
Figure 175. Location of Instrumentation in Valve Test 23 (Plan View)	127
Figure 176. Post-Detonation Condition of Valve BMT (Test 23).....	128
Figure 177. Width of Hole in BMT (Test 23).....	128
Figure 178. Height of Hole in BMT (Test 23).....	129
Figure 179. Detail of Valve Breach (Test 23).....	129
Figure 180. Pressure-Time Histories, xx-lb C4 Charge in Contact with WinTec Protective Structure (Test 23)	130
Figure 181. Decommissioned Compressor Cylinder as Witness Element	131
Figure 182. yy-lb C4 Charge	132
Figure 183. yy-lb C4 Charge Placed Prior to Detonation.....	132
Figure 184. zz-lb C4 Charge.....	133
Figure 185. Corrugated-Steel Retaining Structure.....	134
Figure 186. First Course of Structure Filled with Sand.....	134
Figure 187. Pre-Test Metalith™, Blast-Loaded Side (Test 31).....	135
Figure 188. Pre-Test Metalith™, Back Side (Test 31)	135
Figure 189. Elevation of yy-lb Charge (Test 31).....	135
Figure 190. Location of Instrumentation in Protective Structure Test 31 (Plan View).....	136
Figure 191. Post-Detonation Blast-Loaded Side (Test 31).....	137
Figure 192. Post-Detonation Blast-Loaded Side Detail (Test 31)	137
Figure 193. Post-Detonation Back Side (Test 31)	137
Figure 194. Post-Detonation Witness Element (Test 31)	138
Figure 195. Pressure-Time Histories, yy-lb C4 Contact Charge on Metalith™ Protective Structure (Test 31)	138
Figure 196. Pre-Test Metalith™, Blast-Loaded Side (Test 32).....	139
Figure 197. Elevation of zz-lb Charge (Test 32)	139
Figure 198. Location of Instrumentation in Protective Structure Test 32 (Plan View).....	140
Figure 199. Post-Detonation Blast-Loaded Side (Test 32).....	141
Figure 200. Post-Detonation Back Side (Test 32)	141

Figure 201. Post-Detonation Witness Element (Test 32)	141
Figure 202. Pressure-Time Histories, zz-lb C4 Contact Charge on Metalith™ Protective Structure (Test 32)	142
Figure 203. ICB Protective Structure Panel Configuration	143
Figure 204. Blast-Loaded Side of ICB Panel Structure (Test 33)	143
Figure 205. Back Side of ICB Panel Structure (Test 33).....	144
Figure 206. Location of Instrumentation in Protective Structure Test 33 (Plan View).....	144
Figure 207. Post-Detonation Blast-Loaded Side (Test 33).....	145
Figure 208. Post-Detonation Back Side (Test 33)	145
Figure 209. Breach of Witness Element Plate (Test 33).....	146
Figure 210. Pressure-Time Histories, yy-lb C4 Contact Charge on ICB Protective Structure (Test 33)	146
Figure 211. Target Region on Surface of SEFRC Layer (Test 41)	150
Figure 212. Gantt Chart for SEFRC Cover (Test 41)	151
Figure 213. Torching of Exterior Steel Layers (Test 41).....	151
Figure 214. Torching of Fiber-Reinforced Concrete Layer (Test 41)	152
Figure 215. Chipping Dross away with Hammer and Chisel (Test 41).....	152
Figure 216. Torching of Bottom Steel Layer (Test 41)	152
Figure 217. Minimum 6-in x 6-in Hole in SEFRC Cover (Test 41).....	153
Figure 218. Target Region on Surface of FRP Layer (Test 43).....	153
Figure 219. Gantt Chart for FRP Cover (Test 43)	154
Figure 220. Removal of FRP Layer with Axe (Test 43).....	155
Figure 221. Removal of FRP Layer with Circular Saw and Wrecking Bar (Test 43).....	155
Figure 222. Minimum 6-in x 6-in Hole in FRP Layer (Test 43)	155
Figure 223. Gantt Chart for Polyurea Coating (Test 44)	157
Figure 224. Scoring of the Polyurea Coating (Test 44)	157
Figure 225. Removal of Polyurea Coating with Chisel and Hammer (Test 44).....	158
Figure 226. Minimum 6-in x 6-in Hole in Polyurea Coating (Test 44).....	158
Figure 227. Erection of Red Oak Planks in Metalith™ Cavity (Test 45).....	159
Figure 228. Gap of 6-in between Red Oak and Corrugated Steel Layer (Test 45).....	159
Figure 229. Gantt Chart for Metalith™ with Red Oak (Test 45)	160
Figure 230. Torch Burning Front Wall (Test 45)	160
Figure 231. Circular Saw Cutting the Panel (Test 45).....	161
Figure 232. Removal of Sand from Cavity (Test 45)	161
Figure 233. Torching Back Panel (Test 45).....	161
Figure 234. Man-Passable Hole in Back Wall (Test 45)	162
Figure 235. Gantt Chart for Metalith™ with No Red Oak (Test 45B).....	163
Figure 236. Removal of Sand from Barrier Cavity (Test 45B)	164
Figure 237. Ingress into Barrier Cavity (Test 45B)	164
Figure 238. Man-Passable Hole in Back Wall (Test 45B).....	164

List of Tables

Table 1. Summary of Blast Mitigation Technologies by Category	12
Table 2. Summary of PHMSA Geometry Data for Natural Gas Transmission Line	13
Table 3. Summary of PHMSA Geometry Data for Crude Oil Line	21
Table 4. Summary of Properties Common to the Eight Simulations.....	27
Table 5. Summary of Results from Bulk Explosive Simulations	32
Table 6. Summary of Protection Priority for Pipeline Components.....	41
Table 7. Summary of Possible Assessments by Blast Mitigation Technology and Threat	48
Table 8. Reduced Simulation Matrix for Contact Charge Threat	49
Table 9. LS-DYNA Material Constants for Pipeline Component (*MAT_PIECEWISE_LINEAR_PLASTICITY).....	54
Table 10. Simulation Results for Bare Pipe.....	54
Table 11. LS-DYNA Material Constants for CFRP (*MAT_ELASTIC).....	58
Table 12. Simulation Results for CFRP.....	59
Table 13. LS-DYNA Material Constants for SRT Continuum Material (*MAT_PIECEWISE_LINEAR_PLASTICITY).....	60
Table 14. Simulation Results for SRT	61
Table 15. LS-DYNA Material Constants for Inner and Outer Steel (*MAT_PIECEWISE_LINEAR_PLASTICITY).....	62
Table 16. LS-DYNA Material Constants for Perlite (*MAT_SOIL_AND_FOAM).....	65
Table 17. LS-DYNA Material Constants for Polyurea (*MAT_PLASTIC_KINEMATIC)	67
Table 18. Simulation Results for Polyurea	68
Table 19. Source Characterization Test Matrix	76
Table 20. Typical Capped Pipe Segment Properties.....	83
Table 21. Pipe Test Matrix.....	85
Table 22. Summary of Pipe Contact Charge Tests	113
Table 23. Typical Capped Pipe Segment Properties.....	114
Table 24. Valve Contact Charge Tests	115
Table 25. Summary of Valve Tests.....	130
Table 26. Protective Structure Contact Charge Tests	133
Table 27. Summary of Protective Structure Tests	147
Table 28. Test Matrix for Anti-Tamper Tests.....	148
Table 29. Anti-Tamper Test Results.....	165
Table 30. Summary of Test Results.....	166

Pipeline Blast Mitigation Technologies: Phase 1

1 Phase 1 Introduction

Pipelines are an extensive and critical part of the nation's infrastructure. Nationwide, there are 320,500 miles of natural gas transmission line and 168,900 miles of hazardous liquid line. Lines for local distribution of natural gas total 2.2 million miles.¹ Nearly all natural gas and 65% of hazardous liquids are transported by pipelines. Natural gas provides over 25% of residential and industrial energy needs, while oil products provide 97% of the energy used for transportation. In total, 62% of the energy used in the US is derived from these two sources.²

Despite the importance of pipeline systems, there are few technologies for mitigating their vulnerabilities to explosive attack. To address this need, the Technical Support Working Group (TSWG) contracted Protection Engineering Consultants (PEC) to perform the following three tasks (Contract no. N41756-09-C-4602):

1. Survey of existing research and technology proposed specifically for blast protection of pipelines (*Survey of Existing Technology and Research*, submitted October 15, 2009);
2. Identification and assessment of the vulnerability of pipeline systems and infrastructure (*Pipeline Vulnerability Assessment* submitted December 3, 2009);
3. Assessment of blast mitigation technologies for pipeline protection using analytical and numerical simulations (*Assessment of Blast Mitigation Technologies* submitted January 28, 2010).

The results of Task 1 were submitted in the *Survey of Existing Technology and Research* report which is reproduced as Section 2 in this report. In Section 2, the basic concept of each blast mitigation technology is discussed, the threats they defeat or mitigate are identified, and any tests conducted to support of the vendors' claim are noted. Also, the technologies are organized into five broad groups based on expected mechanical contribution to the pipeline: stiff reinforcement, independent barrier, dependent barrier, crushable layer, and ductile layer.

The results of Task 2 were submitted in the *Pipeline Vulnerability Assessment* report; Task 2 results are Section 3 of this report. To assess vulnerabilities, the basic components and the overall pipeline system are described generically, both for natural gas and liquid lines. General pipeline vulnerabilities, inherent resistance of pipelines to attack, and specific explosive threats applicable to pipelines are then characterized. Finally, the consequences of pipeline failure are examined, both by component and by line type, to establish protection priorities.

In Task 3, the technologies identified in Task 1 for mitigating the vulnerabilities discussed in the Task 2 report were evaluated with analytical and numerical simulations. The Task 3 results are presented in Section 4 of this report.

2 Task 1: Survey of Existing Technology and Research

In this section:

- Existing pipeline blast mitigation technologies are identified;
- The basic concept of each blast-mitigating technology is discussed;

- The threats that they defeat or mitigate are identified;
- The tests that have been conducted to support the vendors' claims are noted.

This report focuses on the expected mechanical contribution of a given technology to the pipeline component it is protecting. Therefore, the blast mitigation technologies are organized into five broad groups, based on expected mechanical contribution:

- Stiff reinforcement
- Independent barrier
- Dependent barrier
- Crushable layer
- Ductile layer

Much of the information reported here was obtained directly from the vendors. Any content without a citation was obtained in this manner. Content obtained in any other way is cited accordingly.

2.1 Stiff Reinforcement

In this approach, the outer wall of the pipeline component is reinforced with a relatively stiff and strong material that increases the strength of the component. The effect of the stiff reinforcement on strength is conceptually illustrated in Figure 1. An increase in ultimate strength results from adding the reinforcing material thickness to the thickness of the component wall.

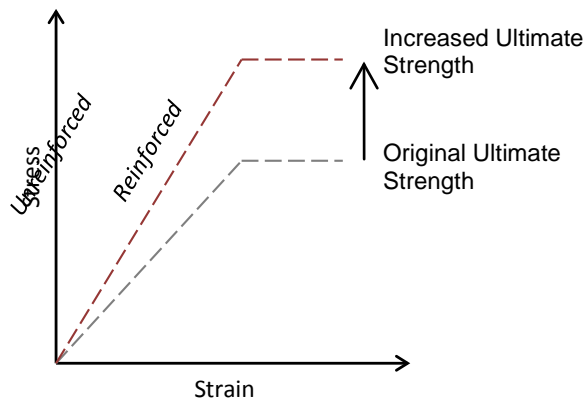


Figure 1. Effect of Adding Stiff Reinforcement on Ultimate Strength

2.1.1 Fiber-Reinforced Polymer

One type of stiff reinforcement is fiber-reinforced polymer (FRP). FRP is a composite material of glass, carbon, or Kevlar™ fibers within a resin matrix. For installation, a structural member is wrapped in a resin-saturated mesh of the fiber and then the liquid epoxy is applied over the mesh. The polymer cures to form a stiff composite layer on the member. This process is shown in Figure 2, where a reinforced concrete column is being retrofitted with FRP. Another installation

approach involves a pre-cured laminate that is simply bonded to the surface of the structure with epoxy.³

FRP has in recent years gained acceptance as a structural reinforcement to increase seismic resistance. One supplier of FRP products, QuakeWrap™ Inc has tested the effectiveness of its product for structural blast mitigation.⁴ In that case, the product was applied to unreinforced masonry walls, but the testing has not included blast mitigation for pipelines.



Figure 2. Installation of FRP on Reinforced Concrete Column⁵

2.1.2 Steel-Reinforced Thermoplastic

Hardwire® LLC has proposed using a high-strength steel mesh embedded in a thermoplastic resin to provide general structural hardening. This concept is similar to FRP, but instead of glass fibers, the embedded reinforcement is 450,000-psi steel mesh. An example of Hardwire® mesh is shown in Figure 3. This steel can be embedded in a variety of resins.⁶



Figure 3. Example of Hardwire® Steel Mesh⁷

Another hardening solution proposed by Hardwire® is their high-strength steel mesh or Dyneema® (a high-strength fiber) integrated with Gorilla™ tape. This product may be wrapped around a pipeline component to harden it.

Hardwire® has developed composite armor for military vehicles, techniques for hardening domestic infrastructure, and blast-resistant panels. A Hardwire® representative noted that these products have been subjected to blast testing at Hardwire®'s in-house test facility. The results from these tests were not made available and, thus, are not discussed here.

2.2 Independent Barrier

An independent barrier is one that is structurally independent of the pipeline component it is protecting. There is no structural integration as was observed with the stiff reinforcement. The barrier simply shields the pipeline from the blast and likely sustains significant damage while doing so. The pipeline is intended to remain in its pre-blast condition.

2.2.1 Steel-Clad Earthen Barrier

Infrastructure Defense Technologies (IDT) has proposed a steel-clad earthen barrier to protect the pipeline, called the Metalith™. This barrier is illustrated in Figure 4. In this approach, corrugated steel cladding is erected and then filled with soil. The compartments for containing the earth are illustrated in Figure 5. The steel panels and soil are intended to prevent significant blast impulse, fragments, and projectiles from reaching the pipeline.

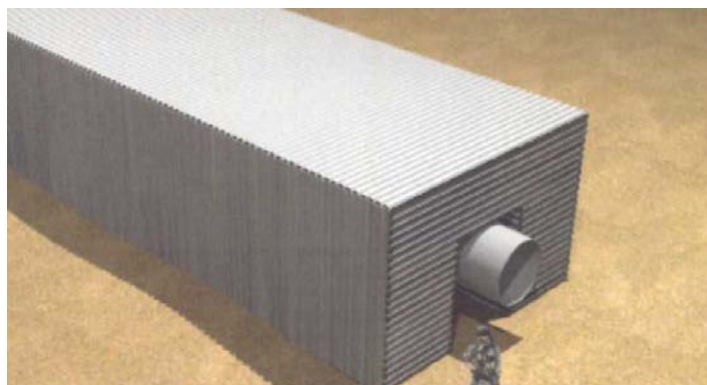


Figure 4. Proposed Metalith™ Barrier for Pipeline Protection⁸



Figure 5. Corrugated-Steel Compartments for Earth⁹

IDT has not tested its barrier system to protect pipelines. However, the company has conducted blast tests on its barriers in a stand-alone configuration, as well as vehicle crash tests. The blast

tests included two detonations near five Metalith™ structures, the first detonation with a charge weight that could be carried by a 15-passenger van, the second with one that could be carried by a minivan. The positions of the charges are shown in Figure 6.

In the first test, the center walls of the 20-foot-standoff and 40-foot structures buckled but permitted no through penetration of shrapnel. The 80-foot and 160-foot structures remained intact structurally and permitted no through penetration. In all cases, blast attenuation (drop in overpressure from blast side to the back side) was at least 90%. In the second test, the center, blast wall buckled, but the structure permitted no through penetration, and the blast attenuation was 99%.

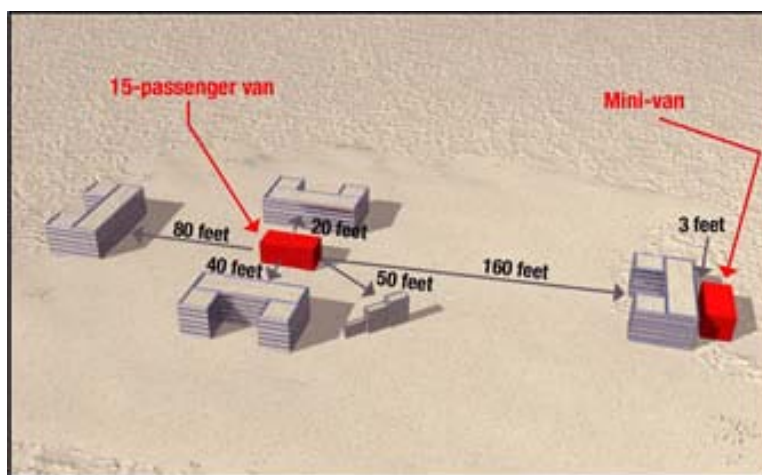


Figure 6. Explosive Tests Conducted on Metalith™ Barriers¹⁰

2.2.2 Lightweight Blast-Resistant Panels

Armor Designs, a subsidiary of Hawthorne & York International, has developed a lightweight panel barrier system. Like IDT, Armor Designs markets their system as a general barrier that could be used for any structure, including pipes, valve stations, manifolds, etc. to protect against blast and ballistic attack. Advertised advantages of the Armor Designs panel system are the following:

- Flexibility of design;
- Easily installed as a retrofit;
- Modular panel replacement in the event of damage to a portion of the barrier;
- Installation without heavy equipment.¹¹

An Armor Designs representative stated that the barrier system has been subjected to blast tests in which it was protecting a pipeline, but data and test results cannot be released due to proprietary agreements. PEC attempted to obtain additional information about the barrier system, but was unsuccessful.

2.3 Dependent Barrier

Like an independent barrier, the primary function of a dependent barrier is to shield the pipeline component from threats, whether blast, ballistic, or physical attack. Unlike the independent barrier, a dependent barrier is structurally dependent on the pipeline; it is not free-standing. The barrier is either mechanically fastened or adhered to the pipeline.

2.3.1 Fiber-Reinforced Concrete

Composite Technologies has developed a pipeline cover system consisting of outer and inner steel layers, separated by a very high-strength concrete core. For this assessment, the product was referred to as steel-enclosed fiber-reinforced concrete (SEFRC). The concrete is placed in forms designed for a specific diameter of pipe and then installed in a “clam-shell” method, as shown in Figure 7, where only the frame portion is shown. The cover is then fixed in place with concealed tamper-resistant fasteners.



Figure 7. Clam-Shell Installation of SEFRC Pipe Cover Frame¹²

Composite Technologies reports that they have performed extensive modeling and testing of their product, including:

- Blast testing;
- Ballistic testing;
- Resistance to chop-saw attack;
- Resistance to thermal attack, such as torching;
- Resistance to sledgehammer impact;
- Fire testing;
- Environmental durability testing.

According to the manufacturer, a diamond-shaped contact charge was placed on the surface of an SEFRC barrier that covered a steel cable and the cable survived but with some deformation. The

tested cable was not under tension, and Composite Technologies expects that a tensioned cable would have exhibited little deformation.

2.3.2 Protective Jacket

WinTec Security reported the development of a protective jacket designed to defeat ballistic and portable drill threats. This product has been classified as a barrier, but it also has attributes of a ductile coating, discussed below, due to the bonding agent that adheres to the pipe.

A sleeve that is slipped over the pipeline and secured, as shown in Figure 8, is intended to provide the protection. Tightening of the fastener releases a bonding agent that joins the sleeve to the pipe, providing self-sealing capabilities. This bonding agent is intended to provide structural reinforcement.

WinTec Security has stated that the jacket is designed to defeat ballistic threats by permitting the rounds to penetrate the pipe and then providing sealing around the resulting hole. According to WinTec, these calibers can be defeated even for high-pressure pipelines:

- 7.62 x 39 mm
- 7.62 x 51 mm
- 7.62 x 54 mm
- Up to .50 Cal M-2 ball

The jacket is designed to defeat a portable drill threat with an outer proprietary protective layer that stops the drill bit. Material within the jacket seizes the drill bit to prevent further rotation.¹³



Figure 8. Protective Jacket Concept proposed by WinTec Security¹⁴

2.4 Crushable Layer

In this approach, a layer of crushable material is installed on the surface of the pipeline component. Failure of that material during a blast event is expected to reduce the peak pressures applied to the component and thereby reduce the likelihood of penetration.

BlastGard® has proposed its crushable material BlastWrap™ for pipeline blast mitigation. BlastWrap™ is heat-treated perlite (a volcanic glass) contained within 3-in compartments, as shown in Figure 9. The compartments are composed of flexible films, and they also contain fire-quenching admixtures for suppressing the blast fireball. BlastGard® states that their product has the following advantages:

- Reduces blast impulse and pressure;
- Quenches fireballs and post-blast fires;
- Prevents sympathetic detonation;
- Highly durable in extreme environments;
- Scalable and adaptable to most structural geometries;
- Lightweight;
- Non-toxic and ecologically friendly.¹⁵



Figure 9. BlastWrap™ Sample¹⁶

BlastGard® has performed blast tests on a section of pipeline. Three tests were performed, one test on an unprotected pipe, one test with a 3-in layer of BlastWrap™, and one with a 6-in layer of BlastWrap™. The pipe segment had a diameter of 24-in and a 0.375-in wall thickness; the threat was an xx-lb C4 charge. In the first test, with the charge in intimate contact with the pipe, an 8-in diameter breach was created. For the 3-in and 6-in standoffs, the pipe was dented but did not fail.¹⁷

2.5 Ductile Layer

For this approach, a ductile material is applied to the exterior surface of the pipeline component. The material can either be sprayed on or installed in sheets. Vendors of these ductile materials claim two advantages from installing the material on a given structure:

- The composite structure (original component plus ductile layer) has greater resistance to localized penetration and perforation, decreasing the likelihood of fragmentation;
- The ductile material is self-sealing and thereby prevents loss of liquid material in the event of perforation.

2.5.1 Polyurea Coating

A spray-on polyurea coating has been proposed by Specialty Products Inc. (SPI). SPI markets its polyurea elastomer coating for pipeline blast mitigation as Dragonshield BC™.

SPI participated in a set of demonstrations at the 2007 Nevada Automotive Test Center Technology Rodeo that illustrate the blast-mitigating properties of its coating. In that demonstration, aluminum panels 36-in x 36-in x 0.75-in, with and without polyurea coatings, were subjected to close-in blast loading. The post-blast condition of the coated panels was compared to that of the uncoated panels. The coated panels were reported to exhibit significantly less deformation and penetration.

SPI has also tested the self-sealing capacity of its material. The material was installed on Humvee doors, which were then fired upon using a common military round. The material was observed to rapidly seal the holes such that they were nearly undetectable.

SPI has also examined the effect of their material on the response of masonry walls, where the polyurea is sprayed on the interior (non-blast-loaded) side of a masonry wall to provide ductile reinforcement.

2.5.2 Polyurethane Coating

BASF advertises a polyurethane coating for blast mitigation but technical details beyond the limited information on its website were not available.¹⁸ BASF also produces a steel-polyurethane-steel composite that is commonly installed on ocean-going vessels. That material has been subjected to impact testing, but it is unclear how it could be used as a retrofit for a pipeline. Additional details of relevant testing were not obtained.

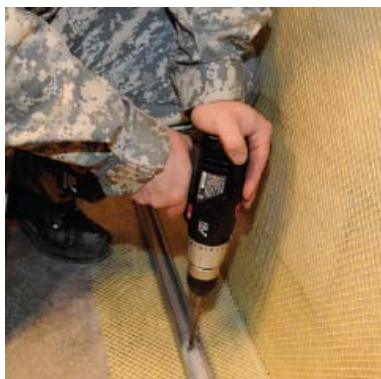
2.5.3 General Polymer Coating

Two companies, DefensTech International Inc and Mid-American Group, both advertise polymer coatings for blast mitigation. DefensTech states that they have performed blast tests on pipeline segments, but the details of the tests were not obtained.

Mid-American Group has not performed blast tests on pipeline segments but has performed hydrostatic tests. The intent of those tests was to show their coating's effect on the structural response of the pipe when subjected to internal hydrostatic pressure. For those tests, a pipeline segment was capped at both ends, coated with their material, and then pressurized. Additional details of the testing were not obtained.

2.5.4 Fiber-Reinforced Polyurethane

Berry Plastics™ advertises a fiber-reinforced polyurethane called the X-Flex™ Protection System. The fiber is aramid, which is commonly used in a stiff epoxy matrix to form a structural composite. The X-Flex™ System is a ductile material because polyurethane serves as its matrix. It is installed in sheets like wall paper, as shown in Figure 10. The fiber is then anchored to the floor and ceiling slabs, adjacent to the wall, as shown in Figure 11.

Figure 10. X-Flex™ Installation Process¹⁹Figure 11. X-Flex™ Floor Anchoring²⁰

X-Flex™ has been blast tested when installed as a retrofit on a masonry wall. Berry-Plastics™ has suggested that X-Flex™ System could be used for pipeline retrofits but has conducted no testing. Durability testing has included heat and humidity testing. The current formulation of the polyurethane is not flame-retarding, but Berry is developing a flame-retardant version.

2.6 Summary Table

Table 1 is a summary of the blast mitigation technologies discussed in the previous sections. The table includes the categories and subcategories, vendor, product name if available, and the website of each technology.

Table 1. Summary of Blast Mitigation Technologies by Category

Category	Subcategory	Vendor	Product Name	Website
Stiff Reinforcement	Fiber-Reinforced Polymer	QuakeWrap™		http://www.quakewrap.com/
	Steel-Reinforced Thermoplastic	Hardwire™		http://www.hardwirellc.com/
Independent Barrier	Steel-Clad Earthen Barrier	Infrastructure Defense Tech.	Metalith™	http://www.themetalith.com/index.html
	Light-Weight Blast-Resistant Panels	Armor Designs, Inc.		http://www.armordesigns.com/products-energy.html
Dependent Barrier	Fiber-Reinforced Concrete	Composite Technologies		http://www.composite-technologies.com/blast.html
	Protective Jacket	WinTec Security	Pipe Jacket	http://www.wintecusa.com/pipeline_protection.html
Crushable Layer	Compartmentalized Heat-Treated Perlite	BlastGard®	BlastWrap™	http://www.blastgardintl.com/
Ductile Layer	Polyurea Coating	Specialty Products Inc.	Dragonshield BC™	http://www.specialty-products.com/index.php?page=dragonshield-bc
	Polyurethane Coating	BASF		http://www2.basf.us/urethanechemicals/Specialty_Systems/sm_index.html
	Polymer Coating	DefensTech Int. Inc.		http://www.defenstech.com/
		Mid-American Group	Line-X	http://www.midamericangroup.com/xperts.html
	Fiber-Reinforced Polyurethane	Berry Plastics™	X-Flex™	http://www.xflexsystem.com/content.aspx?page=company

3 Task 2: Pipeline Vulnerability Assessment

For Task 2, the vulnerabilities of pipeline systems to explosive attack were assessed. The goals were to identify the components of a pipeline system that are vulnerable to explosive attack; evaluate the level of vulnerability in terms of qualitative and quantitative measures; and prioritize those vulnerabilities based on the consequences of an attack.

Toward that end, the basic components and the overall pipeline system are described generically in Section 3.1 and 3.2, for natural gas and liquid lines respectively. The vulnerability of pipeline components to explosive threats and the specific explosive threats that could be applied to a pipeline are discussed in Section 3.3. The consequences of pipeline failure are examined in Section 3.4, both by component and by line type, to establish priorities for protecting the components. Finally, conclusions from the assessment are drawn in Section 3.5.

3.1 Natural Gas Pipeline

3.1.1 Basic Components

3.1.1.1 Line Pipe

Line pipe is generally characterized by diameter, wall thickness, and pipe grade, with associated minimum yield strength. The diameter of a gas transmission line ranges from 20 to 42-in²¹, but it can be as large as 48-in. A common flow speed on a gas line is 70 feet per second, and the flow capacity of a large line can be 1 billion cubic feet per day. In some cases, a gas line is composed of multiple lines in parallel that have been installed over time to increase capacity.²²

To estimate average wall thicknesses, maximum operating pressures, and minimum yield strengths, data was obtained from the Pipeline and Hazardous Materials Safety Administration (PHMSA).²³ A statistical summary of the results is provided in Table 2.

Table 2. Summary of PHMSA Geometry Data for Natural Gas Transmission Line

Parameter	Average Reported	Minimum Reported	Maximum Reported
Wall thickness [in]	0.36	0.13	1.25
Maximum Allowable Operating Pressure [psi]	1,030	60	3,640
Specified Minimum Yield Strength [psi]*	48,500	24,000	70,000

**Values greater or less than these minimum and maximum values were reported in the data, but they are considered spurious and are not included in this table.*

3.1.1.2 Valve

There are a variety of valve mechanisms used in the pipeline industry, but three common types are the ball, plug, and check mechanisms. The ball valve mechanism is shown in Figure 12. The

mechanism includes a ball with a port through it along one axis. In the open orientation, the axis of the port is aligned with the direction of flow, and liquid can pass through the valve. In the closed orientation, that axis is perpendicular to flow, and the ball blocks the flow of the liquid. A side elevation view of a ball valve is shown in Figure 13.



Figure 12. Ball Valve Mechanism²⁴



Figure 13. Side Elevation View of Ball Valve²⁵

Figure 14 is a photograph of a plug valve. Its mechanism consists of a cylindrical or conical plug that can be raised or lowered in the valve cavity to permit or block flow.



Figure 14. Plug Valve²⁶

An example of a check valve is shown in Figure 15. Check valves permits flow in only one direction. There are many methods for restricting flow directionally, and these include spring-loaded balls or pivoting spring-loaded mechanisms.



Figure 15. Check Valve²⁷

Common practice is to match the design pressure of the valve to that of the line pipe. In that case, the wall thicknesses of the valve and line pipe are comparable. However, depending on valve availability at the time of installation, the walls of the valves may be thicker than the line pipe. In most cases, the thickness of the line pipe wall can be taken as a lower limit for the thickness of the valve wall.

3.1.1.3 Manifold

Pipeline manifolds are combinations of pipe, valves, flanges, and fittings, assembled for a specific purpose or application. They permit and manage flow among intersecting pipelines. An example of a manifold is shown in Figure 16. Depending on application, manifolds can cover a variety of areas, but component diameters will be comparable to those of the line they join, from 20-in to 48-in.



Figure 16. Pipeline Manifold

3.1.1.4 Compressor

A wide array of compressors can be used to maintain pipeline pressurization. Gas turbine centrifugal, electric motor centrifugal, and gas engine reciprocating compressors are shown respectively in Figure 17 through Figure 19. In the past, compressors were almost solely powered by gas extracted from the line itself, but recent regulation has mandated use of compressors powered by electric motors.

In contrast to liquid pumps, as discussed below in Section 3.2.1.2, PEC was not able to obtain the location and magnitude of the minimum wall thickness for a typical compressor due to proprietary restrictions. However, discussion with personnel in the compressor industry revealed that the most vulnerable part of a compressor to be cross head guide assembly, shown in Figure 20. Each compression cylinder is joined to the crankshaft via the cross head guide assembly, and damage to this assembly would necessitate costly and time-consuming repair to the compressor.

Figure 17. Centrifugal Compressor: Gas Turbine²⁸



Figure 18. Centrifugal Compressor: Electric Motor²⁹



Figure 19. Reciprocating Compressor: Reciprocating Gas Engine³⁰

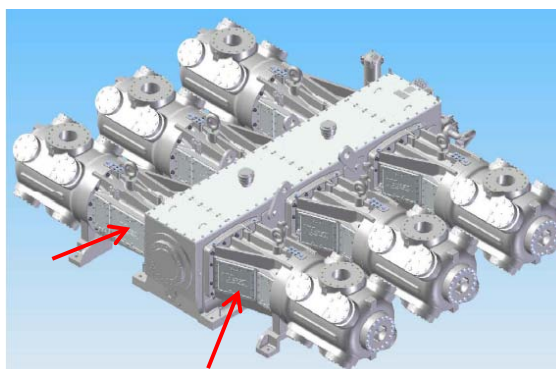


Figure 20. Location of Cross Head Guide Assembly³¹

3.1.2 Stations

Gas pipeline stations are assemblages of the components discussed in Section 3.1.1, along with any instrumentation specific to that station type. There are four main types of station: compressor, block valve, metering, and maintenance, as discussed in the following sections. In general, these stations are installed aboveground for ease of access during maintenance. They also tend to be located in remote areas with minimal access control and little surveillance.

3.1.2.1 Compressor Station

Compressor stations are spaced 50 to 100-miles along the line.³² The pressure drop from one station to the next is generally from 1000-psig to 500-psig. The capacity of a compressor station is set by the flow rate of the line, and consequently, a compressor station can vary in size

significantly. Figure 21 is a photograph of a large compressor station, and it includes labels of the constitutive parts.

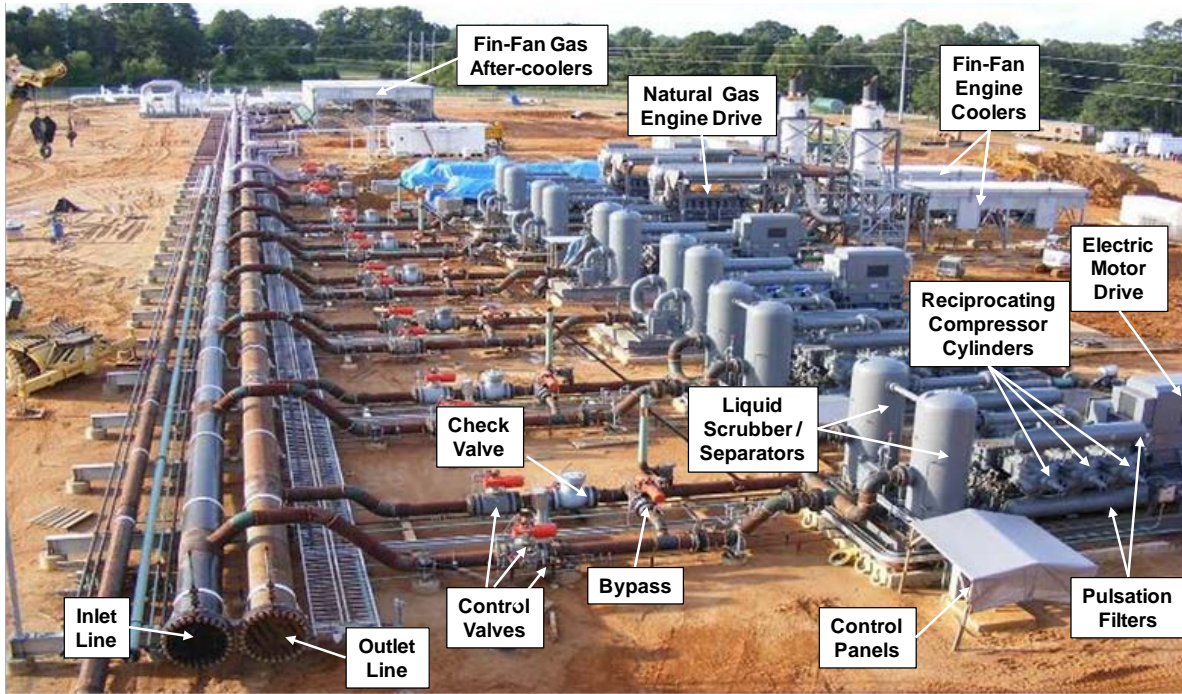


Figure 21. Large Natural Gas Compressor Station³³

3.1.2.2 Metering Station

Metering stations are commonly near compressor stations for ease of operation and maintenance. Their purpose is to measure the volume of gas that has passed through the line over a given time period. Station size depends upon the size of the associated line. Small and large metering stations are shown in Figure 22 and Figure 23, respectively.



Figure 22. Small Metering Station³⁴



Figure 23. Large Metering Station³⁵

3.1.2.3 Block Valve Station

Block valves stop flow during emergencies and scheduled maintenance, and their mechanisms can include ball or plug. They are spaced every 5-miles in populated areas, and 20-miles elsewhere, commonly as part of a larger station. In some cases, they are located separate from a station, in a standalone configuration.³⁶

3.1.2.4 Maintenance Station

Pig stations permit ingress and egress of diagnostic devices known as pigs. These devices travel along the line cleaning it or inspecting it for structural deficiencies. An example of a pig station with pig launcher is shown in Figure 24.

Another type of maintenance station is an odorization station. These stations are aboveground along a gas line and facilitate addition of Mercaptan to the gas. The distinctive odor of Mercaptan permits identification of gas leaks.



Figure 24. Pig Launcher Station

3.1.3 Storage Facilities

Storage facilities are particularly important in the natural gas industry because the industry practices peak shaving. To meet peak winter demand, the industry maintains an auxiliary source of gas near markets, stored as liquefied natural gas or liquefied petroleum gas, but operates pipelines well below capacity for the rest of the year. This approach allows the gas industry to

maintain a relatively small flow capacity compared with peak demand without service interruption to consumers.

Storage facilities have all the components of a compressor station, as pictured in Figure 21, including compressors, scrubbers, coolers, valves, and a control room. The difference is that the gas is compressed into storage tanks rather than down the gas line.³⁷

3.1.4 Control Centers

Pipeline control centers can be distributed or consolidated. If distributed, there are several control centers, each for a segment of pipeline. A consolidated control center directs the entire pipeline from a single location.

Processed pipeline measurements are relayed to the appropriate control center using a Supervisory Control and Data Acquisition (SCADA) system. Both computers and human operators continually monitor SCADA output. In the event of an emergency, SCADA allows operators to quickly shutdown a line. Given their importance to controlling the line, the components of the SCADA system typically have redundancy.

Data acquisition from field instrumentation on the line is performed by Remote Terminal Units (RTUs), which interface with SCADA.³⁸ Values recorded by an RTU include pressure, temperature, flow rate, and specific gravity. RTUs also monitor pressures in routing and storage areas.³⁹

3.2 Liquid Pipeline

3.2.1 Basic Components

The components of liquid lines are line pipe, valves, and manifolds. Liquid line pipe and pumps are discussed in this section; liquid valves and manifolds are essentially equivalent to those of gas, as discussed in Section 3.1.1.

3.2.1.1 Line Pipe

Pipe for liquid lines is specified by diameter, wall thickness, and pipe grade. The diameter of the pipe depends on its function. If the liquid is crude oil, it is collected from production sites by gathering lines; the gathering lines join trunk lines, which actually transport the oil. Gathering lines typically have diameters 2- to 8-in, whereas trunk lines typically have diameters 8- to 24-in, but they can be as large as 48-in. Oil moves through the pipeline at speeds of 4.4 to 11.7 feet per second.⁴⁰

The PHMSA data also includes hazardous liquid incidents, and crude oil incidents were examined to estimate average pipeline parameters, such as wall thickness. Table 3 is a summary of wall thicknesses, maximum allowable operating pressure, and specified minimum yield pressure reported in the PHMSA data.⁴¹



Figure 27. Photograph of Pump for 20-in Crude Line⁴⁴

3.2.2 Pump Stations

A liquid line includes pump stations, block valve stations, metering stations, and maintenance stations. Liquid stations function similarly to the gas line stations discussed in Section 3.1.2 except that liquid lines do not require odorization.

Booster pump stations maintain the head and thus flow rate of the line, and they are located every 20 to 100 miles. Their principal component is a pump, typically centrifugal and electrically powered, but the pumps can be powered by diesel engines or gas turbines.⁴⁵ As shown in Figure 28, the station includes valves and pipe segments to connect the pump to the pipeline.



Figure 28. Typical Pump Station⁴⁶

An originating pump station is located at the head of a line and can also include metering equipment, supervisory control and data acquisition equipment, and scraper traps. Scraper traps permit ingress and egress of pigs.⁴⁷

Liquid block valves are required on both sides of pump stations and at major waterways.⁴⁸ Figure 29 is an example of a typical block valve station for a liquid line.



Figure 29. Typical Block Valve Station⁴⁹

3.2.3 Storage Facilities

Storage facilities, also known as storage fields or tank farms, reduce fluctuation in a pipeline by providing a buffer supply of the liquid. They are commonly used for petroleum products. The tanks can be belowground or aboveground, as shown in Figure 30.

The tanks typically operate near atmospheric pressure. They commonly are designed to resist vehicular impact but are not hardened against explosive attack. They are also typically unguarded but commonly have containment measures in place for a spill event, like the levees shown in Figure 30.⁵⁰



Figure 30. Petroleum Tank Farm⁵¹

3.2.4 Control Centers

The control centers of liquid lines function similarly to those of natural gas lines, as discussed in Section 3.1.4.

3.3 Vulnerabilities to Explosive Threats

3.3.1 Access to Critical Pipeline Components

Pipelines and the industries they support are everywhere. A few statistics on pipeline assets and operators illustrates this point⁵²:

- Natural gas transmission lines: 320,500 miles
- Natural gas transmission line operators: over 700
- Natural gas storage facilities: over 400
- Hazardous liquid transmission line: 168,900
- Hazardous liquid line operators: over 200
- Natural gas distribution operators: 1,300
- Natural gas distribution lines: 2.2 million

The sheer size of the pipeline system makes it inherently vulnerable to numerous threats, including explosive, ballistic, sabotage, vandalism, and accidents. Explosive threats include improvised explosive threats (IEDs) and vehicle borne IEDs (VBIEDs). The proximity of pipelines to vehicular infrastructure (roads, parking areas, and bridges) contributes to the vulnerability, allowing easy access for VBIED and other IED threats.

General hardening of pipeline infrastructure against these threats would be exorbitantly expensive. The extent of the infrastructure is simply too great. The extent of the pipeline system has also prevented broad surveillance because of the cost of security personnel and instrumentation for monitoring such a large area.⁵³

There are numerous instances in the continental US of pipelines being conveyed across a body of water as part of a vehicular bridge. Combining bridge and pipeline crossings permits an aggressor access to the line at a critical location, and the repair cost of such a line, as well as the cost of environmental remediation, can be enormous.⁵⁴

3.3.2 Resistance to Explosive Threats

3.3.2.1 Enforced Standoff

Although pipelines are very accessible to explosive attack, they also exhibit some inherent resistance. In many cases, their construction enforces standoff of an explosive charge from the pipeline itself. Increase in standoff greatly decreases the impulse applied by the charge to the pipeline. This fact is illustrated in Figure 31, which shows the decrease in peak reflected impulse applied by a sphericalxx-lb TNT charge with increasing standoff. This curve was generated using CONWEP, a weapons-effects software based on UFC 3-340-01⁵⁵.

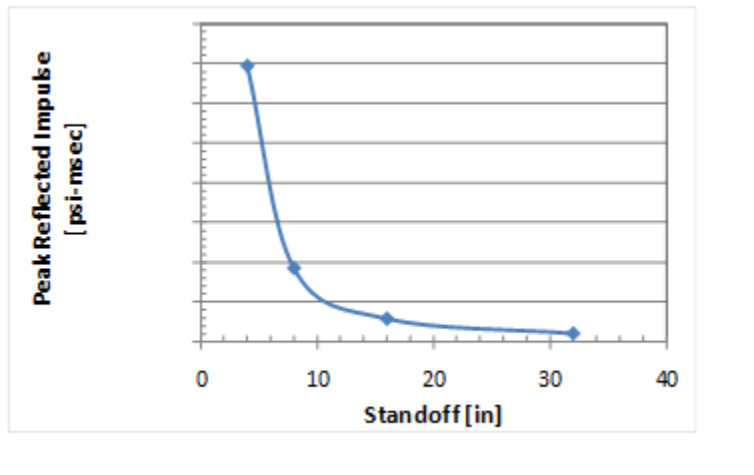


Figure 31. Peak Reflected Impulse versus Standoff for xx-lb TNT Charge

In many cases, burial requirements provide standoff. Nearly all pipelines in the continental US are belowground, as required by federal regulations, and the typical soil cover is 30-in to 36-in.⁵⁶ The presence of the soil reduces the vulnerability of the pipeline to rupture. Natural Resources Canada (NRCan)⁵⁷ has confirmed this fact through testing of buried line pipe segments.

The aggressor may choose to remove soil to place the charge immediately adjacent to the line, but such an approach increases the likelihood of detection. However, if the soil is not removed, a much larger amount of explosives would be required to rupture the pipe. Furthermore, the aggressor would need to unload the vehicle carrying the explosives to reduce the standoff; otherwise, the explosion may not rupture the pipe.⁵⁸

In cases where the pipeline is aboveground, such as over 400 miles of the Trans-Alaska Pipeline System (TAPS)⁵⁹, the pipeline is often covered with insulation which provides some standoff. An example of a heavily insulated segment of TAPS is shown in Figure 32. In order to place a charge directly on the pipeline, the aggressor would have to remove the insulation.⁶⁰



Figure 32. Heavy Insulation on the Trans Alaska Pipeline System (TAPS)⁶¹

3.3.2.2 Structural Resistance

In general, both liquid and natural gas lines have significant internal pressure. Blast testing has shown that a larger charge mass is required to fail a pressurized line than an unpressurized line. This difference is likely due to the internal pressure increasing the blast required for failure.⁶²

The circular cross section of a pipeline provides additional resistance to explosive attack when the aggressor threat is bulk explosives. For a flat surface, as shown in Figure 33 (a), the entire presented area is orthogonal to the path of the shock wave. Because the presented area of a circular cross section recedes from the shock wave, as shown in Figure 33(b), the magnitude of the applied impulse can be as much as 20% less than what is applied to the square section.⁶³ As a result, a larger charge is required to fail a circular cross section than a square cross section with edge length equal to the diameter of the circle.

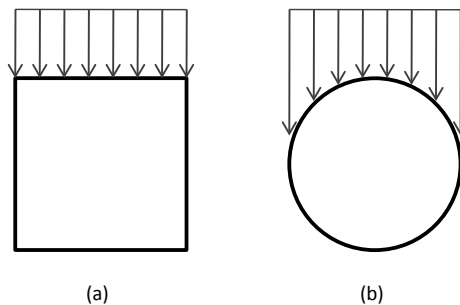


Figure 33. Shock Pressure Accumulation for (a) Square Cross Section and (b) Circular Cross Section

3.3.2.3 Redundancy

Pipeline systems include redundant capacity to minimize supply disruption if repairs become necessary. Many pipelines include a built-in looped line to bypass critical segments of pipeline, such as compressor or pump stations. Block valves can isolate the station if it is damaged. In cases where this looped line has not already been installed, pipeline operators can install aboveground bypass for a damaged segment of the line in a matter of hours.

Control systems are also highly redundant. In many cases, SCADA systems have double or even triple redundancies. Manual backups that bypass SCADA are also available.⁶⁴ Use of manual backups decreases the flow rate of the line but prevents loss of the line altogether. One estimate is that a gas pipeline can operate at 70% capacity without SCADA, as long as a mechanical pressure gauge is operating at the damaged point.⁶⁵

The result of these redundancies is that the US pipeline system is resilient, and a single attack is unlikely to cause a major disruption. In fact, multiple attacks would be required for any major disruption.⁶⁶ However, significant environmental damage could result from a limited attack.

3.3.3 Vulnerability to Specific Explosive Threats

Vulnerability can be defined with a number of different metrics, such as peak stress, plastic strain, amount of deflection, extent of fracture, etc. The required accuracy in predicting

avulnerability metric need not be higher than the certainty with which the threat is known or can be defined. To evaluate a particular pipeline component vulnerability, the actual magnitude and location of the explosive threat would need to be specified, perhaps by a government agency or other regulatory body. For the evaluations performed in this section, a specific threat is not specified; rather, the size of the charge is varied in order to determine the minimum explosive weight that will cause a failure.

For the purposes of this assessment, vulnerability is defined as a fracture, rupture or penetration of a pipeline component by an explosive threat, i.e., an opening is created, be it a crack or hole. While a pump, compressor, or valve may become inoperable due to deflection of the outer wall coming into contact with the internal components, the prediction of this would require that the structural details and materials of the component be known and that the explosive threat be well-defined. Component details vary considerably by manufacturer and are generally proprietary. Consequently, these details were not explicitly modeled in this assessment. In addition, only general definitions of the explosive threat are known. Therefore, vulnerability metrics based on failure of the component wall are appropriate.

3.3.3.1 Bulk Explosive

A bulk explosive threat is a relatively large charge weight, such as 50-lb TNT or greater, detonated at a distance from the pipeline. The explosion generates a high-pressure shock wave that propagates through the air before striking the target.

To assess the vulnerability of an aboveground pipeline to a bulk explosive threat, eight finite element analysis (FEA) simulations were developed. For all eight simulations, the charge was assumed to be TNT. The segment of pipeline was 100-ft long which should be sufficiently long that the boundary conditions at the end of the pipe do not affect the response of the pump, compressor, and valve components. The pipe diameter was 24-in, and the wall thickness was 0.25-in; these were chosen as typical values. Symmetry was employed such that the length of the model was 50-ft. The material properties for API 5L Grade X60 line pipe were used; that grade has a yield strength of 60,000 psi and ultimate strain of approximately 20%.⁶⁷ Finally, the pipe had an internal pressure of 800 psi. These properties are summarized in Table 4, and the layout of the simulations is illustrated in Figure 34.

Table 4. Summary of Properties Common to the Eight Simulations

Property	Value
Segment Length	100-ft
Internal Pressure	800-psi
Diameter	24-in
Wall Thickness	0.25-in
Pipe Yield Stress	60,000 psi
Pipe Ultimate Strain	20%

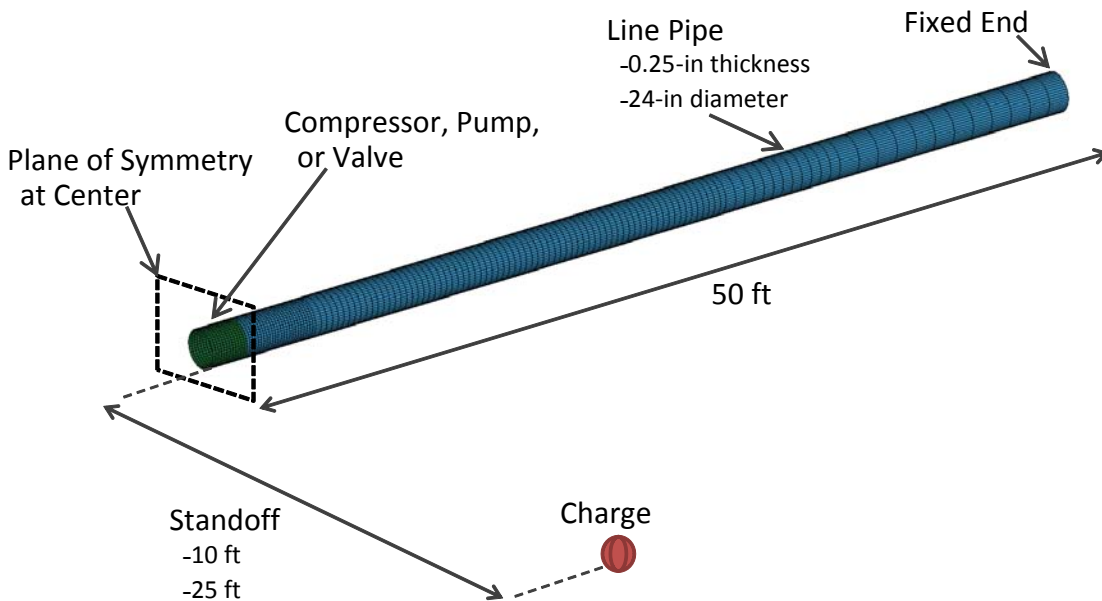


Figure 34. Layout of FEA Model for Bulk Explosive Simulations

Two cases were considered for each of three variables, resulting in the eight cases shown below in Table 5:

1. Standoff: 10-ft or 25-ft
2. Pipe content: gas or liquid
3. Center component: valve or pump

In developing the FEA model for bulk explosives, several approaches were considered. To maintain efficiency and keep simulation time short, the model did not explicitly include the charge and the air between the charge and the pipeline. Instead, CONWEP, a weapons-effects software based on UFC 3-340-01⁶⁸, was utilized to develop basic pressure and impulse loading predictions for particular charges and standoffs. These loads were then applied using pre-defined loading regions on the pipe.

As the blast propagates outward from the charge, the shockwave does not uniformly load the entire pipe. It first strikes the center of the pipe on the side facing the charge; the loading is highest in this area due to its proximity and normal angle to the charge. The shock takes longer to arrive at points further down the length of the pipe, where the intensity is reduced due to the increased standoff and increased obliquity of the pipe to the charge (Figure 35).

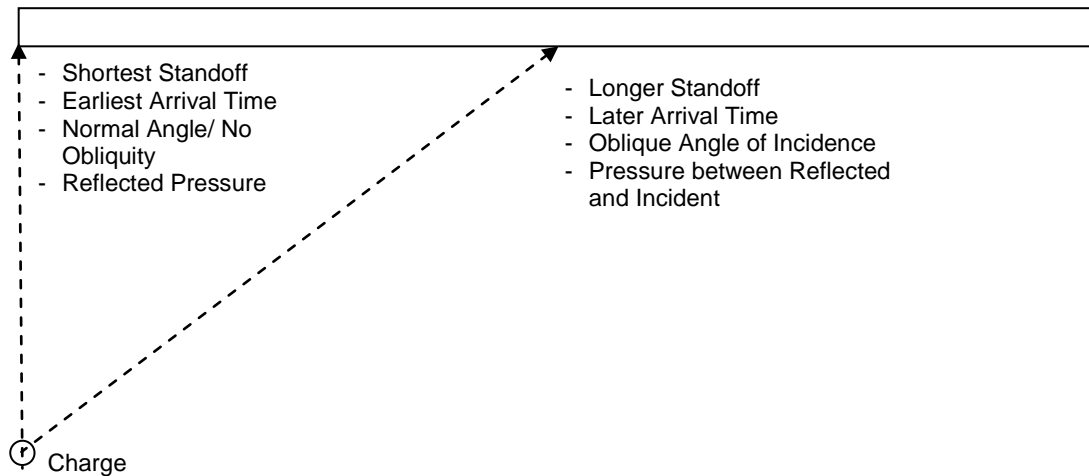


Figure 35. Longitudinal Pipeline Loading Considerations

The shock was further reduced on circumferential regions of the pipe due to decreases in the degree of shock reflection, a phenomenon discussed in Section 3.3.2.2. It was assumed that the upper, lower, and rear faces of the pipe received incident pressure/impulse loading. The direct frontal area of the pipe received reflected pressure. Areas of the pipe between the front-most edge and the top or bottom received loads that were adjusted for the angle of incidence. This arrangement is shown in Figure 36.

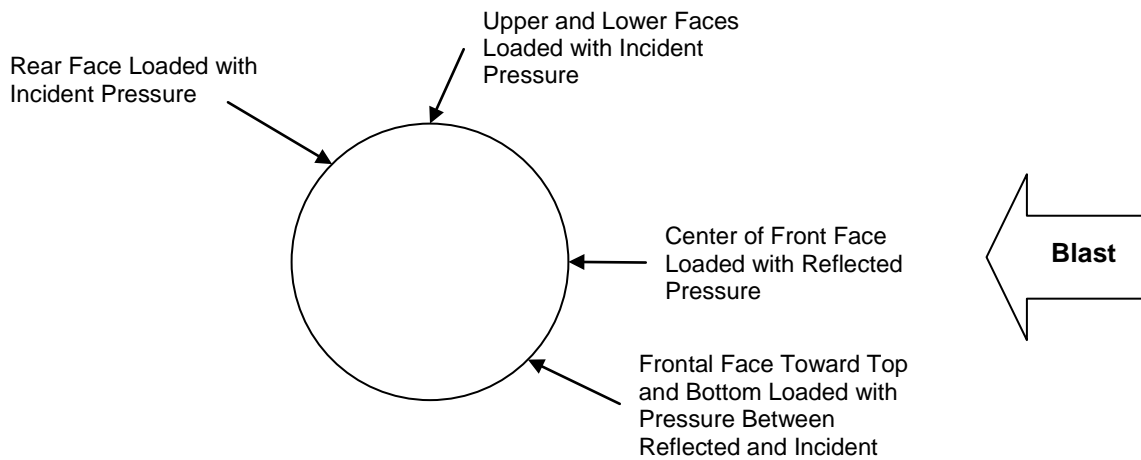


Figure 36. Circumferential Pipeline Loading Considerations

The pipeline model was partitioned lengthwise into 11 longitudinal loading regions and 5 circumferential loading regions. The overall angle of incidence for each of these 55 loading regions was calculated separately from the FEA model. Impulse adjustment factors were developed using data from UFC 3-340-02.⁶⁹ These correction factors were then applied to the baseline load data derived from CONWEP. Thus, the final loading on the pipe accounted for the standoff, angle of incidence, and time of arrival for each load segment.

The model pipe was filled in two different ways to correspond with natural gas and liquid lines, which proved to be important to dynamic structural response for the following reasons. First, gas and liquid lines have different masses per unit length, and structural mass is critical to dynamic response. Second, the internal pressure due to the gas or liquid affects how the line pipe ruptures⁵⁷. Third, the liquid in the pipe increased resistance because a confined liquid resists load. For both the gas and liquid cases, the contents of the line were pressurized to 800-psi. In the gas case, a pressure was simply applied to the interior face of the line pipe; in the liquid case, the liquid was explicitly modeled with solid elements and pressurized to 800-psi. For convenience, the properties of water were used for the liquid.

The effect of the valve, compressor, or pump (compressor for gas content, pump for liquid) on structural response was modeled as a distinct segment of pipe. A case including a manifold was not explicitly modeled, but the compressor or pump simulation case was taken to provide a good approximation of the boundary conditions imposed by the manifold. Like the pump, the manifold would be relatively massive and constrained against displacement due to mounting supports.

The valve, compressor, or pump was included as a 4-ft long segment of pipe with 1.0-in wall thickness, illustrated by the green part in Figure 34. A 1.0-in wall thickness was selected based on discussions with pipeline component distributors. Based on the discussion in Section 3.1.1.2, the valve was expected to provide minimal inertial resistance beyond that of a segment of pipe; it was modeled as an elastic-only steel material. However, from Section 3.1.1.3 and Section 3.2.1.2, the pump or compressor was expected to contribute greater inertial resistance, given their size and construction. As a result, in the pump or compressor cases, the density of the center section was increased to 100 times that of the valve cases to prevent the center section from moving, effectively creating a fixed boundary condition.

As shown in Figure 37 and Figure 38, the increase in mass for the pump or compressor altered the deformed shape of the line pipe due to the inertial restraint. In the case of the valve, the 100-ft length of pipe deflected like a fixed-fixed beam. The maximum observed deflection was at the mid-span, where the simulated valve was placed. For the pump or compressor case, the line pipe behaved more like a continuous beam, fixed at either end with a support in the middle.

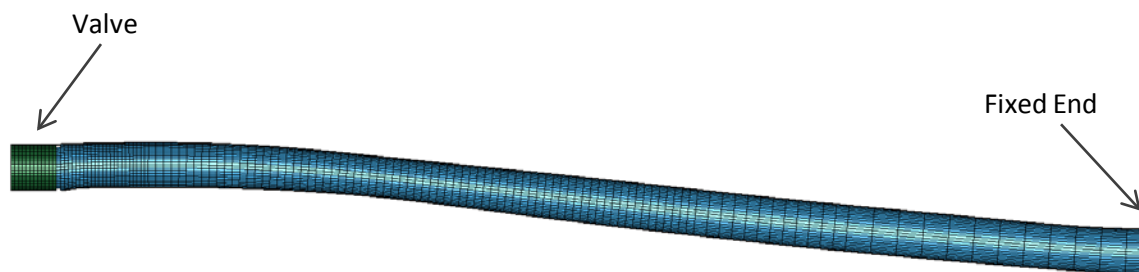


Figure 37. Typical Deformed Shape for Valve Case
(Valve Section with Density of Steel)



Figure 38. Typical Deformed Shape for Pump or Compressor Case
(Pump or Compressor with Mass 100 times that of Valve)

Again, for this set of simulations, failure was taken to be rupture of the pipe. Although deformation of the line pipe could impair service by reducing operating pressure or preventing maintenance, it was not considered to be failure since a hole was not created and product would not leak out.

Rupture of the line pipe was defined as failure of any finite element (discrete region of pipe defined by mesh) at the middle of the line, near the valve, pump, or compressor. Element failures elsewhere along the length of the pipe were regarded as spurious. Elements at a distance from the valve, pump, or compressor were increased in length to reduce run time, and their aspect ratio resulted in artificial failures. Also, failure near the center of the line was expected a priori from interaction of larger instantaneous shear stresses resulting from proximity to the charge and overall flexural stresses.

The results of the eight simulations are shown in Table 5, with the TNT charge weight that was calculated to rupture or perforate the pipe in the last column. An immediate observation is that large charge weights are required to rupture line pipe at a standoff as small as 10-ft. The smallest charge weight is ww- lb, when the line contains liquid, the standoff is 10-ft, and the center component is a pump. The line containing liquid and having a valve failed to rupture at any charge weight for a 25-ft standoff. Therefore, it is concluded that bulk explosives at these standoffs are a relatively ineffective threat to domestic pipelines.

Table 5. Summary of Results from Bulk Explosive Simulations

Sim. No.	Pipeline Contents	Charge Standoff [ft]	Component at Center	Charge Weight (TNT) [lb]
1	Gas	25	Valve	xx
2	Gas	25	Compressor	xx
3	Gas	10	Valve	xx
4	Gas	10	Compressor	xx
5	Liquid	25	Valve	No Failure
6	Liquid	25	Pump	xx
7	Liquid	10	Valve	xx
8	Liquid	10	Pump	xx

Summary:The large volumes of bulk explosive required to rupture a pipeline at standoffs greater than 10-ft are concluded to be an ineffective threat against pipeline infrastructure.

3.3.3.2 Contact Charge

A contact charge consists of a relatively small charge weight, such as 50-lb TNT or less, placed in direct contact with a target. This threat is distinct from a charge with standoff because the blast energy is directly applied to the pipe.

Analytical Model

As a preliminary analysis, an existing analytical model developed by Jones for breach of flat steel plates subjected to close-in spherical charges was modified to determine the vulnerability of pipeline components to contact charges. While the surface of a pipe is curved and it is unlikely an aggressor would use a spherical charge shape, this model was deemed suitable for performing a rough, first-order assessment of breaching in a pipe. It is conservative to assume that the pipeline component is a flat plate, since curvature provides additional resistance to the applied blast energy through compressive arching. Therefore, the predicted hole diameters should be an upper limit on actual hole diameters.

In this model, the impulse applied to the plate, was determined using the Kingery-Bulmash polynomial curve fits.⁷⁰ As shown in Figure 39, to represent a contact charge, the charge standoff was taken to be the radius of the spherical charge. Equations discussed in N. Jones “Plastic Failure of Ductile Beams Loaded Dynamically”⁷¹ were used to calculate the energy applied to the plate and the energy required to fail the plate for a given hole diameter. The hole diameter was varied until these two energies were equal, and this hole diameter was defined to be the size of the breached area. The results for two plate thicknesses, 0.35-in and 1.00-in, are shown in Figure 40. A thickness of 0.35-in is representative of line pipe and valves, and 1.00-in is representative of pumps and compressors. From the figure, ww-lb of TNT causes a hole diameter of 11-in in a 0.35-in plate and 4.0-in in a 1.00-in plate.

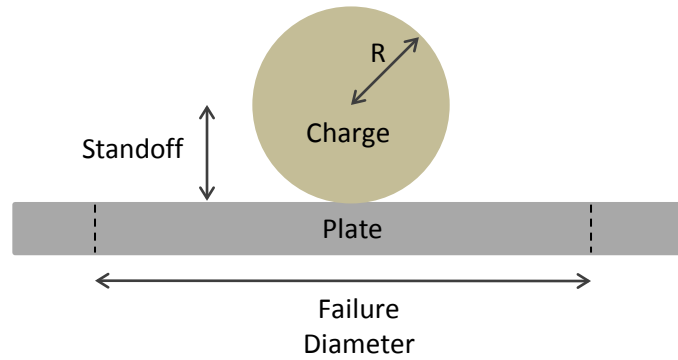


Figure 39. Conceptual Scheme of Contact-Charge Analysis

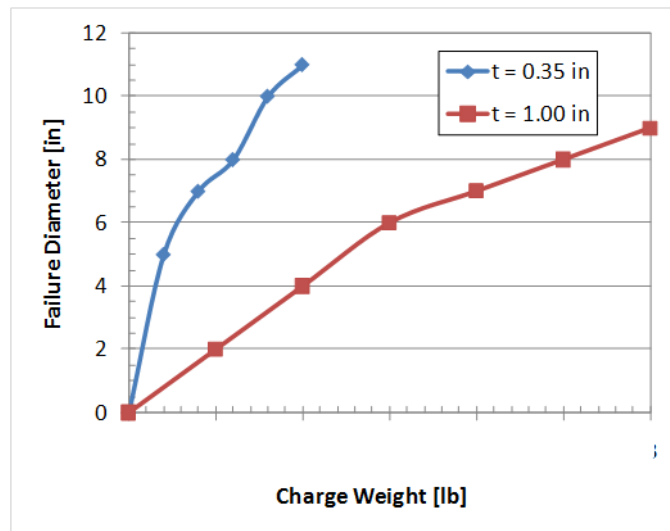


Figure 40. Hole diameter versus Spherical Charge Weight TNT: 0.35-in and 1.00-in

The assumptions made when applying the analytical model proved too conservative for line pipe with relatively thin walls. For example, when the wall thickness was reduced to 0.25 in, unrealistically large hole diameters were predicted. Another limitation of the analytical model is that it fails to include the effect of pressurized gas and liquid on the response of the pipe wall. A further limitation is that the Kingery-Bulmash equations are not necessarily valid for such small standoffs. Therefore, an FEA model was developed to simulate contact charges detonated on a pipeline.

FEA Model

An FEA model was created for a pipe with a diameter of 24-in, a wall thickness of 0.25-in, and 60,000-psi steel. C4 was chosen for the charge, as it is a common explosive type. The explosive was explicitly modeled along with the air and liquid using fluid formulations. These were coupled to the solid pipeline model using an Arbitrary Lagrangian-Eulerian (ALE) capability in LS-DYNA (Figure 41).

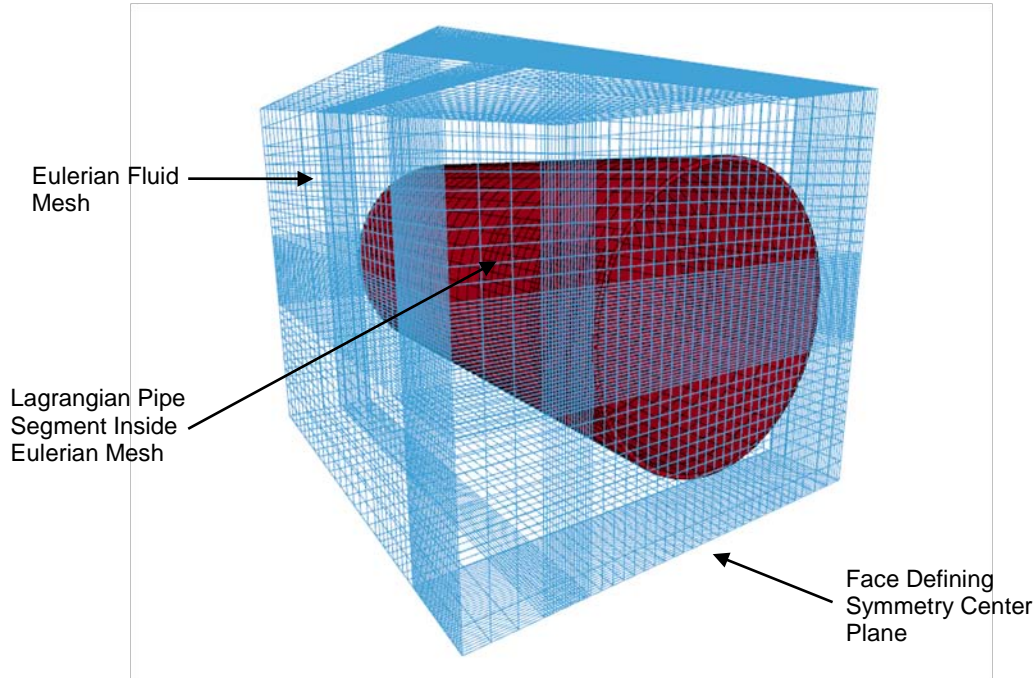


Figure 41. C4 Contact Charge ALE Model Before Fluid Fill

The pipe was modeled with shell elements as shown in Figure 42. Smaller elements were used in the region near the charge, since this is a region of high stress gradients in the pipe. The pipe section was suspended in an Eulerian mesh of solid elements. The region outside the pipe was filled with air, while the region inside the pipe was filled with either a gas or a liquid. The properties of water were used for the liquid. A box-shaped contact charge was placed immediately adjacent to the pipe as shown in Figure 43 where one half of the model is shown. The charge shape was changed to a box from a spherical shape because it was deemed that a spherical charge did not represent a realistic threat. Standard material values for the C4 were employed.

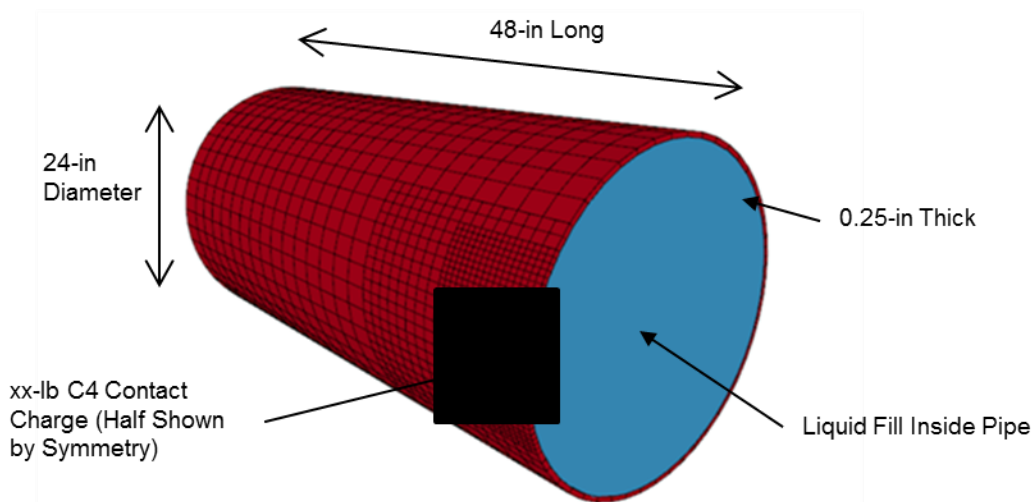


Figure 42. Contact Charge ALE Model After Fluid Fill (air outside pipe omitted for clarity)

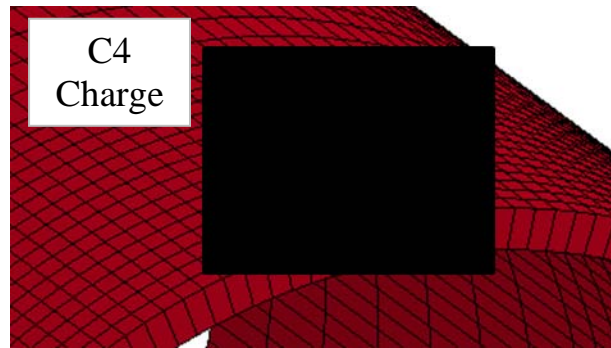


Figure 43. Detail of Box-Shaped C4 Charge on Bare Pipe
(Half Shown by Symmetry)

Three cases were modeled:

1. Empty pipe
2. Gas-filled pipe at 800-psi
3. Liquid-filled pipe at 800-psi

For the gas-filled pipe, the gas itself was not explicitly modeled; an empty pipe was used with a pressure load applied to the inside face. For the liquid-filled pipe, an incompressible liquid was explicitly modeled, but in an unpressurized state. The stress state in the pipe itself was imposed by applying a pressure load to the inside face, just as done for the gas-filled case. This two-step approach was used for simplicity and efficient simulation times. Since the liquid is incompressible, the mechanical performance was essentially identical to a liquid under pressure.

To validate the contact charge model, a test performed by BlastGard International was replicated.⁷² Although the documentation from the test is sparse, it did serve as a useful baseline. In that test, aww-lb C4 contact charge was applied to an unpressurized, water-filled 24-in OD x 0.375-in pipe comprised of API-5L X-42 steel. The charge was found to produce an 8-in diameter hole in the pipe. This case was repeated using the LS-DYNA model, and the charge produced an 8.8-in diameter hole, as shown in Figure 44. This correlation between the model and the test was deemed sufficient to validate the modeling approach.

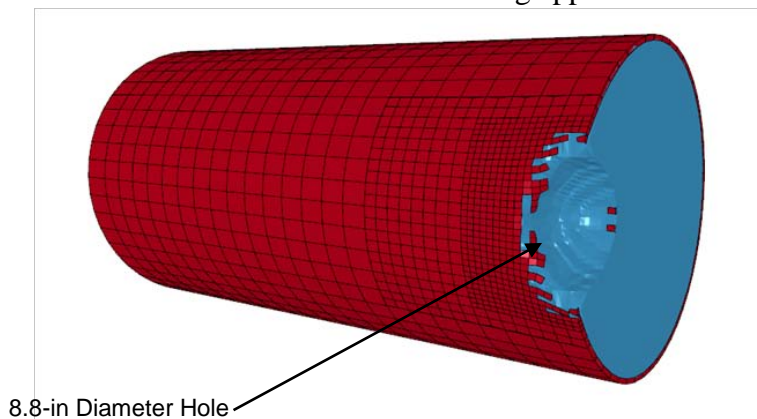


Figure 44. Contact Charge ALE Model Validation Case

In each of the three simulation cases, the initial charge size was ww-lbs, which breached the pipeline. The charge size was progressively decreased in order to find the threshold for pipeline failure. It was found that charges as small as ww-lbs produced holes in this particular pipe configuration for all three cases. While pipelines with larger wall thicknesses will require a larger charge to breach, these analyses highlight that typical pipeline components are vulnerable to small contact charges, with weights as low as ww-lb C4.

Summary: From the analysis, it was concluded that pipeline components are vulnerable to contact charges.

3.3.3.3 Shaped Charge

Conical Shaped Charge

Shaped charges are a common military ordnance but are also used for drilling activities, instantaneous release of sections of rockets, and engineered demolition charges.

The most common type of shaped charge is the conical, or cylindrical, shaped charge. As shown in Figure 45, the conical charge is composed of a copper-lined cone embedded in high explosive (HE). At ignition, the copper cone collapses and forms a metal jet which is ejected from the casing along with a lower velocity slug. The jet makes a deep and narrow penetration in the target material.⁷³

From calculations performed in CONWEP, which is based on UFC 3-340-01,⁷⁴ a ww-in shaped charge will penetrate ww-in of steel and ww-in of earth. Therefore, even buried pipeline components are vulnerable to shaped charge attack. While the diameter of the perforation caused by a shape charge is small, a pressurized component may fracture due to the stress concentration. In addition, the blast from the HE will interact with the perforated area, increasing the chance of failure.

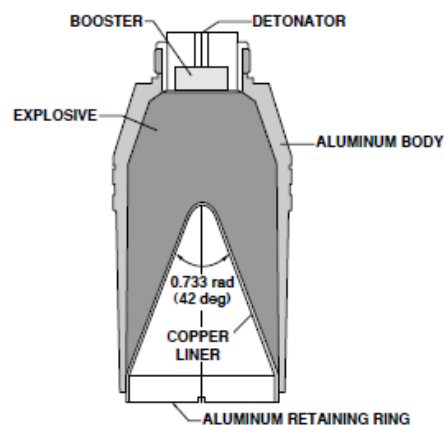


Figure 45. Section of Conical Shaped Charge⁷⁵

Linear Shaped Charge

The mechanics of a linear shaped charge is similar to conical shaped charges, in that the high explosive compresses a liner of copper or other metal, creating a jet of near-molten material. Linear shaped charges have a V- or chevron-shaped profile which creates a continuous, knife like jet that is very effective in cutting metals and other hard materials. Examples of linear shaped charges are shown in Figure 46. Commercially available linear shaped charges with ww-lbs/ft of RDX/TNT (a medium sized shaped charge) will cut through ww-in of mild steel.



Figure 46. Linear Shaped Charge⁷⁶

Summary: Given the considerable penetration capability of linear and conical shaped charges, all pipeline components are vulnerable to this explosive threat.

3.3.3.4 Flyer Plate

The configuration of the flyer plate threat is shown in Figure 47. It consists of a circular, concave plate, usually copper, backed by high explosives. Detonation of the explosives ejects the flyer plate with sufficient force that it deforms, becoming a convex high-velocity projectile with considerable penetration capacity. According to engineers with expertise in the technology, flyer plates can have diameters as small as 6-in and as large as 36-in, and a common diameter-to-thickness ratio is 25.

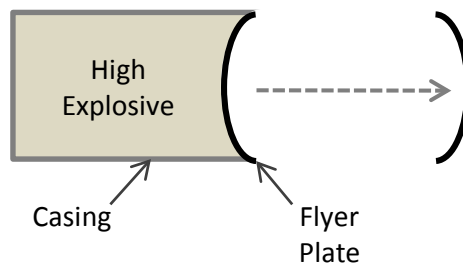


Figure 47. Flyer Plate Configuration

Preliminary analysis was performed to determine the penetration characteristics of this type of threat. The failure energy was calculated as in Section 3.3.3.2, using equations presented in Jones.⁷⁷ The applied energy was equal to the kinetic energy of the flyer plate, where the speed of the flyer plate was obtained using the Gurney equation, as discussed in Vigil, *A Scaling Law*

*Describing the Penetration of Reinforced Concrete Barriers by Explosively Driven Flyer Plates.*⁷⁸ The failure energy and applied energy were equated to determine the hole diameter, given the thickness and strength of the target plate.

For the calculations, the ratio of charge mass to flyer plate mass was 1.0 so that the initial velocity of the plate was consistent with the experimental data cited by Vigil.⁷⁹ Figure 48 illustrates the distribution of the explosive assumed for the analytical model. It was assumed to be radially offset from the flyer plate a distance resulting in a mass equal to that of the flyer plate. In practice, the explosive would be distributed as in Figure 47, for convenience and efficient use of explosive.

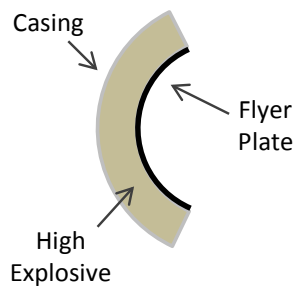


Figure 48. Assumed Explosive Distribution for Analytical Model

The conclusion from the analysis is that a ww-in diameter flyer plate can form a ww-in diameter hole in ww-in of 50,000-psi steel. While this analytical model shares the limitations of the analytical model for the contact charge discussed in Section 3.3.3.2, there was no need to perform FEA modeling, since flyer plates are an overwhelming penetration threat against standard pipeline components.

Summary: All aboveground pipeline components are vulnerable to flyer plate threats of any reasonable size.

3.4 Consequences of Pipeline Failure

To identify which pipeline components have the highest priority for protection, the consequences of component failure are evaluated in this section. The importance of the type of product (gas or liquid) is also evaluated.

3.4.1 Consequences by Component Failure

3.4.1.1 Line Pipe

Failure of line pipe due to explosive attack would have the immediate consequence of line product leaking into the environment. The volume of product lost depends on the distance between the block valves and the reaction time of the operators to shut the line down. Loss of a large volume of hazardous liquid would result in considerable costs for environmental remediation and property repair. Even if the damage caused by the threat were minimal, such as

a small perforation, the internal pressure of the line could cause circumferential rupture about the section of the line or linear rupture along the axis of the line. In those cases, a large volume of product would be lost as well.

Nevertheless, a properly functioning control system would signal loss of integrity shortly after the attack, enabling operators to seal the block valves on either side of the line rupture. Operators would then be able to repair the line quickly, often within 24 hours. Line pipe is the most readily available and lowest-cost pipeline component. Therefore, failure of a single segment of pipe would likely have minimal downstream effects.

3.4.1.2 Manifold

Failure of a manifold would also result in product leakage, but depending on the configuration, that volume leaked could be greater than for line pipe failure. Manifolds join multiple lines, and the volume of the product between block valves for all lines supported by the manifold could be lost.

In addition, replacing manifolds is more costly and time-consuming than replacing line pipe. For a given line diameter, more welding is required to install a manifold, and installation tolerances are smaller because the manifold must accommodate all the lines that it joins. Therefore, protection of a manifold has higher priority than protection of line pipe.

3.4.1.3 Valve

The downstream effects of loss of a valve could be significantly greater than loss of line pipe or manifold, especially if the aggressor damages a block valve. In this scenario, an operator would have more difficulty sealing off the leak, particularly if control instrumentation is damaged during the attack, and a larger volume of product would likely be lost than if only a pipe segment were damaged. In addition, valves have lower availability and are more costly than line pipe. As a result, protection of valve has higher priority than protection of the line pipe or manifold.

3.4.1.4 Compressor or Pump

As discussed in Section 3.3.2.3, loss of a pump or compressor would not disable an entire line because stations have built-in looped lines, and when they do not have such a bypass, it can be constructed in a matter of hours. However, it is commonly observed that loss of three pump stations would be sufficient to take out an entire line.⁸⁰

Replacing a badly damaged pump or compressor station can take six months or longer, and the flow rate of the line would be diminished throughout that repair period. A significant part of the time required to repair a pump or compressor station is having a replacement pump or compressor fabricated. Large units are commonly custom-fabricated overseas to meet the needs of a particular line, and they are the most costly components on the line. Therefore, compressors and pumps are generally regarded as particularly critical pipeline assets and have higher priority for protection than eitherline pipe, manifolds, or valves.

3.4.1.5 Storage Tank

As discussed in Section 3.1.3 and Section 3.2.3, storage tanks serve as a buffer in the pipeline system, whether for peak shaving on a gas line or surplus storage on a liquid line. Therefore,

loss of a storage tank or even several storage tanks likely would not impair service; it would just damage or eliminate spare capacity. Therefore, because loss of a tank likely would not impair the operation of the pipeline as a whole, its priority for protection is below that of valves, manifolds, and pumps or compressors.

However, damage to a tank could result in significant loss of product. A tank farm design, particularly with liquid lines, includes containment measures to minimize environmental impact. In the case of gas tanks, the product may be dissipated into the atmosphere, depending on topography and atmospheric conditions. If the gas is constrained or confined, there is the possibility of explosion and fire, depending on how the gas mixes with air and on the existence of an ignition source. Although this hazard exists for any gas line component, it is particularly great for a storage tank due to the large volumes of product involved. Therefore, because the potential for product loss is considerable, the protection priority of a storage tank is above that of line pipe.

3.4.1.6 Control Center

As noted in Section 3.1.4, the SCADA control system is integral to pipeline operation. Loss of a SCADA element at a given location will decrease the flow rate of the line. In addition, if an element is lost, there are compatibility issues with replacing the technology because SCADA systems have been installed gradually since the middle of the twentieth century.⁸¹ These considerations have led previous vulnerability reports to recommend that SCADA be listed among critical facility assets.⁸² However, the elements of the SCADA control system generally are not hardened. Because protection of the control system is typically distinguished from physical hardening and the focus of this research is physical hardening, protection of the control system is beyond the scope of this effort.

3.4.1.7 Priority for Component Protection

Protection priority for the pipeline components is summarized in Table 6, from highest to lowest. Compressors and pumps have highest priority. They are costly to replace, and their loss can impair flow rates for months due to the long lead times required to procure them. Loss of valves can result in large product spills, and they are important to controlling the line, relatively costly, and require relatively long lead times to procure. Therefore, they have second priority.

Failure of manifolds can result in significant product leakage, and they can be costly and time-consuming to replace, though likely not requiring the procurement lead times of pumps, compressors, and valves. Loss of a storage facility can also result in large spills, but they are largely controllable, and loss of a storage facility would not necessarily impair line service. Line pipe is readily available and low cost, and rupture of a line pipe segment can be repaired in a matter of hours. For these reasons, manifolds, storage facilities, and line pipe have third, fourth, and fifth priority for protection, respectively.

The control center was not included in this ranking. It is a critical asset, but its protection is generally considered separate from physical hardening, the subject of this research effort.

Table 6. Summary of Protection Priority for Pipeline Components

Protection Priority	Component	Reason for Priority
1	Compressor or Pump	Long replacement time, large cost, line service impairment
2	Valve	Large-volume product loss, intermediate replacement time, line service impairment, cost
3	Manifold	Intermediate-volume product loss, intermediate replacement time
4	Storage Facility	Controlled, large-volume product loss
5	Line Pipe	Intermediate-volume product loss, easily repaired or replaced
Not considered	SCADA	Protection typically distinguished from physical hardening and therefore outside the scope of this effort

3.4.2 Consequences by Line Product Type

3.4.2.1 Natural Gas Pipeline

In general, there are seven possible consequences of a natural gas line failure:

- Product loss
- Replacement/repair costs
- Environmental damage
- Property damage
- Human evacuation
- Human injury and fatality
- Interruption of service

Identification of these consequences is based on the data⁸³ collected by Pipeline and Hazardous Materials Safety Administration (PHMSA) with the exception of interruption of service. Interruption of service has been added to the PHMSA list because both immediate and downstream consequences of a pipeline failure are of concern.

If a leak develops in a natural gas line and the gas is not confined or constrained, it will be dissipated into the environment with no remediation costs; however, there are costs associated with product loss. If the gas is constrained or confined near an ignition source, it may ignite, and immediate consequences could include environmental damage, property damage, human evacuation, and human injury and fatality.

In recent years, the interdependence of natural gas lines and the electrical grid has increased. Historically, gas lines have been independent of the electrical grid. However, recent regulation

has required the use of electric compressors, and industry representatives speculate that 6 to 7% of natural gas compressors are electric.⁸⁴ In addition, power generation from natural gas has increased such that a significant number of electrical plants are fired by natural gas. Because of this interdependence of the gas pipeline system and electrical grid, compressor failure on a gas line supporting a power plant could have cascading effects. In such a scenario, loss of a compressor station could lead to loss of a power plant. Loss of a plant may cause loss of sectors of the electrical grid, which in turn renders multiple gas lines without power. Without compressors, the lines eventually depressurize and shut down additional power plants, which would cripple additional sectors of the power grid. However, it should be noted that the gas pipeline system rarely operates at peak capacity. Peak shaving allows gas lines to meet peak winter demand using storage tanks near the gas market and operate well below capacity the rest of the year. Therefore, though the effects of interrupting service could cascade, actually interrupting service with an explosive attack would likely require considerable planning and coordination. A relatively unsophisticated attack could cause loss of redundant capacity and place strains on the gas system, but the attack would need to target critical nodes at specific times to actually interrupt service.^{85,86}

3.4.2.2 Liquid Pipeline

The potential consequences of a liquid line incident are similar to those for a gas line, as listed above. All of these consequences can be costly in the case of liquids, depending on the specifics of the incident and product. The type of product in a liquid line clearly has a large impact on the costs of product loss, environmental damage, property damage, and human injury and fatality. Loss of finished product is generally more costly than loss of raw product because the finished product has undergone a refining process. In addition, finished products can be especially toxic, which increases the hazard it poses to the environment, property, and humans.⁸⁷

As with gas lines, interruption of service can be economically significant for any industry that relies heavily upon liquid products. Compared with gas, the domestic supply of liquids, both finished and raw, is small, a fact which amplifies the consequences of service interruption. For example, interruption of service to a refinery could have national consequences by causing spikes in fuel costs due to limited supplies of gasoline and diesel.⁸⁸

Interruption of jet fuel service could also have national consequences for the US airport system. US airports almost solely rely on a dedicated line for direct delivery of jet fuel.⁸⁹ Loss of this line at a single major airport could disrupt air travel nationally, given the interdependence of US airports.

3.5 *Conclusions from Pipeline Vulnerability Assessment*

Several conclusions can be drawn from this assessment.

- Both natural gas and liquid pipelines are assemblages of line pipe, valves, compressors or pumps, storage facilities, and control centers. Therefore, vulnerability assessment of a pipeline system reduces to the assessment of the individual components.
- The extent of the pipeline system and its proximity to other infrastructure render it vulnerable to a variety of threats. The sheer size of the pipeline system has prevented

general hardening and surveillance, even of critical assets. Also, its proximity to other infrastructure permits relatively unhindered access to the pipeline components.

- Although pipelines are vulnerable to attack, they also have inherent resistance. Nearly all pipeline in the continental US is belowground, and the cover soil provides charge standoff. Aboveground lines may be insulated, and insulation provides enforced standoff as well. The internal pressure, mass, and circular cross section of the pipeline increase its resistance to bulk explosive attack.
- The pipeline system and its components are vulnerable to all four explosive threats that were considered: bulk explosives, contact charges, shaped charges, and flyer plates.
- A large amount of bulk explosives is required to fail pipe at standoffs greater than 10 ft.
- Relatively small contact charges, common linear and conical shaped charges, and relatively small flyer plate threats will fail pipeline components.
- From the point of view of line contents, natural gas lines are vulnerable to post-rupture fire or explosions, if the gas is constrained or confined near an ignition source. In addition, the interdependence of gas lines with the electrical grid could result in the cascading failure of both.
- The contents of liquid lines, particularly finished product, can cause significant environmental impact, and the small domestic supply of liquid products can intensify the effect of loss of a liquid line. Loss of dedicated lines, like those that supply jet fuel to airports, can also have significant consequences.

Discussion of failure consequences by component suggests the following priority for component protection, from highest to lowest: compressor or pump, valve, manifold, storage tank, and line pipe. This ranking is based primarily on the time and cost required to replace the component, which correlates with time of service interruption, and the relative volume of product expected to leak due to a failure, which is related to cost of product loss and environmental remediation.

4 Task 3: Assessment of Blast Mitigation Technologies

In Task 3, the technologies identified in Task 1 for mitigating the vulnerabilities discussed in the Task 2 results were evaluated with numerical simulations. The Task 3 results are presented in this section.

4.1 Development of Numerical Simulation Matrix

Eight blast mitigation technologies were discussed in Section 2 and summarized in Section 2.6, and four explosive threats were discussed in Section 3.3.3. To develop the Task 3 simulation matrix, the technologies and threats were arranged in a table as thirty-two possible assessment cases, shown in Table 7.

The blast-mitigation technologies form the rows, and the threats form the columns. The table is populated by labels for each possible assessment. For example, fiber-reinforced polymer subjected to the bulk explosive threat would be assessment 1.1.

As discussed in Section 3.3.3.1, for the bulk explosive threat, very large charge weights would be required to fail a segment of bare pipeline for reasonable standoffs. Obtaining such a large explosive weight is difficult and if a capable adversary did have such a large amount, he would likely use it for more dramatic results. As concluded in Section 3.3.3.3 and Section 3.3.3.4, the shaped charge and flyer plate threats can be defeated with extensive hardening, but such approaches would be too costly and would greatly hinder routine operation and maintenance.

Therefore, the bulk explosive, shaped charge, and flyer plate threats were excluded from the Task 3 assessment, leaving the contact charge threat to be examined. These exclusions eliminated columns 1, 3, and 4 from Table 7.

Focusing on contact charges was further warranted by the fact that the majority of explosive attacks have involved contact charges of 50-lbs or less. Therefore, past events and the assessment of the capabilities of the other threats suggested prioritizing contact charges as the main threat to consider and that 50-lbs is a reasonable upper limit for a charge weight.

The simulation matrix was further reduced by eliminating those technologies for which adequate technical information could not be obtained. Armor Designs, Inc. and WinTec Security did not provide sufficient detail about their technologies so that they could be modeled in a contact charge scenario, and they were consequently excluded from consideration. These additional exclusions eliminated rows 4 and 6 in Table 7.

The steel-clad, earth-filled barrier of Infrastructure Defense Tech, Metalith™, is able to defeat contact charges, since, by definition, the charge cannot be placed on or near the pipeline. Because this barrier approach permits the pipeline to be enclosed in a soil layer of arbitrary thickness, it can be used to harden a pipeline to resist a contact charge of any practical charge weight. In addition, the Metalith™ approach should be capable of stopping the shaped charge and flyer plate threats, provided there is sufficient soil thickness.

Because Metalith™ will defeat the contact charge for reasonable soil thicknesses (a foot or more will provide standoff and significant mass) and the shaped charge and flyer plate threats can be assessed using software such as CONWEP, the Metalith™ barrier was not modeled in the Task 3 simulations. Consequently, row 3 was removed from Table 7.

Therefore, given those exclusions, Table 8 provides a summary of the technologies that were numerically simulated. The first column in the table references the section in the report where the simulation of each technology is discussed.

Table 7. Summary of Possible Assessments by Blast Mitigation Technology and Threat

			Column No.	1	2	3	4
Row No.	Mitigation Category	Subcategory	Vendor	Bulk Explosive	Contact Charge	Shaped Charge	Flyer Plate
1	Stiff Reinforcement	Fiber-Reinforced Polymer	QuakeWrap™, Sika, Fyfe	1.1	1.2	1.3	1.4
2		Steel-Reinforced Thermoplastic	Hardwire™	2.1	2.2	2.3	2.4
3	Independent Barrier	Steel-Clad Earthen Barrier	Infrastructure Defense Tech	3.1	3.2	3.3	3.4
4		Light-Weight Blast-Resistant Panels	Armor Designs, Inc.	4.1	4.2	4.3	4.4
5	Dependent Barrier	Steel Encased Fiber-Reinforced Concrete	Composite Technologies	5.1	5.2	5.3	5.4
6		Protective Jacket	WinTec Security	6.1	6.2	6.3	6.4
7	Crushable Layer	Compartmentalized Heat-Treated Perlite	BlastGard®	7.1	7.2	7.3	7.4
8	Ductile Layer	Polyurea Coating	Specialty Products Inc.	8.1	8.2	8.3	8.4
		Polyurethane Coating	BASF				
		Polymer Coating	DefensTech Int. Inc.				
			Mid-American Group				
Fiber-Reinforced Polyurethane	Berry Plastics™						

Table 8. Reduced Simulation Matrix for Contact Charge Threat

Report Section No.	Category	Subcategory	Vendor
4.3.2.1	Stiff Reinforcement	Fiber-Reinforced Polymer	QuakeWrap™, Sika, Fyfe
4.3.2.2		Steel-Reinforced Thermoplastic	Hardwire™
4.3.3	Dependent Barrier	Steel-Encased Fiber-Reinforced Concrete	Composite Technologies
4.3.4	Crushable Layer	Compartmentalized Heat-Treated Perlite	BlastGard®
4.3.5	Ductile Layer	Polyurea Coating	Specialty Products Inc.
		Polyurethane Coating	BASF
		Polymer Coating	DefensTech Int. Inc.
			Mid-American Group
Fiber-Reinforced Polyurethane	Berry Plastics™		

4.2 Contact Charge FEA Model

In the literature search performed in Task 1, limited experimental data and essentially no engineering evaluations were found in regards to the vulnerability of unprotected and protected pipeline components from explosive threats of any kind. Therefore, to assess the vulnerabilities of existing pipelines and the performance of the candidate blast mitigation technologies, PEC employed a combination of engineering judgment, analysis approaches, and numerical methods.

4.2.1 Modeling Approach

To assess the contact charge threat, a revised version of the finite-element analysis (FEA) model described in Section 3.3.3.2 was used. As before, the contact charge was composed of C4. The geometry of the charge was a box with dimensions in these ratios, as shown in Figure 43:

- Height = w
- Width = w
- Length = w

The Arbitrary Lagrangian Eulerian (ALE) technique was used, in which the pipeline was modeled with Lagrangian elements and the explosive, external air, and liquid/gas in the pipe were modeled as Eulerian.

The Task 3 quarter-symmetry model and dimensions are shown in Figure 49. Quarter-symmetry was used to reduce run times, and figures in this report that illustrate half-symmetry or no

symmetry are simply reflections of the underlying quarter-symmetry model. Other revisions to the Task 2 model discussed in Section 3.3.3.2 included elimination of model instabilities by modifying the Lagrangian mesh on the solid parts and refining the Eulerian mesh.

For all simulations, the pipe had a 24-in diameter, and the wall was 0.75-in thick, as shown in Figure 49. The wall thickness was increased from the Task 2 thickness of 0.25-in to 0.75-in because the larger value is a minimum wall thickness more commonly observed in pumps and compressors. As discussed in Section 3.4.1.7, pumps and compressors have the highest priority for protection. Because contact charge failure is highly localized, it was not necessary to alter the geometry of the pipeline component to make it visibly more like a pump or compressor or to simulate a suite of diameters. The 24-in diameter circular wall of a pipe provided a reasonable approximation of the curved wall of a pump or compressor.

Failure was defined as breach of the pipeline component. It is possible that a contact charge could render a pump or compressor inoperable without breach of the side wall. However, modeling the innerworkings of a pump or compressor was beyond the scope of this effort, leaving wall breach as the best indication of failure.

Based on discussions with pump and compressor manufacturers and distributors, the material of the pipeline component was assumed to be API X60 steel, which has a nominal yield strength of 60,000 psi and an ultimate strain of 20%. As discussed in Section 4.3.1, a bilinear elastic-plastic constitutive model was used to represent the pipe steel, and modest strain-hardening was included.

For each combination of charge weight and blast mitigation technology, two pipe contents were modeled: gas and liquid. For the gas-filled pipe, the gas itself was not explicitly modeled; an empty pipe was used with a pressure load applied to the inside face.

For the liquid-filled pipe, an incompressible liquid (specific gravity 1.0) was explicitly modeled, but in an unpressurized state. The stress state in the pipe itself was imposed by applying a pressure load to the inside face, just as done for the gas-filled case. This two-step approach to the liquid-filled case was used for simplicity and efficient simulation times. Since the liquid is essentially incompressible, the mechanical performance was essentially identical to a liquid under pressure.

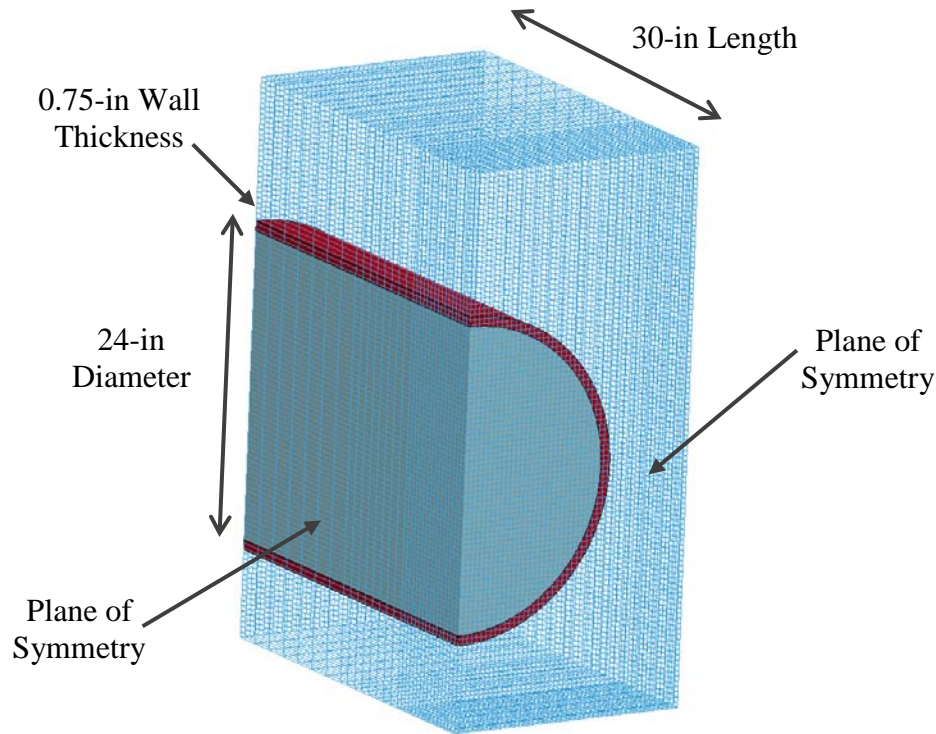


Figure 49. Quarter-Symmetry Model

All faces of the Eulerian right parallelepiped shown in Figure 49 except those labeled *plane of symmetry* were defined as non-reflecting using the LS-DYNA keyword *BOUNDARY_NON_REFLECTING. As a result, pressures on those faces of the Eulerian mesh were not amplified due to reflection. These non-reflecting boundaries allowed the explosive products to continue to expand and exit the system (Eulerian mesh), just as would occur in an outdoor environment.

These non-reflecting boundaries cannot be applied to Lagrangian solids. Therefore, a 30-in length was used for the pipeline component so that reflections at the end of the component did not interfere significantly with stresses in the component near the charge. If the speed of sound in steel is taken to be 5,960-m/s, then it takes the reflected stress wave 256-usec to cover the 60-in distance from charge to end and back again. But by that time in most simulations, the hole diameter of the pipeline component was near convergence. For example, as shown in Figure 50, for a ww-lb charge the hole diameter was 3.4-in at 260-usec after detonation, whereas the final hole diameter was 3.6-in. As such, the pipe length was deemed long enough for reasonable damage estimation.

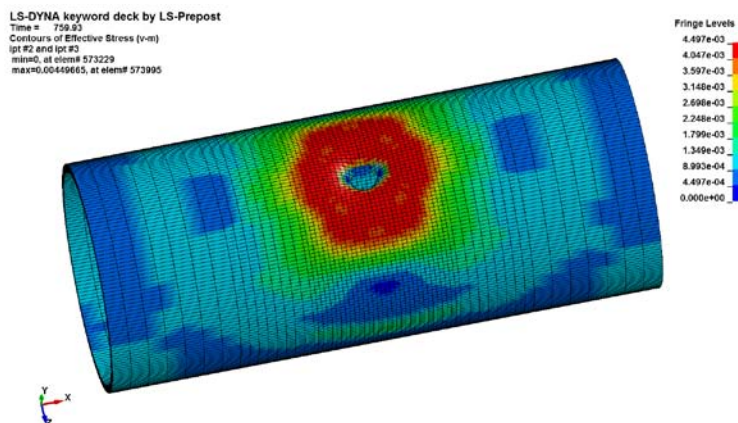


Figure 50. Hole diameter: Bare Pipe ww-lb Gas Content at 260-usec
(Reflections about XY and YZ Planes)

The contact charge was box-shaped as shown in Figure 43. The properties of the C4 for the material model and equation of state were the same as employed in the Task 2 modeling.

For purely computational reasons, null parts were included for the pipeline component in all models. Parts in LS-DYNA are assemblages of finite elements. The null part was simply a shell part of identical dimensions to the component shell part, and the nodes of the two were merged. The null part was included so that the component could effectively have two sets of shell normal vectors, one pointing outward and one pointing inward. The outward vectors permitted the pipeline component to interact with the Eulerian fluids outside of it, and the inward ones permitted interaction with the internal fluids. In all cases, the mass of the component was split between the pipeline component part and the null part, which had the LS-DYNA material definition *MAT-NULL.*MAT_NULL only added mass to the system, not strength.

4.2.2 Modeling Issues

Three issues have bearing on these simulation results: the constitutive models, the refinement of the mesh, and the presence of sliding energy in some of the models.

4.2.2.1 Constitutive Models

The greatest source of uncertainty in these simulations was the constitutive models for the blast mitigation materials. In some cases, the constitutive model had not been calibrated to the material strengths used for the simulation. For example, the steel-encased high-performance concrete discussed in Section 4.3.3 has a compressive strength significantly higher than the concrete used to calibrate the LS-DYNA constitutive model. In other cases, the actual material constants inputted through the constitutive models were known only approximately. This issue is discussed for each simulation in which it was a factor.

4.2.2.2 Mesh Refinement

In some cases, particularly for smaller charge weights, a finer Lagrangian mesh would have allowed greater precision in predicting the exact hole diameter. For small charges and small hole diameters, the characteristic dimension of the Lagrangian mesh was coarse with respect to the

hole diameter. However, reducing the mesh size would have exponentially increased run times because the Eulerian mesh would need to be refined proportionately. Therefore, the precision of the small hole diameters is low, approximately ± 0.5 -in, which is the largest dimension of the pipe shell elements near the charge.

4.2.2.3 Sliding Energy

Relatively large values of sliding energy were observed in some of the simulations, particularly in those for the fiber-reinforced polymer. LS-DYNA handles contact between node-defined surfaces using a contact algorithm. Sliding energy is a measure how much the nodes of one surface penetrate the nodes of another, when the two surfaces are in contact. The sliding energies did not affect the energies critical to the simulation—internal and kinetic—and instances where the sliding energy was high resulted in hole diameters that were consistent with similar instances where it was low. Therefore the relatively large values of sliding energy were deemed acceptable.

4.3 Contact Charge Simulation Results

4.3.1 Bare Pipeline Component

As a basis for comparison, a bare pipeline component was modeled to determine its resistance to a contact charge, in the absence of retrofitting. The wall of the pipeline component was modeled using shell elements with a thickness of 0.75-in to match the wall thickness of the component. The charge was positioned directly in contact with the component, as shown in Figure 51. The component had a 24-in diameter and 30-in length. These dimensions were retained for all simulations except with the steel-encased fiber-reinforced concrete, as discussed in Section 4.3.3. Both gas and liquid contents were modeled.

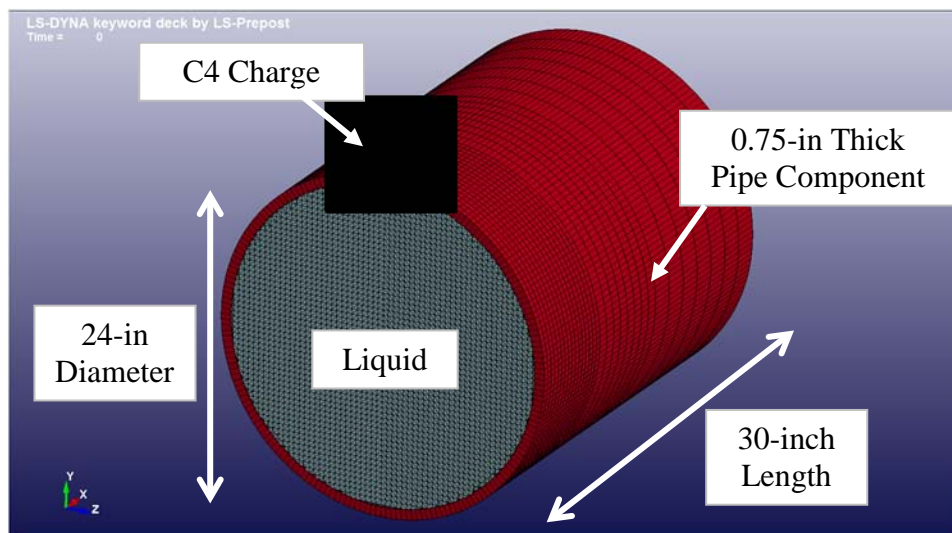


Figure 51. Bare Pipe Component Model (Reflection about XY Plane)

The material properties of API X60 line pipe were used for the pipeline component. These were included in the LS-DYNA *MAT_PIECEWISE_LINEAR_PLASTICITY constitutive model using the material constants shown in Table 9. These constants were used for the pipeline component in all models. The simulation was actually conducted with the units g-cm-usec (10^{-6} sec), but the material constants are reported in English units for consistency within the report.

Table 9. LS-DYNA Material Constants for Pipeline Component (*MAT_PIECEWISE_LINEAR_PLASTICITY)

Parameter	LS-DYNA Symbol	Value	Units
Density	RO	7.33E-04	lb-s ² /in ⁴
Young's Modulus	E	2.90E+07	psi
Poisson's Ratio	PR	0.32	
Yield Stress	SIGY	6.00E+04	psi
Tangent Modulus	ETAN	2.90E+04	psi
Failure Strain	FAIL	0.20	

Ten simulations were performed on the bare pipe model, and the variables were the weight of the C4 charge and the contents of the pipe. The results from these simulations are summarized in Table 10. As shown in the table, a charge of ww-lb was the smallest charge required to breach the pipeline component wall for both liquid and gas contents.

The hole diameters in the gas cases were larger than in the liquid cases for two reasons. First, the liquid added mass to the structure, increasing its inertial resistance to the high-rate loading by the contact charge. Second, the liquid is incompressible and inertially confined inside the pipe which added structural resistance. Inertial confinement was present even though the boundary at the end of the pipe was non-reflecting because the loading rate was much higher than the response time of the liquid.

Table 10. Simulation Results for Bare Pipe

C4 Charge Weight [lb]	Pipe Component Contents	Failure Diameter [in]
ww	Liquid	No failure
ww	Liquid	1.2
ww	Liquid	2.9
ww	Liquid	3.4
ww	Liquid	4.2
ww	Gas	No failure
ww	Gas	2.8
ww	Gas	3.6
ww	Gas	4.5
ww	Gas	4.5

Figure 52 through Figure 55 illustrate detonation of a ww-lb charge on a bare pipe with liquid contents. For clarity, only the pipe and C4 charge are rendered. After 40-usec, the gas generated by the C4 detonation has expanded from the initial position in Figure 52 to the position in Figure 53. After 140-usec, it has reached the position in Figure 54. By that time, the gas began to interact with the non-reflecting boundary of the Eulerian mesh, as shown in Figure 55.

Figure 56 through Figure 58 illustrate the initial von Mises stress state of the pipe and propagation of the von Mises stress during the detonation. The fringe stress legend on each figure is in units of $g/(cm\text{-}usec^2)$, consistent with the original simulation units. Figure 56 shows the pipe uniformly stressed by 800-psi internal pressure, immediately prior to detonation. Thereafter, the C4 charge quickly stresses the pipe to yield, and by 140-usec, a significant number of elements have failed, reaching the ultimate strain of 20% through the thickness of the shell. Figure 59 illustrates the breach in the bare pipe with liquid contents due to a ww-lb charge at 1000-usec.

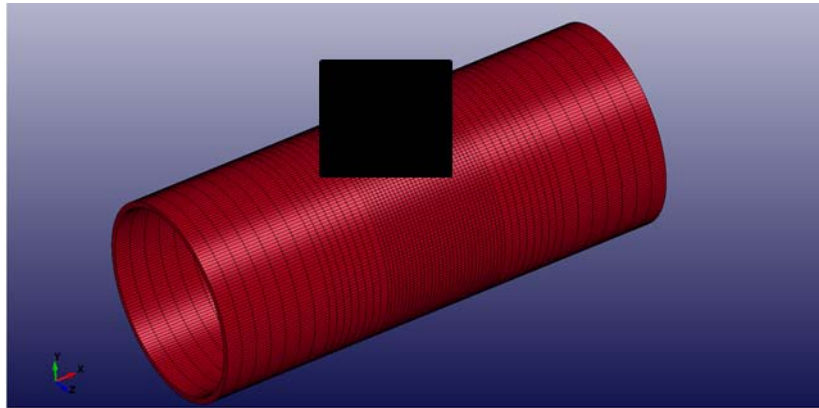


Figure 52. Bare Pipe ww-lbC4 Charge Liquid Content, Initial Condition (Reflections about XY and YZ Planes)

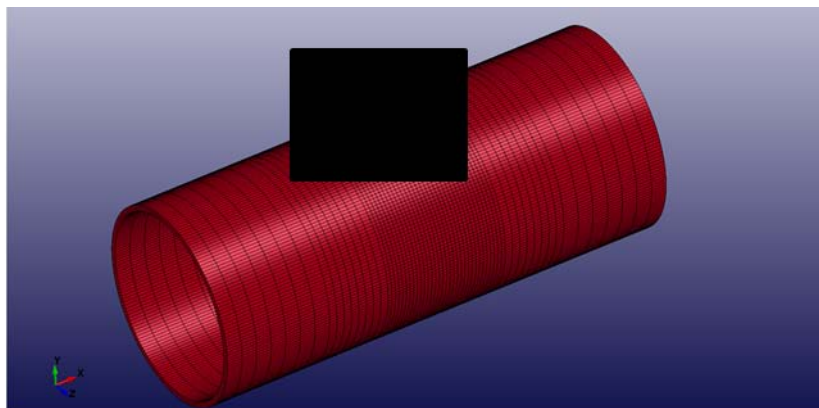


Figure 53. Bare Pipe ww-lbC4 Charge Liquid Content, 40-usec after Detonation (Reflections about XY and YZ Planes)

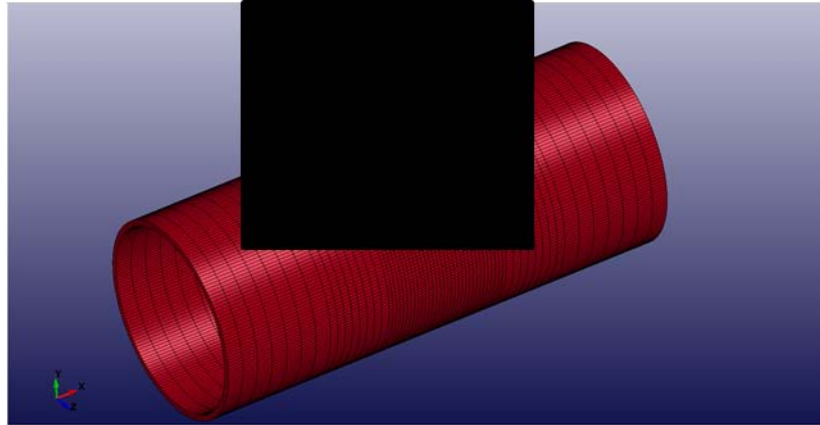


Figure 54. Bare Pipe ww-lbC4 Charge Liquid Content, 140-usec after Detonation (Reflections about XY and YZ Planes)

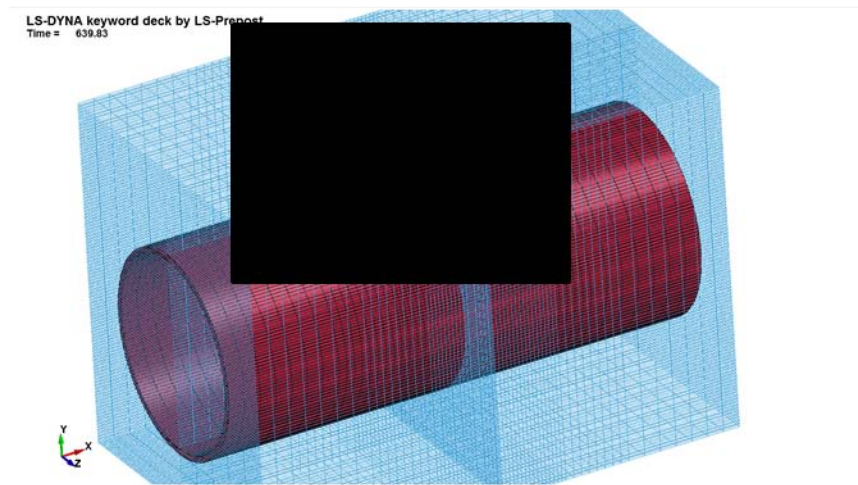


Figure 55. Bare Pipe ww-lbC4 Charge Liquid Content, 140-usec after Detonation Eulerian Mesh Rendered (Reflections about XY and YZ Planes)

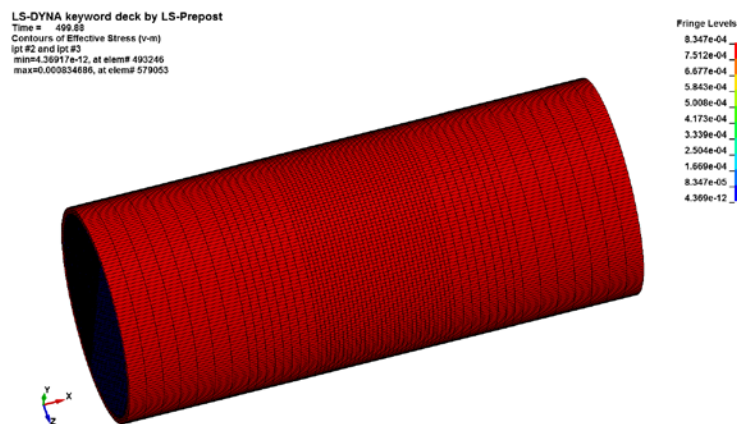


Figure 56. Bare Pipe ww-lbC4 Charge Liquid Content, Initial Condition, Von Mises Stress (Reflections about XY and YZ Planes)

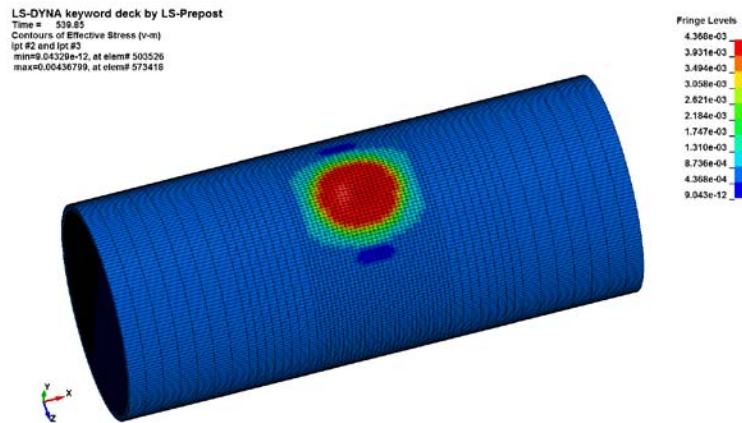


Figure 57. Bare Pipe ww-lbC4 Charge Liquid Content, 40-usec after Detonation, Von Mises Stress (Reflections about XY and YZ Planes)

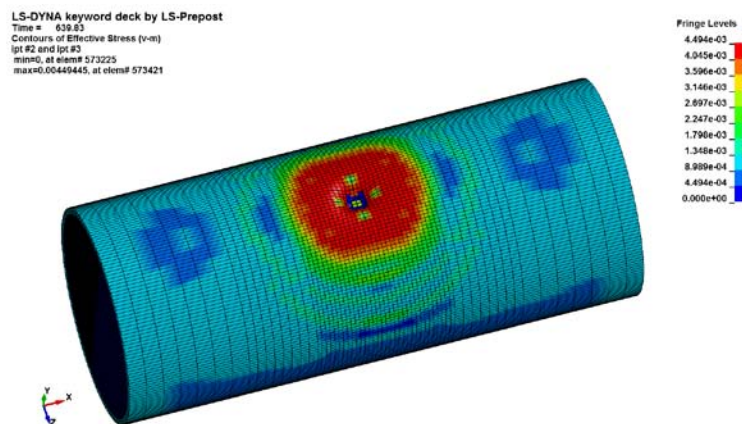


Figure 58. Bare Pipe ww-lbC4 Charge Liquid Content, 140-usec after Detonation, Von Mises Stress(Reflections about XY and YZ Planes)

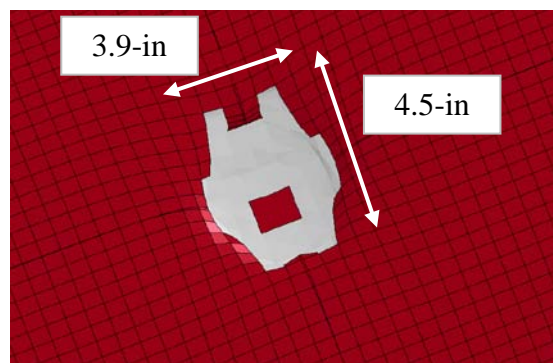


Figure 59. Hole Diameter: Bare Pipe ww-lbC4 Charge Liquid Content at 1000-usec (Reflections about XY and YZ Planes)

4.3.2 Stiff Reinforcement

4.3.2.1 Fiber-Reinforced Polymer

For the fiber-reinforced polymer simulations, the fiber was assumed to be carbon. The carbon fiber reinforced polymer (CFRP) was modeled as shell elements offset from the 0.75-in thick pipe component. The thickness of the CFRP was 0.50-in because that is the maximum practical thickness for a field installation, based on correspondence with the CFRP vendors. The model is illustrated in Figure 60.

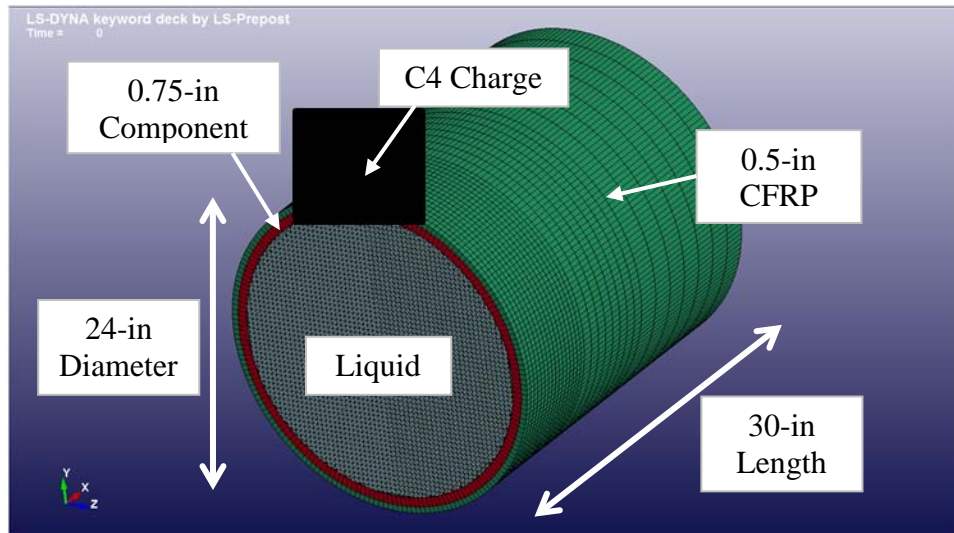


Figure 60. CFRP Model (Reflection about XY Plane)

Material constants were obtained for CFRP from the vendors QuakeWrap™ and Sika Corporation, and representative values were input for the constitutive model. The LS-DYNA constitutive model *MAT_ELASTIC was used, and an erosion criterion of 1.3% for maximum principal strain accounted for material failure. These values are shown in Table 11.

Table 11. LS-DYNA Material Constants for CFRP (*MAT_ELASTIC)

Parameter	LS-DYNA Symbol	Value	Units
Density	RO	1.4E-04	lb-s ² /in ⁴
Young's Modulus	E	9.49E+04	psi
Poisson's Ratio	PR	0.22	
Max Principal Strain	MXEPS	1.3%	

To account for adhesion between the resin matrix of the CFRP and the pipeline component, the LS-DYNA contact definition CONTACT_TIEBREAK_SURFACE_TO_SURFACE was used. The shear and normal strengths of the contact were 7,150-psi, which is the tensile strength of the resin matrix. The shear strength of the resin was not explicitly known, and therefore the generous assumption was made that it was equal to the tensile strength of the resin.

Ten simulations were conducted, five with liquid and five with gas contents. As shown in Table 12, a charge weight of ww-lbs was the smallest charge to breach for both the liquid and gas cases. The breach diameter for the liquid was 1.1-in, and for the gas, it was 2.5-in. Again, this difference was due to the mass and compressibility differences of liquid and gas. The hole diameter for the ww-lb charge liquid case is shown in Figure 61. Only the pipe and liquid are rendered in the figure, for clarity.

Table 12. Simulation Results for CFRP

C4 Charge Weight [lb]	Pipe Component Contents	Failure Diameter [in]
ww	Liquid	No failure
ww	Liquid	No failure
ww	Liquid	1.1
ww	Liquid	2.5
ww	Liquid	3.4
ww	Gas	No failure
ww	Gas	No failure
ww	Gas	2.5
ww	Gas	4.1
ww	Gas	4.9

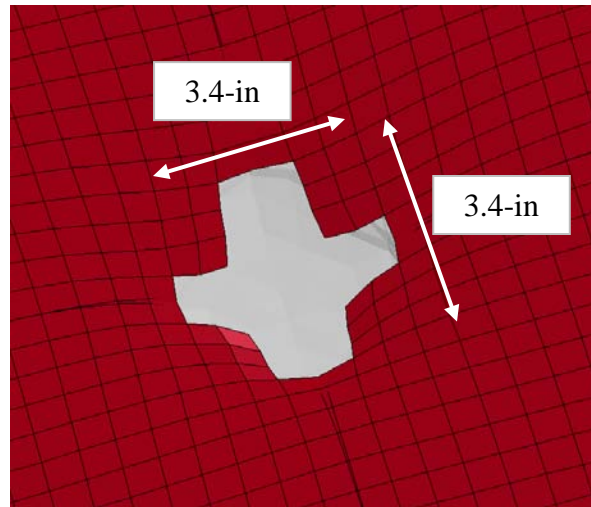


Figure 61. Hole Diameter: CFRP ww-lbC4 Charge Liquid Content at 1000-usec (Reflections about XY and YZ Planes)

4.3.2.2 Steel-Reinforced Thermoplastic

In contrast to CFRP, the details of applying steel-reinforced thermoplastic (SRT) to a civil engineering structure are not widely available. Therefore, for the purposes of these simulations, SRT was assumed to be qualitatively similar to CFRP: strong fibers adhered to a structure using a resin matrix.

The SRT was modeled using shell elements 0.5-in thick, assumed to be the maximum practical thickness for installation, as with the CFRP. Consequently, the model used for the SRT was equivalent to the one illustrated in Figure 60 except that SRT was modeled in place of CFRP.

The constitutive model was *MAT_PIECEWISE_LINEAR_PLASTICITY, and the SRT was modeled as a continuum where strength and mass properties were “smeared” through the thickness. The volume fraction of the steel fiber was assumed to be 40%. The separate densities, Young’s moduli, and yield stresses were then weighted by volume to determine the corresponding continuum material constants. A Poisson ratio of 0.35 was assumed for the continuum, which is a value close to that of steel and fiber glass. A failure strain of 0.75% was used. The tangent modulus was 10% of the Young’s modulus to provide some strain hardening over the short interval of plastic strain. These material constants are provided in Table 13. The same contact definition used to adhere the CFRP to the pipe component was used for the SRT.

Table 13. LS-DYNA Material Constants for SRT Continuum Material (*MAT_PIECEWISE_LINEAR_PLASTICITY)

Parameter	LS-DYNA Symbol	Value	Units
Density	RO	3.77E-04	lb-s ² /in ⁴
Young's Modulus	E	1.17E+07	psi
Poisson's Ratio	PR	0.35	
Yield Stress	SIGY	1.84E+05	psi
Tangent Modulus	ETAN	1.18E+06	psi
Failure Strain	FAIL	0.75%	

The results of ten SRT simulations are shown in Table 14. A charge of ww-lb was the smallest charge required to breach both the liquid-containing and gas-containing component protected with SRT. The hole diameter for the ww-lb charge liquid case is shown in Figure 62. In the figure, only the pipe and liquid are rendered, for clarity.

Table 14. Simulation Results for SRT

C4 Charge Weight [lb]	Pipe Component Contents	Failure Diameter [in]
ww	Liquid	No failure
ww	Liquid	No failure
ww	Liquid	1.1
ww	Liquid	2.2
ww	Liquid	3.5
ww	Gas	No failure
ww	Gas	No failure
ww	Gas	1.6
ww	Gas	3.8
ww	Gas	5.0

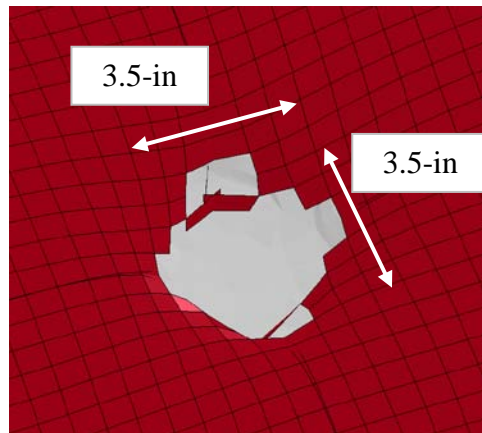


Figure 62. Hole diameter: SRT ww-lbC4 Charge Liquid Content at 1000-usec (Reflections about XY and YZ Planes)

4.3.3 Steel-Encased Fiber-Reinforced Concrete

Composite Technologies is capable of installing their steel-encased fiber-reinforced concrete (SEFRC) product in a variety of thicknesses and geometries, i.e., the shape can follow the contour of a pump or valve that is not circular in cross-section. A thickness of 5-in was selected for the high-performance concrete (HPC) core in this analysis as a realistic geometry. The inner and outer layers of steel on the SEFRC were assumed to be 0.25-in thick, based on review of vendor literature about the product. The overall geometry is presented in Figure 63. Again, other dimensions and configurations are possible, as the product can be tailored for different applications.

The HPC core was modeled using solid elements, as shown in Figure 63. The inner and outer steel layers were modeled as shell elements. The 30-in model length was increased to 44-in to

ensure that blast-wave reflections from the end of the model did not have sufficient time to significantly influence the response of the model near the detonation.

The inner and outer steel layers were assumed to be conventional 50,000-psi steel and were characterized using the LS-DYNA constitutive model *MAT_PIECEWISE_LINEAR_PLASTICITY. These constants are provided in Table 15.

Table 15. LS-DYNA Material Constants for Inner and Outer Steel
(*MAT_PIECEWISE_LINEAR_PLASTICITY)

Parameter	LS-DYNA Symbol	Value	Units
Density	RO	7.33E-04	lb-s ² /in ⁴
Young's Modulus	E	2.90E+07	psi
Poisson's Ratio	PR	0.32	
Yield Stress	SIGY	5.0E+04	psi
Tangent Modulus	ETAN	2.90E+04	psi
Failure Strain	FAIL	20%	

The LS-DYNA constitutive model used for the HPC core was *MAT_CONCRETE_DAMAGE_REL3. Material constants are proprietary to the vendor and are not provided in this report. Regardless, the HPC core is concrete of a very high compressive strength, but the constitutive model *MAT_CONCRETE_DAMAGE_REL3 was developed for normal-strength concrete. Therefore, the material model used strength, modulus, and failure surface parameters based upon the compressive strength of the HPC material and scaling proportions typical for normal-weight concrete. In actuality, the HPC material may have somewhat different failure surface shapes than this scaling method yields, but the significant effort required to develop material constants for HPC was outside the scope of this effort. Thus, the concrete model could be improved with other constants, but for the purposes of this project, the default formulation, with the higher strength, was used.

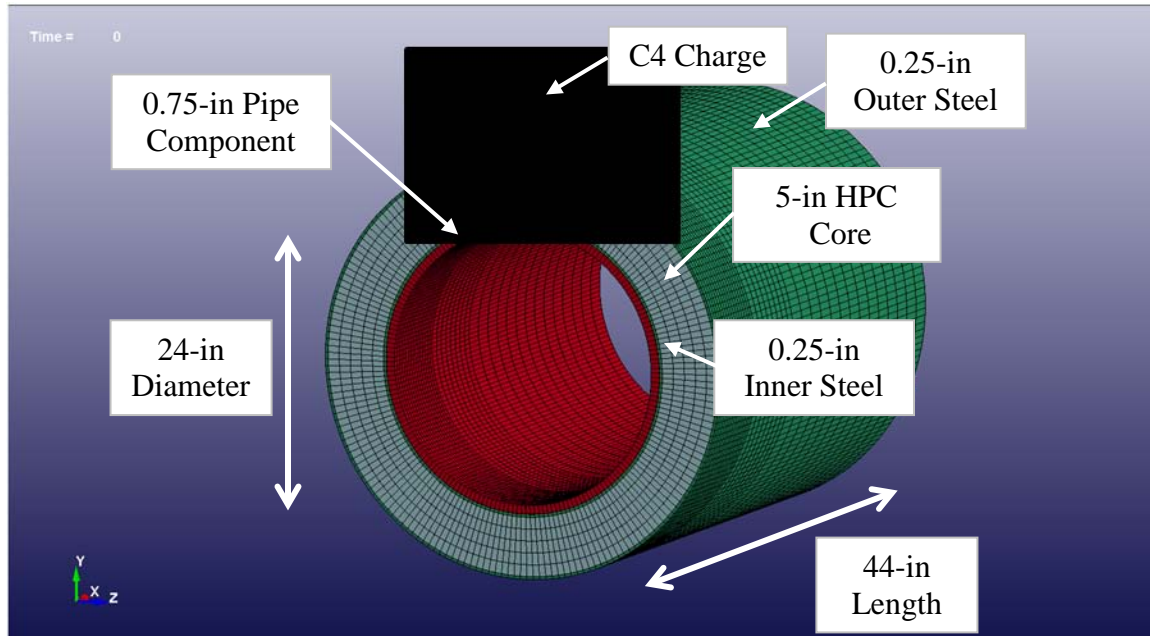


Figure 63. SEFRC Model, Gas-Filled Case (Reflection about XY Plane)

Although there is composite action between the HPC core and the inner and outer steel layers, adhesive and frictional resistance between the HPC core and the steel encasing layers was assumed to be zero. Transmission of load among the parts by bearing was modeled using the LS-DYNA contact `CONTACT_AUTOMATIC_SINGLE_SURFACE`.

To improve coupling between the solid elements of the HPC core and the explosive, a 0.125-in thick shell part with dimensions identical to the outer face of the solid part was included. Nodes of the shell part were merged with the nodes of the outer face of the solid part. The shell part was `*MAT_NULL` and had the density of water. The shell part added negligible mass and no strength to the structure and was regarded structurally as the equivalent of a packaging material, for example.

The minimum C4 charge weight required to breach the pipeline component protected with the SEFRC was over ww-lbs, whether the contents of the component were liquid or gas. Hole diameters are not reported for charge weights greater than ww-lbs because long run times were required for the SEFRC model to reach equilibrium. The model had significantly more elements than the other models and significantly more mass. The large amount of mass in the SEFRC product increased the clock time for the entire model to reach equilibrium.

An example of the SEFRC resisting a ww-lb contact charge is shown in Figure 64. The von Mises stresses in the figure illustrate how the HPC core carries stresses around the pipeline component as a compression ring. This frame was recorded early in the response, at 110-usec after detonation.

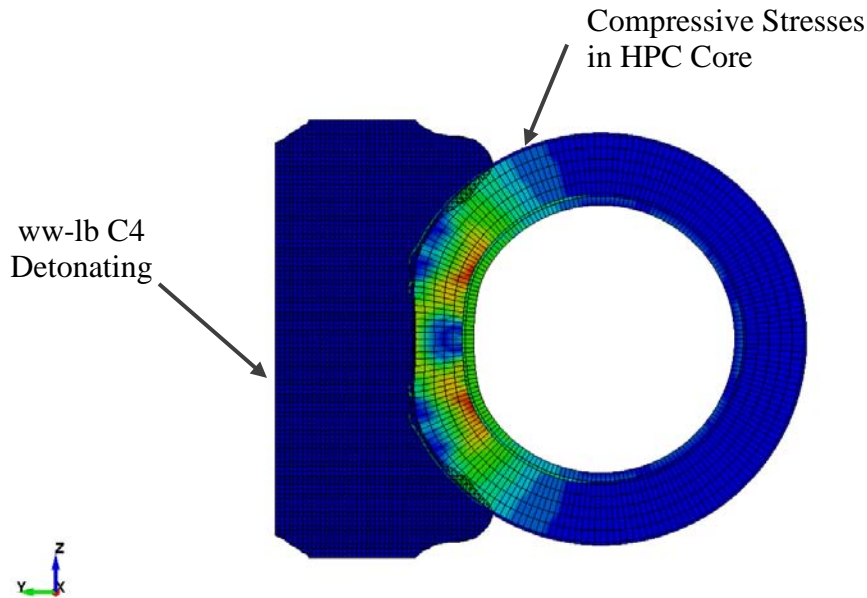


Figure 64. Von Mises Stresses in the Composite Technologies System 110-usec after Detonation (Front View, Reflection about XY Plane)

4.3.4 Compartmentalized Heat-Treated Perlite

Since the compartmentalized, crushable perlite inherently provides standoff due to its thickness, two simulations were performed to determine the benefits of just standoff and of standoff with the crushable perlite. In the first simulation, a ww-1b charge was placed at a 3-in standoff from the pipeline component with only air in the intervening space. In the second case, a 3-in layer of perlite was placed between the charge and the pipeline component. These two configurations are illustrated in Figure 65 and Figure 66, respectively. Only the charge, pipe component, and perlite are rendered for clarity.

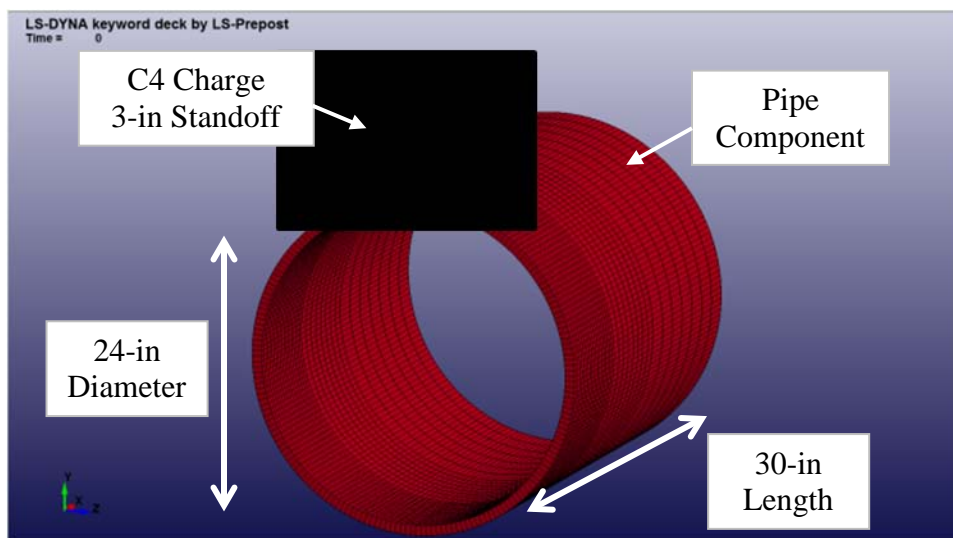


Figure 65. Pipeline Component with 3-in Charge Standoff (Reflection about XY Plane)

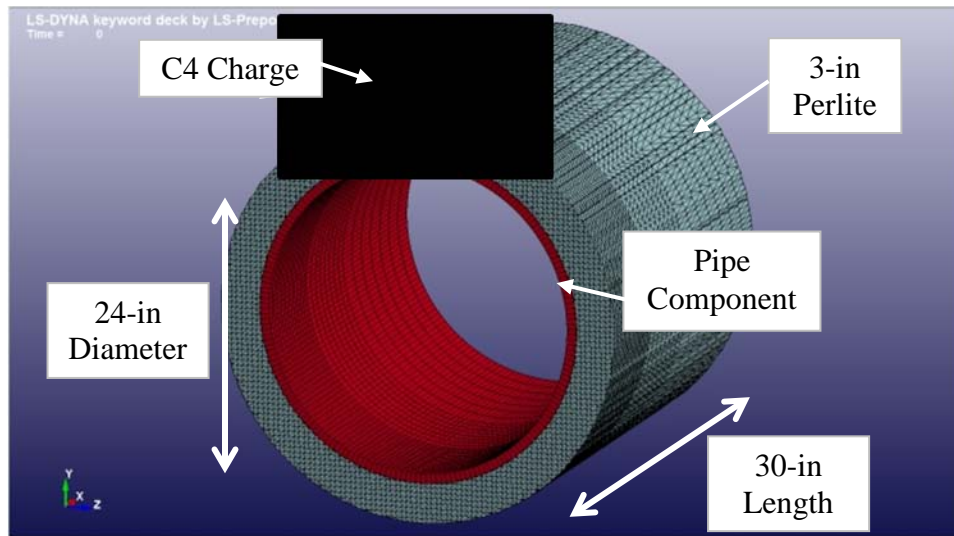


Figure 66. Pipeline Component with 3-in Perlite Layer (Reflection about XY Plane)

The perlite was modeled as an Eulerian fluid using the LS-DYNA constitutive model *MAT_SOIL_AND_FOAM; early attempts at representing the perlite using a Lagrangian material failed due to its lack of strength and low density. The material constants shown in Table 16 were used for the model, as well as the curve of pressure versus volumetric strain shown in Figure 67. Fields not shown were set to default except that the volume-crushing option was turned on. The strength properties of perlite were derived by down-scaling sandy soil properties based on the density ratio of the materials. These properties are not necessarily the exact properties of perlite; however, they provide a reasonable level of accuracy for the scope of this research.

Table 16. LS-DYNA Material Constants for Perlite (*MAT_SOIL_AND_FOAM)

Parameter	LS-DYNA Symbol	Value	Units
Density	RO	9.32E-06	lb-s ² /in ⁴
Shear Modulus	G	3.77E+01	psi
Yield Constant	A0	7.57E-01	psi ²
Pressure Cutoff	PC	-1.89E-01	

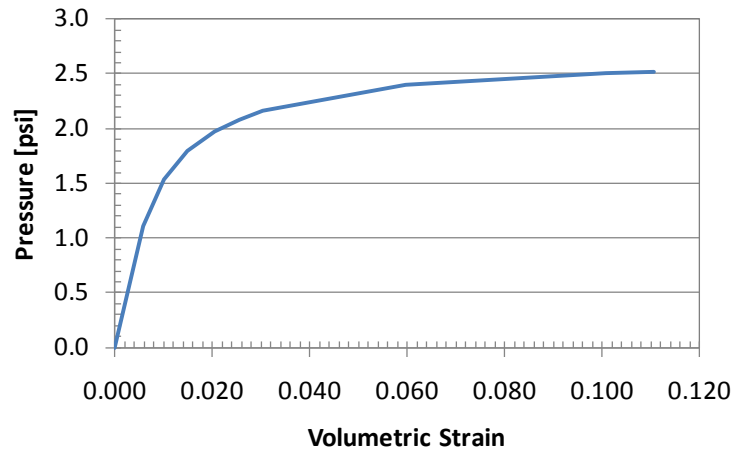


Figure 67. Assumed Pressure versus Volumetric Strain for Perlite

The condition of the perlite 1000-usec after the C4 detonation is shown in Figure 68. The quarter symmetry model is reflected about two axes and Eulerian fluid inside the component representing the gas is colored white to highlight the breach region. Details of the failure region with and without perlite shown in Figure 69 (a) and (b) respectively illustrate that the perlite marginally reduces the characteristic dimensions of the breach area.

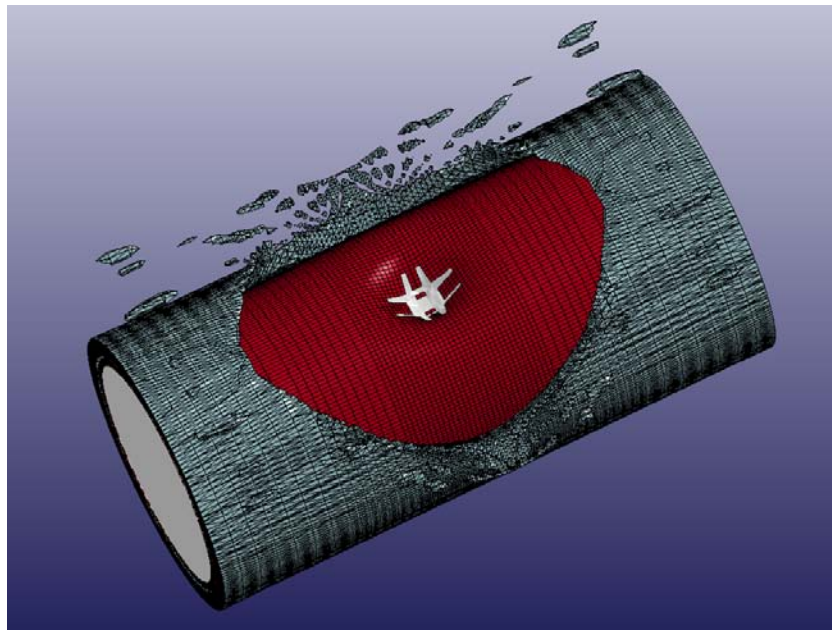


Figure 68. Condition of Perlite 100-usec after C4 Detonation (Reflections about XY and YZ Planes)

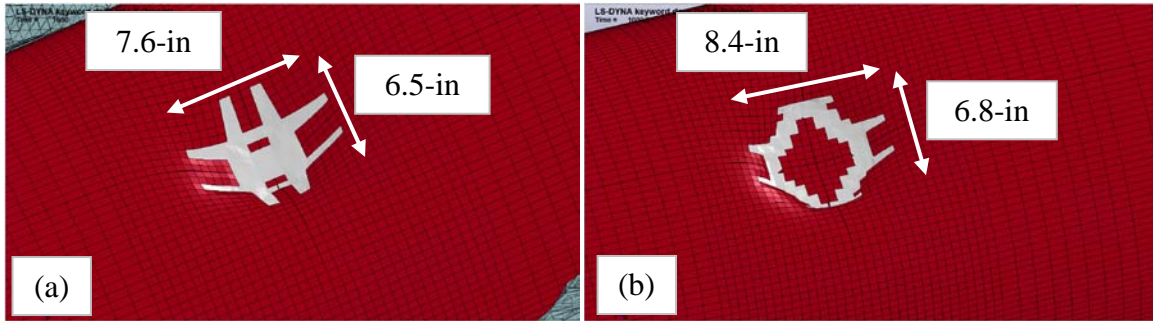


Figure 69. (a) Pipe Component with Perlite (1000-usec)
 (b) Pipe Component without Perlite (1000-usec)

4.3.5 Ductile Polymer

The ductile polymer was assumed to have the properties of a spray-on polyurea. Many of the vendors of ductile polymer retrofits discussed in the Task 1 *Survey of Existing Technology and Research* use polyureas, and retrofitting a large, civil structure, such as a pipeline, can be efficiently accomplished by spraying the polyurea on the structure.

The polyurea was modeled as shell elements offset from the 0.75-in thick pipe. The polyurea was made 0.5-in thick because that is the maximum practical thickness for a spray-on installation, based on past research conducted by PEC on polyureas. As a result, the polyurea model was identical to the CFRP model shown in Figure 60 except that the outer retrofit layer was polyurea, not CFRP.

The LS-DYNA constitutive model *MAT_PLASTIC_KINEMATIC was used for the polyurea. The material properties are provided in Table 17. The density, Poisson’s ratio, and failure strain of polyurea are widely known, and representative values were used. Past research conducted by PEC has shown that the Young’s modulus of polyurea increases significantly for high strain rates and that the yield strength increases about 10%. Therefore, to account for rate effects, a factor of 10 was applied to the static Young’s modulus and 1.1 to the static yield stress. No data was available on the tangent modulus of polyurea, and consequently 0.5% of the Young’s modulus was selected to provide moderate strain hardening from the yield strain to the failure strain of 250%. All other values on the constitutive model were LS-DYNA defaults.

Table 17. LS-DYNA Material Constants for Polyurea (*MAT_PLASTIC_KINEMATIC)

Parameter	LS-DYNA Symbol	Value	Units
Density	RO	1.21E-04	lb-s ² /in ⁴
Young’s Modulus	E	6.50E+05	psi
Poisson’s Ratio	PR	4.85E-01	
Yield Stress	SIGY	3.07E+03	psi
Tangent Modulus	ETAN	3.25E+02	psi
Failure Strain	FAIL	250%	

As with the CFRP and SRT, ten simulations were performed on the polyurea model, the variables being the charge weight and contents of the pipe. The results are shown in Table 18. A charge weight of ww-lb was sufficient to breach the liquid case, whereas a charge weight of ww-lb was sufficient to breach the gas case.

Figure 70 illustrates the hole diameter for a ww-lb charge with liquid contents. In one direction, the failure dimension is 3.4-in, and in the other it is 4.0-in. These were averaged to get the value of 3.7-in reported in Table 18.

Table 18. Simulation Results for Polyurea

C4 Charge Weight [lb]	Pipe Component Contents	Failure Diameter [in]
ww	Liquid	No failure
ww	Liquid	No failure
ww	Liquid	1.3
ww	Liquid	2.7
ww	Liquid	3.7
ww	Gas	No failure
ww	Gas	1.2
ww	Gas	2.9
ww	Gas	4.2
ww	Gas	4.8

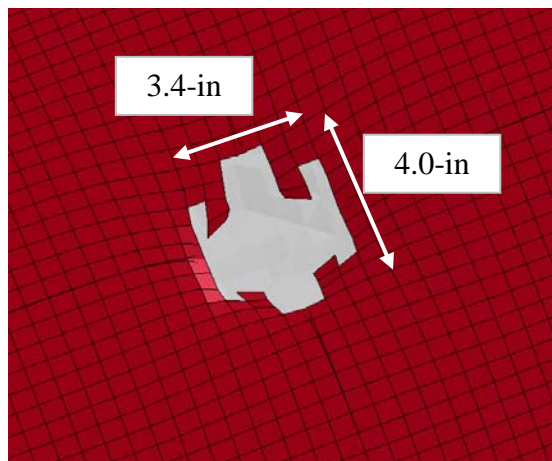


Figure 70. Hole diameter for ww-lb C4 Charge Liquid Contents (Reflections about XY and YZ Planes)

4.4 Assessment by Criteria

The blast mitigation technologies were assessed according to the following set of criteria:

- Protection Level. The protection level is the maximum charge weight, at a certain standoff, or as the shortest standoff at a set charge weight, that the technology will protect against. In the case of contact charge, this criterion is simply charge weight.
- Cost. The cost includes installing, maintaining, and replacing a blast mitigation technology; life cycle costs are also important.
- Robustness. Robustness is important for connections to valves, pumps, and other critical components, since the toughness of the technology will be related to ductility of the connection.
- Adaptability. Adaptability is the ability to retrofit existing pipelines and related components of different sizes and in a variety of environments.
- Durability. The blast mitigation technology should provide protection over an extended period of time in harsh environments, as pipelines have a long design life.
- Environmental Impact. The composition of the blast mitigation materials should be environmentally benign.

Of these, the protection level is clearly the most important, and that criterion divides the blast mitigation technologies discussed in this report into two categories: those that provide marginal benefit and those that provide significant benefit. The marginal benefit of the compartmentalized heat-treated perlite has already been discussed. Figure 71 illustrates that the CFRP, SRT and polyurea also provide marginal benefit. In general, the hole diameters of the protected components are only slightly smaller than those of the bare pipe, and in some cases they are even larger. Therefore, none of these technologies are likely to significantly increase the protection level of a bare pipeline component subjected to the contact charge threat.

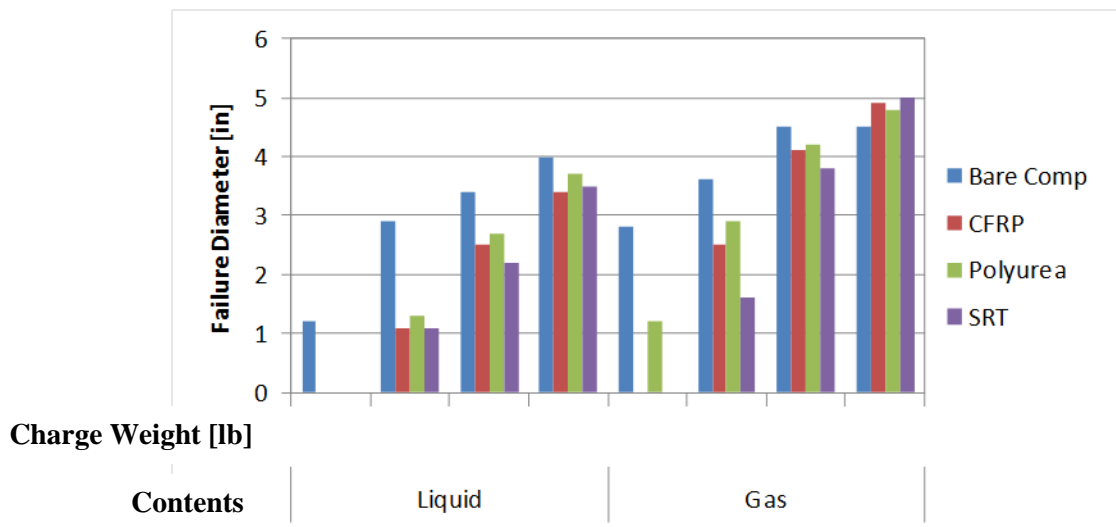


Figure 71. Hole Diameter by Charge Weight, Contents, and Blast Mitigation Technology

In contrast to the other products, the steel-encased fiber-reinforced concrete (SEFRC) cover from Composite Technologies increases the protection level significantly. As discussed in Section 4.3.3, the SEFRC analysis showed the cover can resist greater than a ww-lb C4 charge without permitting breach of a 0.75-in thick pipeline component.

Moving on to the other criteria, the SEFRC vendor has stated that the cost of installing its product is highly dependent on the particular design threat and the geometry of the structure to be hardened. Consequently, the vendor could not provide general installation costs. Maintenance costs are likely low, given that the technology is a combination of steel and concrete, both of which can be readily weatherized. Furthermore, the fact that the cover is installed with removable but tamper-resistant bolts suggests that maintenance can be performed without draconian efforts.

Since the SEFRC product is a composite concrete and steel structure, it is quite robust. Composite Technologies has stated that its product is highly adaptable in that it can be cast to fit any geometric configuration. Also, SEFRC is expected to be highly durable because of the proven durability record of high-performance concrete in general.

The other technology that is expected to increase protection level significantly is the Metalith™ barrier system, as discussed in Section 4.1. As with the SEFRC, the installation costs for Metalith™ are highly dependent on threat and the geometry of the pipeline components to be protected. However, maintenance costs could be large because, much of the Metalith™ barrier would need to be removed to perform inspections and repairs.

Otherwise, the Metalith™ barrier is robust, durable, and likely has a low environmental impact. The durability and non-toxicity of steel and virgin soil is obvious. The barrier system is adaptable in that it could be tailored to protect any geometry of pipeline component. However, depending on the design threat, a large volume of material may be required for sufficient protection, and this fact may significantly reduce adaptability. In some cases, there may not be space for the Metalith™ barrier.

4.5 Conclusions from Assessment of Blast Mitigation Technologies

Simulations for a contact charge threat were performed for five distinct blast mitigation technologies. The bulk explosive threat was not considered because of the inherent resistance of pipelines to such a threat. Shaped charge and flyer plate threats were not considered because they are overwhelming and extreme measures are required to defeat them. However, it is noted that Metalith™, the steel-clad earthen barrier by Infrastructure Defense Technologies, should be effective providing enough soil is placed between the flyer plate or shaped charge and the protected pipeline component.

Five blast mitigation technologies were modeled:

- Carbon fiber-reinforced polymer
- Steel-reinforced thermoplastic
- Steel-encased fiber-reinforced concrete

- Compartmentalized heat-treated perlite
- Ductile layer (polyurea)

Only one of the technologies that were modeled, the steel-encased fiber-reinforced concrete (SEFRC), significantly increased the resistance of a generic pipeline component to contact charge attack. Over ww-lbs of C4 was required to breach a component protected by the SEFRC, compared with ww-lbs required to breach an unprotected component. In addition, the SEFRC can likely satisfy the requirements of adaptability, durability, and minimal environmental impact. For these reasons, the SEFRC product is a viable candidate technology for reducing the vulnerability of pipeline components to the contact charge threat.

The other viable candidate is the Metalith™ barrier system. In principle, it could be used to defeat any practical contact charge threat, and it has the attributes of robustness, durability, and low environmental impact. However, maintenance costs may be significant for a pipeline protected with Metalith™ because of the difficulty of getting access to a particular point on the line. Furthermore, the adaptability of Metalith™ is limited by the fact that considerable space may be required to install it.

Pipeline Blast Mitigation Technologies: Phase 2 Explosive Tests

5 Phase 2 Introduction

Phase 2 was initiated upon completion of Tasks 1 through 3, which are discussed in Sections 2 through 4 of this report, respectively. The results of the Task 3 report were used to develop the Phase 2 *Test Plan*, which was executed as Task 5 (Task 4 was project management). The Task 5 explosive tests included source characterization and pipe, valve, and protective structure tests. The source characterization tests, discussed in Section 6 of this report, verified the repeatability of explosive yield for charge configuration used in pipeline component tests. The pipe, valve, and protective structure tests determined the resistance of pipeline components to explosive threats, whether protected by blast mitigation technologies or unprotected. These tests are discussed, respectively, in Section 7 through Section 9. The resistance of certain blast mitigation technologies to removal by an aggressor was also tested in a series of anti-tamper tests, which are discussed in Section 10. Finally, conclusions from the entire Task 5 test series are drawn in Section 11.

6 Source Characterization Tests

6.1 Test Overview

6.1.1 Test Objective

The goal of these tests was to verify the repeatability of explosive yield of the charge configuration used in subsequent tests.

6.1.2 Test Subcontractor

All tests were performed by Southwest Research Institute (SwRI), under sub-contract to PEC. SwRI provided the explosives, water and nitrogen fills, pipe pressurization system, instrumentation, regular and high-speed photography, and on-site test support. The tests were performed at the SwRI test range in Yancey, Texas, approximately 40-miles southwest of San Antonio.

6.1.3 Typical Test Specimen

For the source characterization tests, each specimen was a 4-ft long segment of 24-in diameter API 5L X52 pipe with a wall thickness of 0.375-in. This combination of diameter, wall thickness, and material was chosen to replicate typical pipe used in the pipeline industry and approximately matches the pipe sections that were numerically analyzed in Phase 1. The segments were uncapped and unpressurized.

The 4-ft pipe segments were supported at the ends by reinforced-concrete blocks, as shown in Figure 72. The length of pipe supported at either end was 9-in, as shown in Figure 73, and the clear span between the blocks was 30-in.



Figure 72. Source Characterization Specimen Supported by Reinforced-Concrete Blocks



Figure 73. Supported Length of Source Characterization Specimen

6.1.4 Explosive Threat

The explosive threat was a block-shaped xx -lb C4 charge, with a base ww -in per side and a height of ww -in. The C4 was hand-tamped into a plywood mold until the weight of the charge was xx -lb. The C4 charge is shown in the mold in Figure 74; the charge was removed from the mold for the tests as shown in Figure 75. This geometry was used for all xx -lb charges in the Phase 2 tests.

The exploding bridge wire (EBW) and placement guide used for the tests are shown in Figure 76. The guide was placed on the top center of the C4 block, and the EBW was pressed into the C4 until the top edge of the EBW was flush with the surface of the C4, as shown in Figure 75. Use of the guide ensured consistent penetration depth for all tests. The charge was placed mid-span of the pipe section, at the apex, as shown in Figure 77. The C4 block was sufficiently stiff to retain its shape.

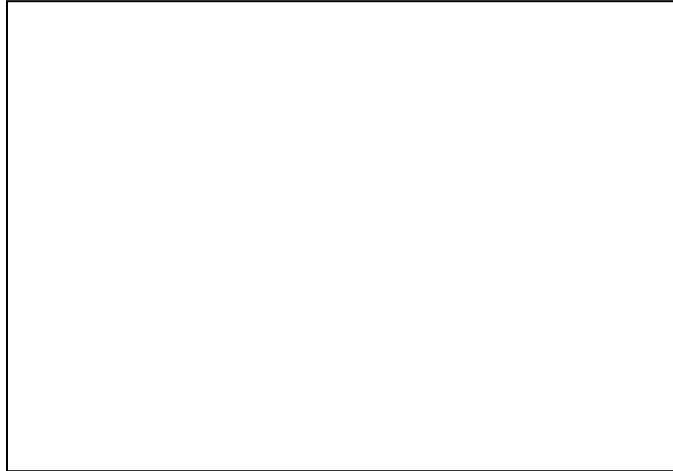


Figure 74. C4 Charge and Plywood Mold

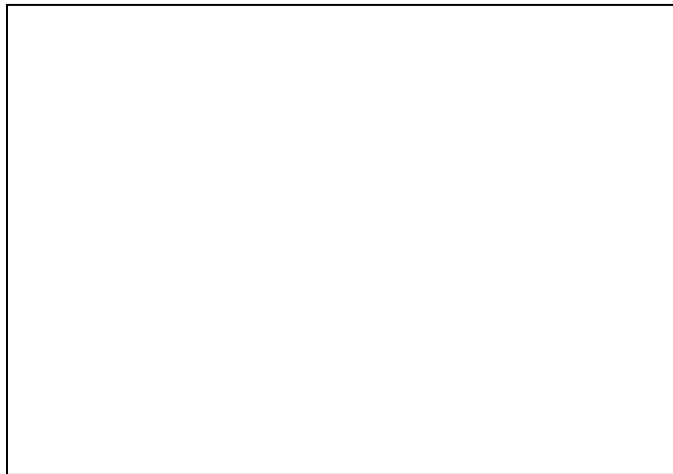


Figure 75. EBW Placed in Top Center of C4 Block



Figure 76. Detail of EBW and Placement Guide



Figure 77. Charge Placed on Source Characterization Specimen

6.1.5 Test Matrix

Five identical tests were performed, as shown in Table 19.

Table 19. Source Characterization Test Matrix

Test	Component	C4 Charge Weight [lb]	Purpose
1	4-ft long piece of 24-diameter X52 pipe with a wall thickness of 0.375-in	xx	Verify repeatability of explosive yield
to			
5	4-ft long piece of 24-diameter X52 pipe with a wall thickness of 0.375-in	xx	Verify repeatability of explosive yield

6.1.6 Instrumentation

Plan and elevation views of the instrumentation layout are shown, respectively, in Figure 78 and Figure 79. This layout was maintained for all five source characterization tests. The elevation of the pressure gauges was nominally equal to the elevation of the charge center, as shown in Figure 79. Data from the pressure gauges was used to assess the repeatability of charge yield. The gauge sampling rate was 1,000,000 data points per second. Camera elevations, which are not included in the figures for clarity, were nominally 60-in from the ground for all tests discussed in this report.

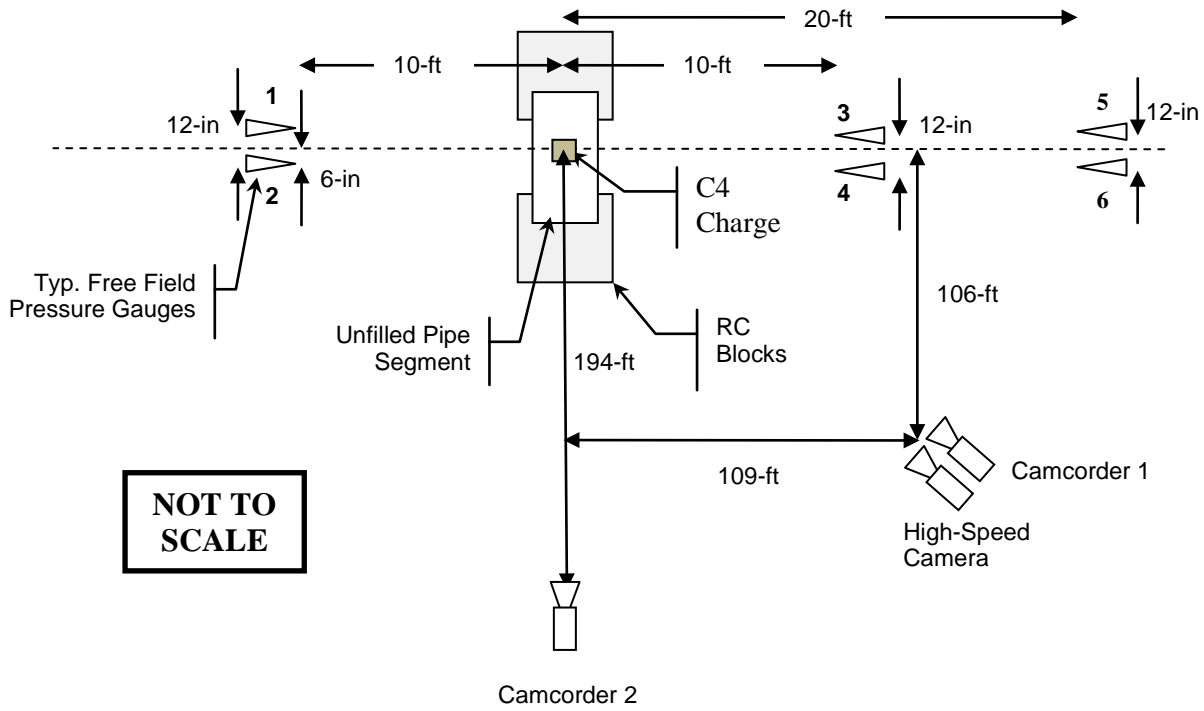


Figure 78. Location of Instrumentation in Source Characterization Tests (Plan View)

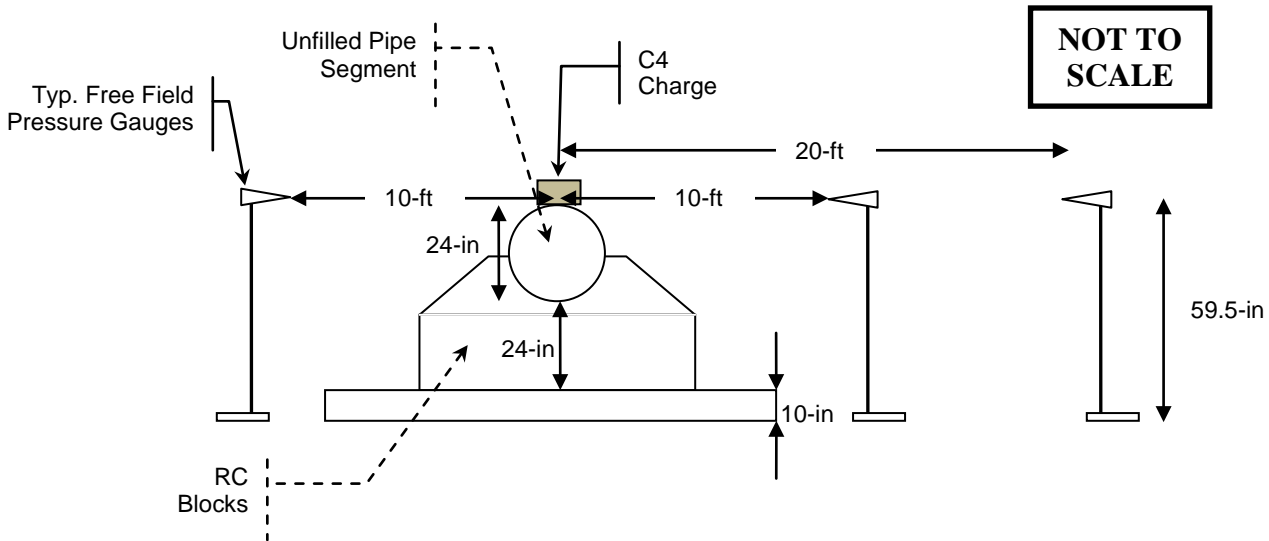


Figure 79. Location of Instrumentation in Source Characterization Tests (Elevation View)

6.2 Test Results

6.2.1 Post-Test Specimen Condition

The post-test condition of the pipe specimens was consistent for all five source characterization tests. Therefore, for brevity, only the post-test condition of the Test 1 specimen, shown in Figure 80 through Figure 85, is discussed. The hole shown in Figure 80 was formed immediately beneath the C4 charge, and its dimensions are shown in Figure 81 and Figure 82. The plug that sheared from the top side of the pipe caused the hole in the bottom side shown in Figure 83. The dimensions of the bottom hole are shown in Figure 84 and Figure 85.



Figure 80. Top of Unfilled Pipe Segment, Post-Detonation Condition (Test 1)



Figure 81. Width of Top Hole in Unfilled Pipe Segment (Test 1)



Figure 82. Length of Top Hole in Unfilled Pipe Segment (Test 1)



Figure 83. Bottom Interior of Unfilled Pipe Segment, Post-Detonation Condition (Test 1)



Figure 84. Width of Bottom Hole in Unfilled Pipe Segment (Test 1)



Figure 85. Length of Bottom Hole in Unfilled Pipe Segment (Test 1)

6.2.2 Repeatability

For each of the five source characterization tests, pressure-time histories were recorded. In Tests 1 and 2, some of the data was corrupted by pipe fragments striking the pressure gauges, but complete data was obtained for Tests 3 through 5. As an example of the data obtained, the pressure-time histories for Test 5 are shown in Figure 86.

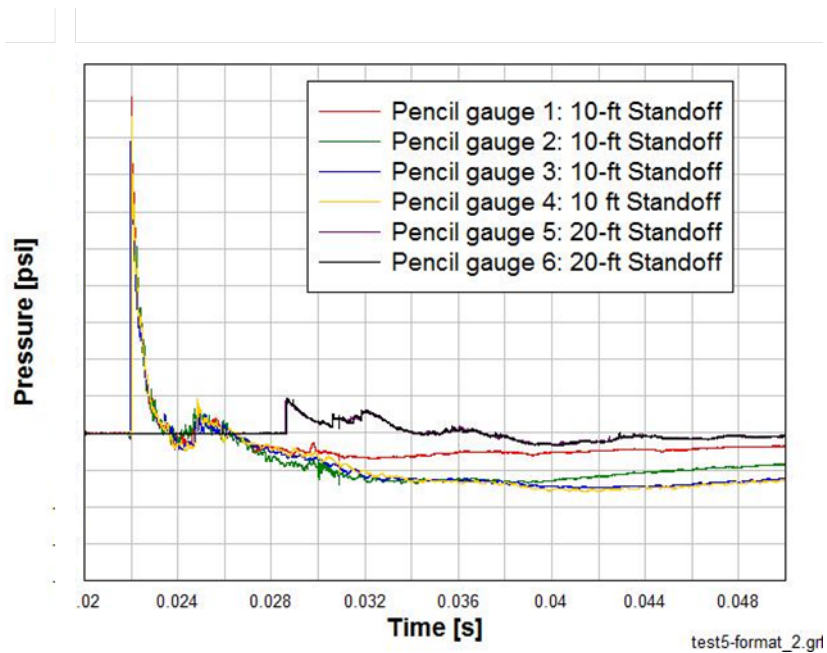


Figure 86. Example Pressure-Time Histories for Source Characterization Tests (Test 5)

The repeatability of the explosive yield was determined from the repeatability of the measured impulse. The impulse of each pressure gauge was calculated by integrating the pressure-time histories. As an example, the impulses for pressure gauges used in Test 5 are shown in Figure

87. The initial peak impulse, also shown in Figure 87, was determined for each gauge by inspection of the impulse histories. The average initial peak impulses for each test, one at the 10-ft standoff and one at the 20-ft standoff, were divided by the corresponding averages across all tests. The resulting ratio of average by test to total average (average for all tests) provided a measure of variability on a per test basis.

The ratio of test average to total average is shown for each of the five tests in Figure 88. From the figure, the average impulse per test ranged from 93% to 105% of the total average, and this variability was deemed acceptable. Corrupt data was not included and the number of data points included in the test average is printed on each histogram bar in the figure. A complete data set for a typical test would include 4 impulse values at 10-ft standoff and 2 impulse values at 20-ft standoff. As shown in Figure 88, data from two of the 10-ft-standoff gauges in Test 1 were corrupt, and in Test 2, there were problems with one of the 10-ft-standoff gauges and two of the 20-ft-standoff gauges.

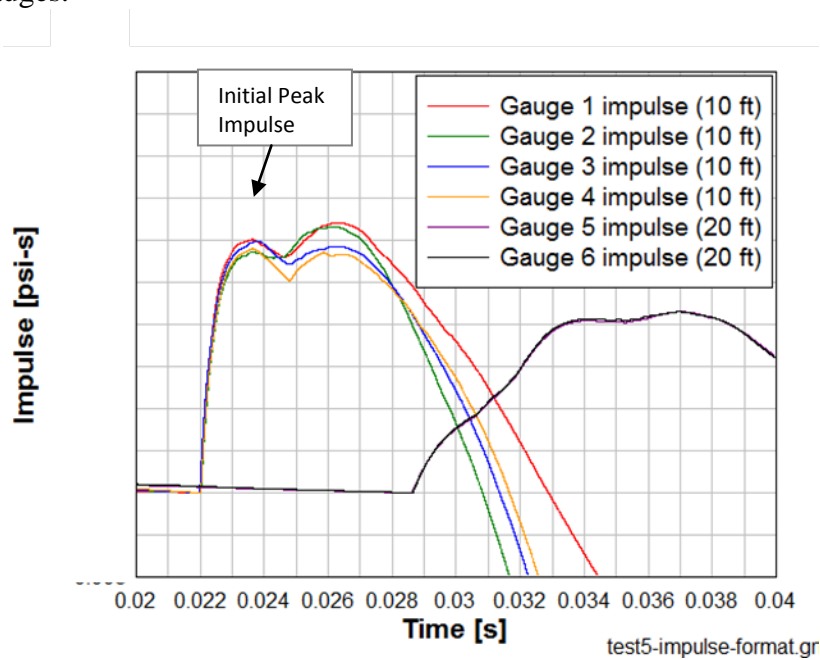


Figure 87. Integrated Pressure-Time Histories to Obtain Impulse (Test 5)

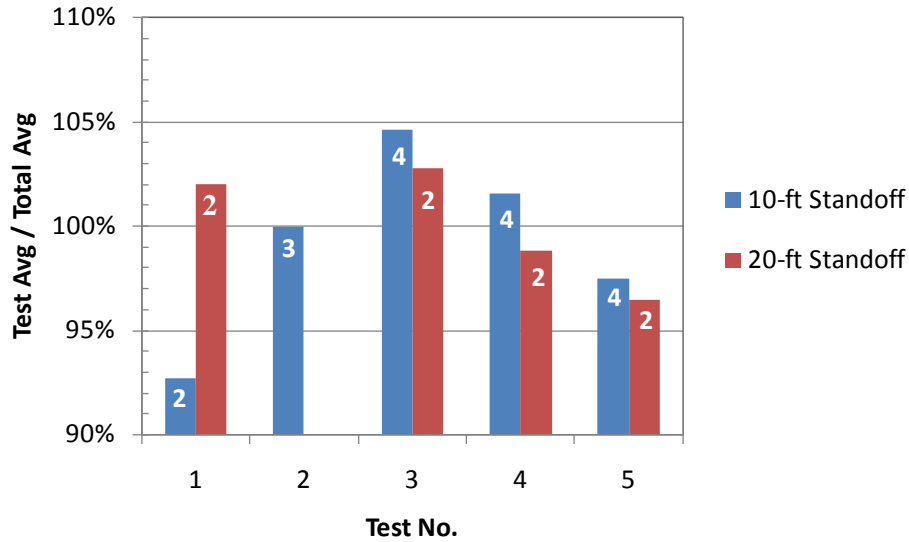


Figure 88. Ratio of Test Average Impulse to Total Average Impulse
(Missing or corrupt data not included)

7 Pipe Tests

7.1 Test Overview

7.1.1 Test Objectives

The goal of these tests was to determine the resistance of bare (unprotected) and protected pipes to small C4 charges, in contact or at a standoff.

7.1.2 Failure Criterion

For the pipe specimens, any breach or cracking of the pipe was defined as a failure. Failure was readily identified during testing as the inability of the specimen to retain internal pressure, which was measured using a remote pressure gauge.

7.1.3 Typical Pipe Specimen

Figure 89 is an illustration of a typical pipe specimen. The pipe length was 20-ft, excluding the elliptical caps welded at the ends to permit pressurization. The wall thickness (0.375-in), diameter (24-in), and material (API 5L X52) are representative of typical pipeline construction. The reinforced-concrete blocks were positioned so that the clear span of the pipe was 14-ft. The properties of the specimen are summarized in Table 20.

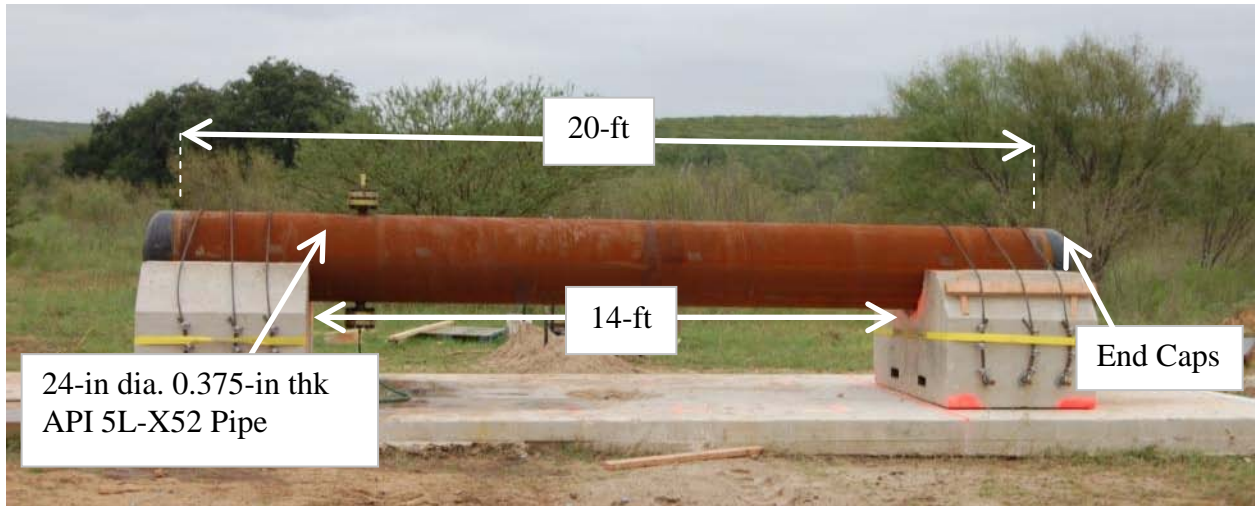


Figure 89. Typical Capped Pipe Segment

Table 20. Typical Capped Pipe Segment Properties

Property	Magnitude/ Description
Diameter [in]	24
Wall Thickness [in]	0.375
Pipe Length [ft]	20
Clear Span [ft]	14
Steel Grade	API 5L X52

The capped pipe segments were identical for all pipe tests. What distinguished the tests were the blast mitigation technologies (BMT) used to protect the pipe segments, the content of the pipe segments (water or nitrogen), and the charge standoff. Specific specimen details are listed in Table 21 and discussed in Section 7.1.5. All specimens, whether water-filled or nitrogen-filled, were pressurized to within 0.5% of 720 psi using nitrogen. The hose and fitting used for pressurization are shown in Figure 90.



Figure 90. Fitting Used for Pipe Pressurization

7.1.4 Explosive Threat

The explosive threat was a xx-lb C4 charge, identical to the typical charge discussed in Section 6.1.4. The charge was placed mid-span, at the apex of the pipe section, as shown in Figure 91, except for Test 11 and Test 17, where the charge was placed at 12-standoff. For cases that included a BMT, the charge was placed in contact with the BMT mid-span, at the apex of the BMT section.

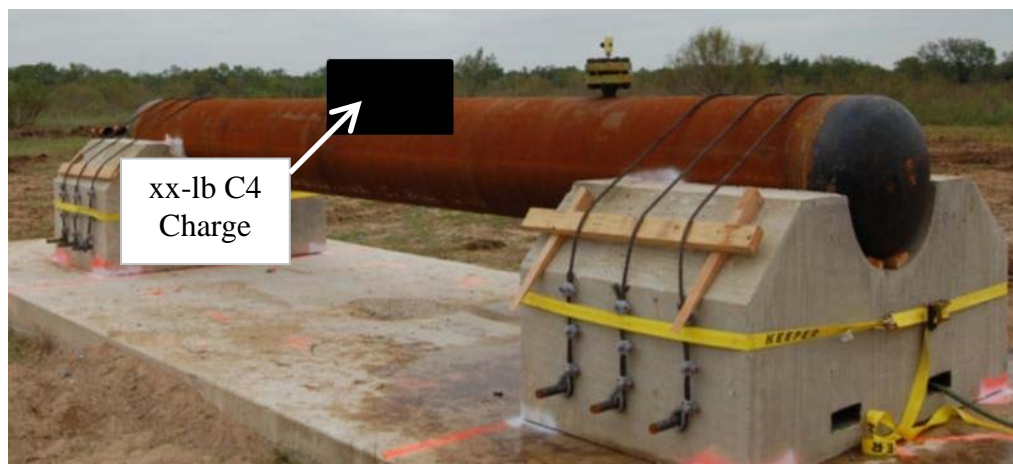


Figure 91. Typical xx-lb C4 Charge Location

7.1.5 Test Matrix

The test matrix is shown in Table 3. All pipe tests included a typical capped pipe segment, as described in Section 7.1.3.

Tests 11 to 14 were performed on pipe specimens filled with water at a pressure of 720-psi. Tests 17 to 20 were performed on pipe specimens filled with nitrogen at 720-psi with similar charge weight and standoff combinations to Tests 11 to 14. Tests 11 and 17 were performed on a bare pipe specimen with the xx-lb C4 charge at a 12-in standoff. Tests 12 and 18 were also performed on a bare pipe specimen with the C4 charge in direct contact with the pipe. Tests 13 and 19 were used to evaluate a steel-encased fiber reinforced concrete BMT with the C4 charge in direct contact with the BMT. Similarly, Tests 14 and 20 were used to evaluate a protective jacket BMT with the C4 charge in direct contact with the BMT.

Since the numerical analyses showed that the composite wrap and polymer coating were unlikely to increase resistance significantly, Tests 15 and 16 were performed only on water-filled pipe segments to evaluate these BMTs. Water was chosen for these tests because it reduces the likelihood of wall failure by increasing both the effective mass of the deforming wall and the resistance to compression. In this way, the composite wrap and polymer coating specimens had the best chance of survival, and if they failed, as predicted, it was not necessary to test the nitrogen-filled case.

Table 21. Pipe Test Matrix

Test	Component	Fill	Blast Mitigation Technology	Charge Weight [lb]	Standoff [in]	Purpose
11	24-in pipe, 0.375-in wall, X52	Water	None	xx	12	Effect of standoff
12	24-in pipe, 0.375-in wall, X52	Water	None	xx	0	Baseline
13	24-in pipe, 0.375-in wall, X52	Water	SEFRC Cover	xx	0	Mitigation evaluation
14	24-in pipe, 0.375-in wall, X52	Water	Protective jacket	xx	0	Mitigation evaluation
15	24-in pipe, 0.375-in wall, X52	Water	FRP composite wrap	xx	0	Mitigation evaluation
16	24-in pipe, 0.375-in wall, X52	Water	Polymer coating	xx	0	Mitigation evaluation
17	24-in pipe, 0.375-in wall, X52	Nitrogen	None	xx	12	Effect of standoff
18	24-in pipe, 0.375-in wall, X52	Nitrogen	None	xx	0	Baseline
19	24-in pipe, 0.375-in wall, X52	Nitrogen	SEFRC Cover	xx	0	Mitigation evaluation
20	24-in pipe, 0.375-in wall, X52	Nitrogen	Protective jacket	xx	0	Mitigation evaluation

7.1.6 Instrumentation

Plan and elevation views of instrumentation layout for the pipe tests are shown in Figure 92 and Figure 93, respectively. At the onset of testing, there was concern that the pressurized pipe would fail catastrophically and damage the pressure gauges. Therefore, in contrast to the source characterization tests, four pressure gauges were used, and the redundant pair of gauges at 10-ft standoff was removed.

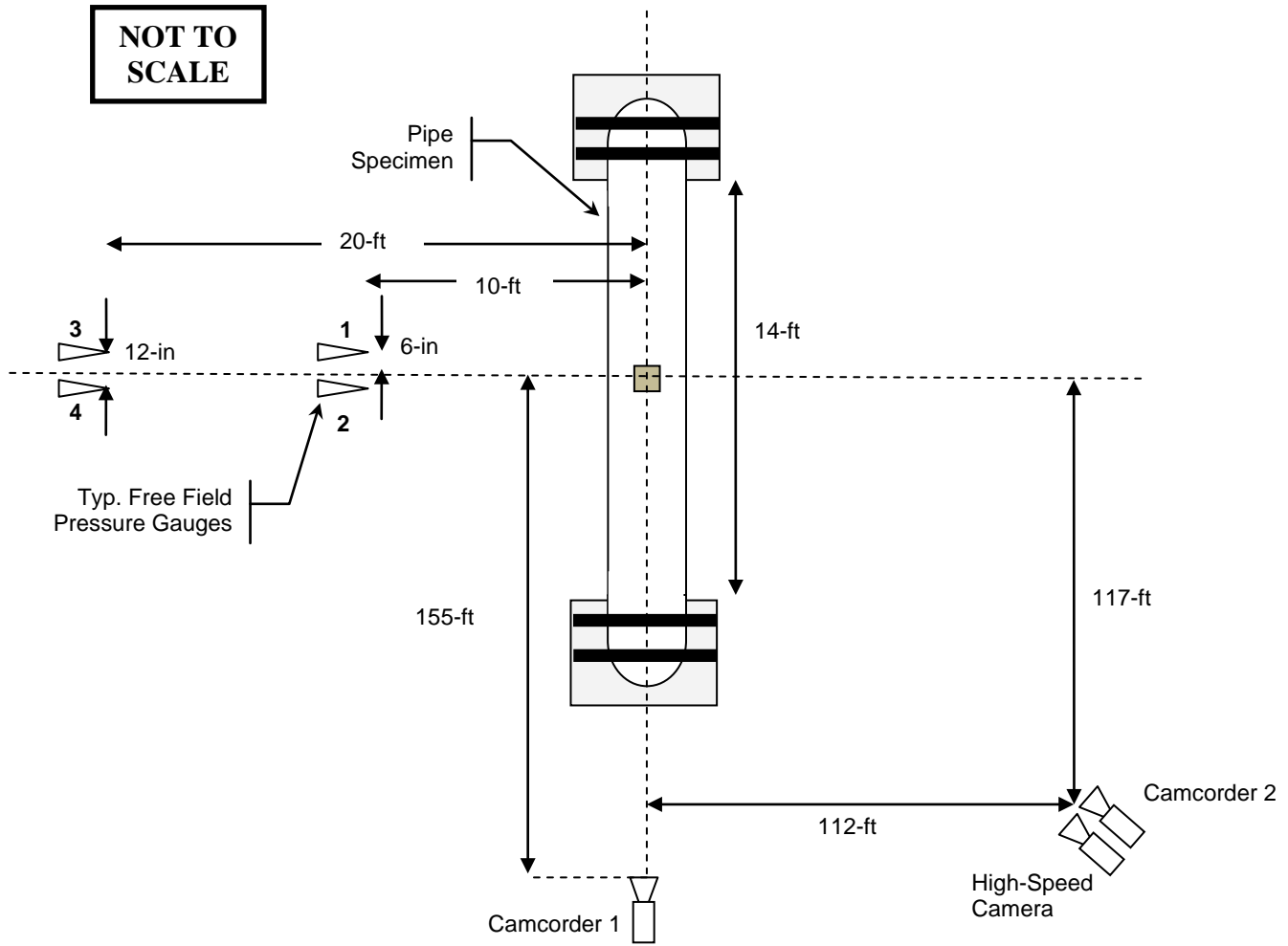


Figure 92. Location of Instrumentation for Pipe Tests (Plan View)

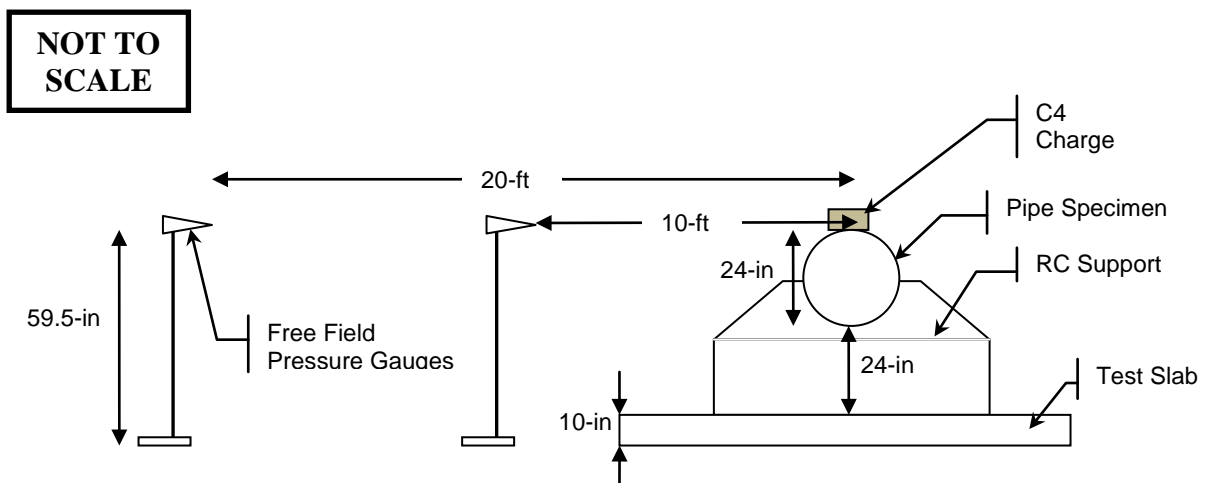


Figure 93. Location of Instrumentation for Pipe Tests (Elevation View)

7.2 Test 11: Water-Filled Pipe, xx-lb C4 Charge at 12-in Standoff

7.2.1 Test Details

In Test 11, a water-filled bare pipe specimen was tested. Prior to pipe pressurization, the charge was placed at a 12-in standoff from the surface of the bare pipe, supported by foam, as shown in Figure 94. The top of the support beneath the charge was open, as shown in Figure 95. In this way, the charge was only supported along its perimeter to minimize the effect of the foam on shock-wave propagation to the pipe surface.



Figure 94. C4 Charge on Foam Support for 12-in Standoff (Test 11)



Figure 95. Hole in Top of Foam Support (Test 11)

7.2.2 Post-Test Condition

As shown in Figure 96 and Figure 97, the xx-lb C4 charge at 12-in standoff did not breach the water-filled bare pipe. The charge caused a dent with the dimensions shown in the figures, but the pipe retained its initial pressure after the test, confirming visual determination of no breach or cracking of the pipe wall.



Figure 96. Depth of Dent in Pipe (Test 11)



Figure 97. Length of Dent in Pipe (Test 11)

7.2.3 Pressure-Time Histories

The pressure-time histories for the four pressure gauges in Test 11 are shown in Figure 98. From the figure, gauges at both the 10-ft and 20-ft standoff reported consistent pressure histories. Comparison of the pressure-time histories of Test 11 with the histories from other pipe tests, as was done in Section 6.2.2 for the source characterization tests, was not possible because each pipe test was unique. For example, the difference in standoff from the target (12-in for Test 11 vs. contact for Test 12) had an effect on pressure-time histories of the two tests, and the effect cannot be readily quantified and removed through calculation. Therefore, pressure-time histories were checked for consistency only on per-test basis.

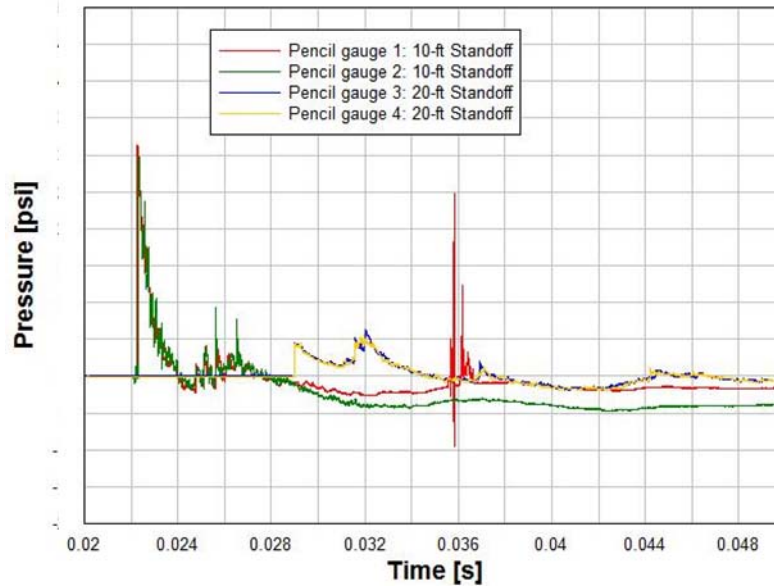


Figure 98. Pressure-Time Histories, xx-lb C4 Charge at 12-in Standoff from Water-Filled Bare Pipe (Test 11)

7.3 Test 12: Water-Filled Pipe, xx-lb C4 Contact Charge

7.3.1 Test Details

The details of Test 12 were identical to those of Test 11 (discussed in Section 7.2.1) except that the charge was in direct contact with the bare pipe, as shown in Figure 99.



Figure 99. C4 Charge in Contact with Bare Pipe (Test 12)

7.3.2 Post-Test Condition

The xx-lb C4 charge in contact breached the water-filled bare pipe. As shown in Figure 100 through Figure 102, the steel sheared around the periphery of the charge, with cracks extending from the corners and from one side. The internal pressure caused the water to vent, as shown in Figure 103 and Figure 104, which are frames taken from the high-speed video. Comparison of the post-test condition of specimens from Test 11 and Test 12 illustrates the importance of standoff for mitigating explosive effects. Increasing standoff from 0-in to 12-in reduces the hole shown in Figure 100 through Figure 102 to the dent shown in Figure 96 and Figure 97, preventing failure of the pipe.

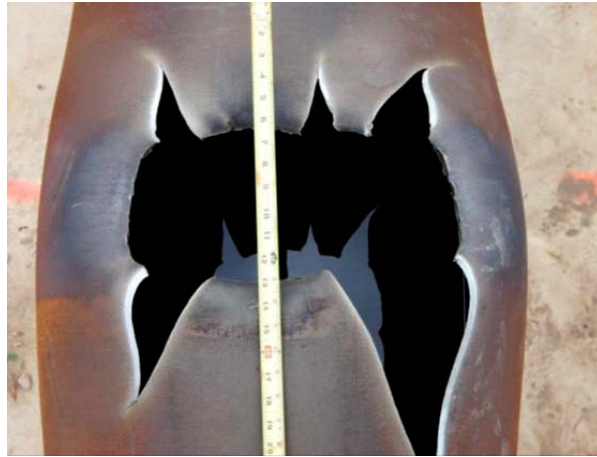


Figure 100. Length of Hole in Pipe (Test 12)



Figure 101. Width of Hole in Pipe (Test 12)



Figure 102. Detail of Hole in Pipe (Test 12)



Figure 103. Water-Filled Pipe, xx-lb C4 Contact Charge (Test 12), at Time = 0 s



Figure 104. Water-Filled Pipe, xx-lb C4 Contact Charge (Test 12) at Time = 0.4369 s

7.3.3 Pressure-Time Histories

The pressure-time histories for Test 12 are shown in Figure 105. The histories of the gauge pairs at the two standoffs (10-ft and 20-ft) were consistent with each other and comparable to the results for Test 11, shown in Figure 98. Pencil gauge 3 was likely struck by a fragment which caused the curve to shift downward approximately 10 psi. If the curve is shifted up, the gauge 3 history corresponds with that of gauge 4.

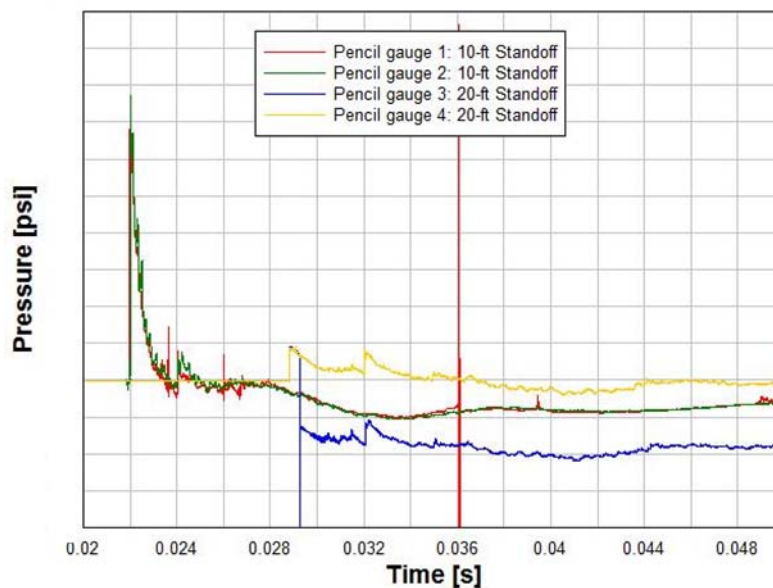


Figure 105. Pressure-Time Histories, xx-lb C4 Contact Charge on Water-Filled Bare Pipe (Test 12)

7.4 Test 13: Water-Filled Pipe with SEFRC Cover, xx-lb C4 Contact Charge

7.4.1 Test Details

For Test 13, Composite Technologies, in association with BAE Systems and a fabricator-subcontractor W Industries (Detroit, MI), designed, fabricated, and installed their proprietary steel-encased, fiber-reinforced concrete (SEFRC) cover system on a typical pipe specimen. For efficient fabrication and installation of the SEFRC, Composite Technologies requested the bare test specimen be sent to their fabricator in Detroit. After installation, the SEFRC-covered specimen was shipped to the test site.

The SEFRC cover consisted of outer and inner steel layers, separated by a high-strength, fiber-reinforced concrete core. The concrete and steel layers were designed and fabricated for the 24-in diameter pipe and then installed in a “clam-shell” method, as shown in Figure 106. In the figure, only the steel frame of the cover is shown. The cover was then fixed in place with bolts. The final covered pipe specimen is shown in Figure 107.



Figure 106. Clam-Shell Installation of SEFRC Cover System⁹⁰

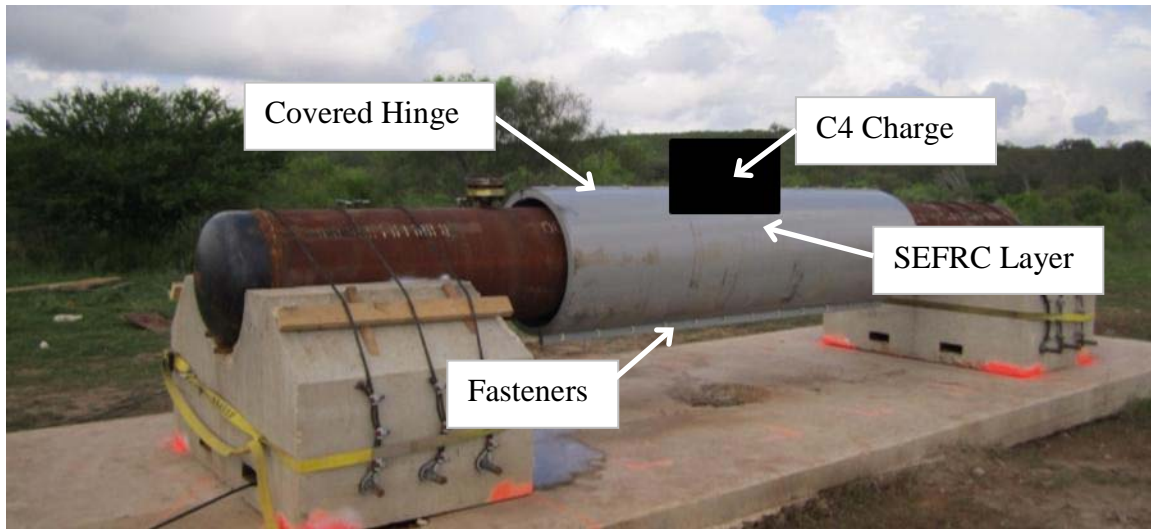


Figure 107. SEFRC Pipe Cover System, Installed on Pipe Specimen (Test 13)

The charge was placed directly on the cover, at its apex, at mid-span along the axis of the specimen. This location essentially corresponded with the joint in the plate covering the hinge, which was expected to be the most vulnerable point in the cover, based on inspection of the test specimen. The charge location is shown in Figure 107 and Figure 108.



Figure 108. C4 Charge Placed at Hinge-Cover Joint (Test 13)

7.4.2 Post-Test Condition

The charge did not breach the water-filled pipe protected by the SEFRC pipe cover. As shown in Figure 109 and Figure 110, the cover was damaged significantly, but the pipe remained intact. As in Test 11, the pipe retained its pre-detonation internal pressure after the detonation.



Figure 109. Width of Hole in SEFRC Cover,
No Breach of Pipe (Test 13)



Figure 110. Depth of Hole in SEFRC Cover,
No Breach of Pipe (Test 13)

7.4.3 Pressure-Time Histories

The pressure-time histories for Test 13 are shown in Figure 111. The histories of the gauge pairs at the two standoffs (10-ft and 20-ft) were consistent with each other.

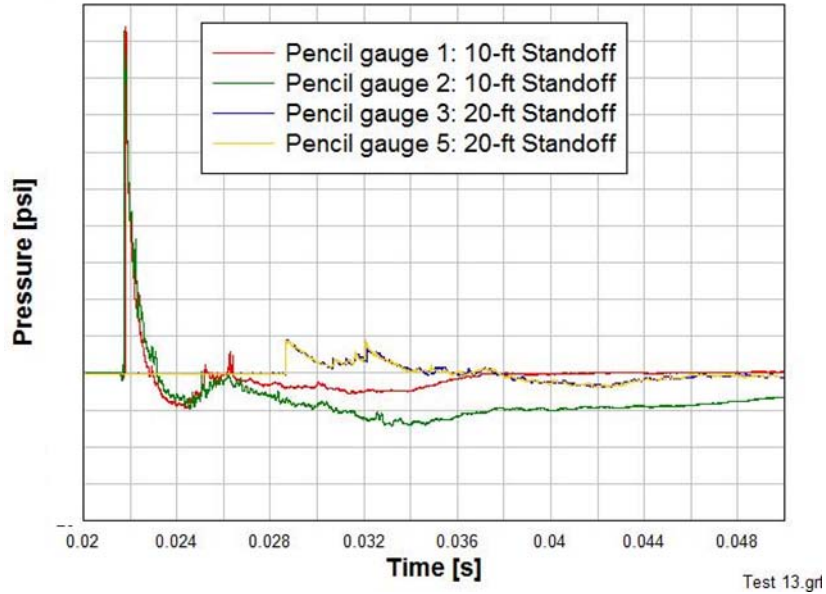


Figure 111. Pressure-Time Histories, xx-lb C4 Contact Charge on SEFRC Pipe Cover (Test 13)

7.5 Test 14: Water-Filled Pipe with Pipe Jacket, xx-lb C4 Contact Charge

7.5.1 Test Details

WinTec has designed a pipe jacket intended to mitigate ballistic and penetration threats. A proprietary layer in the jacket is included to prevent drill penetration by seizing the drill bit. For installation, the jacket is slipped over the pipeline and secured, as shown in Figure 112.

Tightening of the fastener is designed to release a bonding agent that adheres the sleeve to the pipe.



Figure 112. Protective Jacket Concept Proposed by WinTec Security⁹¹

WinTec provided pipe jackets for contact-charge testing with the expectation that the bonding agent would provide structural reinforcement. The jacket BMT installed for Test 14 is shown in

Figure 113. WinTec was unable to provide the requested 10-ft length of jacket and only 4-ft was available. Based on the highly localized failures observed in previous tests, 4-ft was deemed sufficient to cover the area affected by the contact charge. In addition, the jacket could not be readily installed using the fastener system provided by WinTec. Therefore, the jacket was installed on the pipe using ratchet straps as shown in the figure. The charge was placed directly on the jacket at its apex, at mid-span along the axis of the specimen as shown in Figure 114.



Figure 113. Pre-Detonation Condition of Pipe Jacket (Test 14)



Figure 114. Charge Placed on Pipe Jacket (Test 14)

7.5.2 Post-Test Condition

As shown in Figure 115 through Figure 118, the pipe jacket was heavily damaged and the pipe was breached. The difference between damage in the baseline case (discussed in Section 7.3) and the jacketed case was negligible, but crack propagation along the axis of the pipe was less severe in the jacket case. This difference could have been caused by the jacket, by the slightly larger standoff due to the jacket, or by typical variations observed in explosive testing. In this test, the plug driven into the pipe by the contact charge was recovered and is shown in Figure 119.



Figure 115. Post-Detonation Condition of Pipe Jacket (Test 14)



Figure 116. Length of Hole in Jacket-Covered Pipe (Test 14)



Figure 117. Width of Hole in Jacket-Covered Pipe (Test 14)



Figure 118. Depth of Hole in Jacket-Covered Pipe (Test 14)



Figure 119. Steel Plug from Jacket-Covered Pipe (Test 14)

7.5.3 Pressure-Time Histories

The pressure-time histories for Test 14 are shown in Figure 120. The histories of the gauge pairs at the two standoffs (10-ft and 20-ft) were consistent with each other overall, though the measured peak pressures at the 10-ft standoff had different magnitudes.

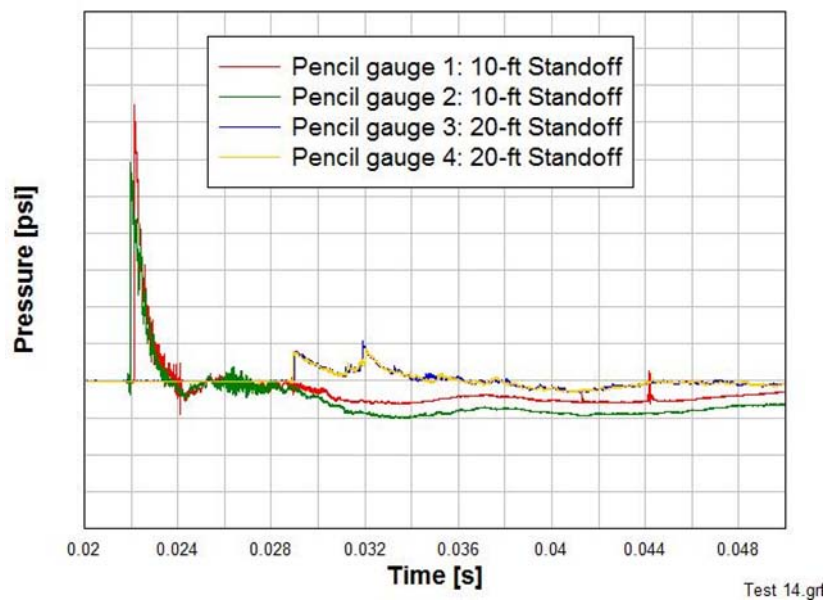


Figure 120. Pressure-Time Histories, xx-lb C4 Contact Charge on Pipe Jacket (Test 14)

7.6 Test 15: Water-Filled Pipe with FRP Layer, xx-lb C4 Contact Charge

7.6.1 Test Details

For Test 15, a nominal 0.5-in thick layer of fiber-reinforced polymer (FRP) was installed on the pipe by PEC and SwRI personnel. The FRP supplier, QuakeWrap™ (Tucson, AZ), provided an engineer familiar with the product to assist with the installation. The FRP was a composite of carbon fibers within a resin matrix. For the installation, the pipe was wrapped in a resin-saturated fabric (Figure 121), and then the liquid epoxy was applied over the fabric as needed. The area of pipe beneath the FRP was sand-blasted prior to installation, to ensure good bond. The polymer cured to form the composite layer shown in Figure 122, which served as the BMT. The charge placed on the FRP BMT is shown in Figure 123.



Figure 121. FRP Installation on Pipe (Test 15)



Figure 122. FRP Installed on Pipe Specimen (Test 15)



Figure 123. C4 Charge in Contact with FRP BMT (Test 15)

7.6.2 Post-Test Condition

When subjected to the xx-lb C4 charge in contact, the FRP failed and the pipe breached, as shown in Figure 124 through Figure 126. As with the pipe jacket from Test 14, the damage mitigation provided by the FRP was negligible, but crack propagation was again less severe than in the baseline case (Section 7.3).



Figure 124. Length of Hole in FRP-Covered Pipe (Test 15)



Figure 125. Width of Hole in FRP-Covered Pipe (Test 15)



Figure 126. Depth of Hole in FRP-Covered Pipe (Test 15)

7.6.3 Pressure-Time Histories

The pressure-time histories for Test 15 are shown in Figure 127. The histories of the gauge pairs at the two standoffs (10-ft and 20-ft) were consistent with each other.

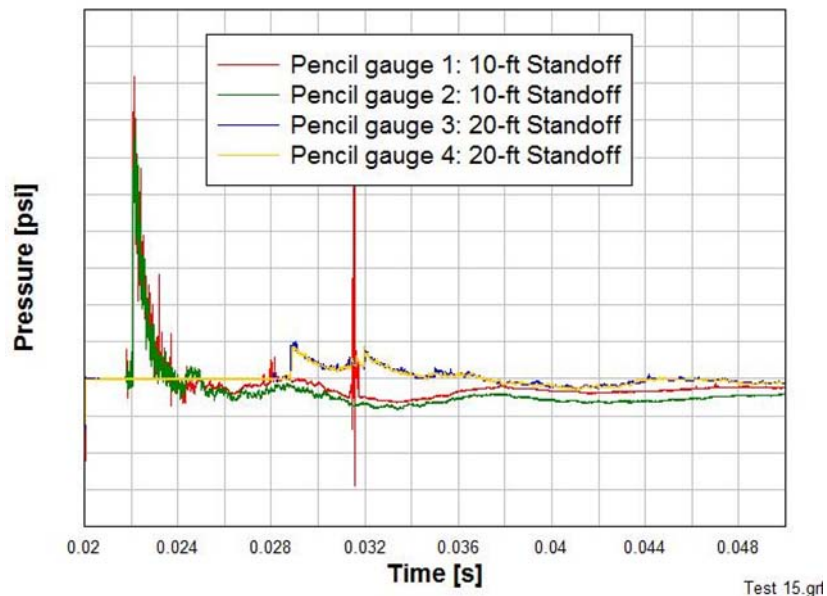


Figure 127. Pressure-Time Histories, xx-lb C4 Charge on FRP Layer (Test 15)

7.7 Test 16: Water-Filled Pipe with Polyurea Coating, xx-lb C4 Contact Charge

7.7.1 Test Details

For Test 16, the BMT was a ductile coating, consisting of a nominal 0.5-in thick polyurea layer applied to the exterior surface of the pipe specimen. The polyurea composition was XS-350, manufactured by Line-X®. Prior to installation, the pipe was sandblasted to provide an optimal bonding surface for the polyurea coating. Then, the coating was installed in multiple spray passes, as shown in Figure 128, until a minimum 0.5-in thick coating was built-up. The completed polyurea specimen and placed C4 charge are shown in Figure 129.



Figure 128. Polyurea Coating Installation (Test 16)



Figure 129. Ductile Coating with Placed Charge (Test 16)

7.7.2 Post-Test Condition

As shown in Figure 130 through Figure 132, the xx-lb C4 charge in contact with the ductile coating breached both the coating and the pipe. The difference between the pipe coated with polyurea and the baseline case was negligible. However, crack propagation was less severe than in the baseline case (Section 7.3).



Figure 130. Length of Hole in Polyurea-Coated Pipe (Test 16)



Figure 131. Width of Hole in Polyurea-Coated Pipe (Test 16)



Figure 132. Depth of Hole in Polyurea-Coated Pipe (Test 16)

7.7.3 Pressure-Time Histories

The pressure-time histories for Test 16 are shown in Figure 133. More noise was observed in the histories than in other tests, likely due to fragment impact on the pressure-gauge stands.

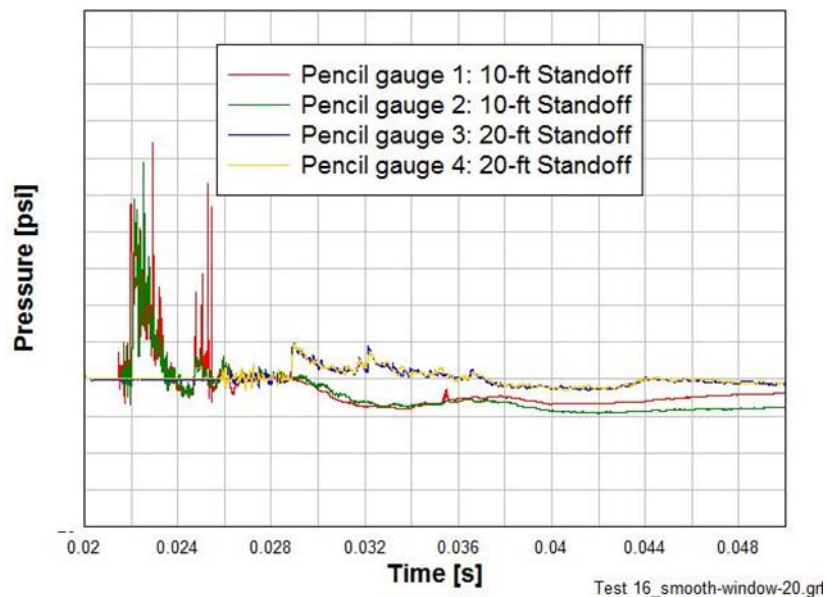


Figure 133. Pressure-Time Histories, xx-lb C4 Contact Charge on Polyurea Coating (Test 16)

7.8 Test 17: Nitrogen-Filled Pipe, xx-lb C4 Charge at 12-in Standoff

7.8.1 Test Details

The specimen in Test 17 was a nitrogen-filled pipe without BMT. Charge standoff was accomplished by using a foam support, as described in Section 7.2.1.

7.8.2 Post-Test Condition

The xx-lb C4 charge at 12-in standoff did not breach the nitrogen-filled bare pipe, as shown in Figure 134 and Figure 135. The charge caused a dent with the dimensions shown in the figures.



Figure 134. Depth of Dent Pipe (Test 17)



Figure 135. Length of Dent in Pipe (Test 17)

7.8.3 Pressure-Time Histories

The pressure-time histories for the nitrogen-filled pipe, xx-lb C4 at 12-in standoff, are shown in Figure 136. Pressure-time history pairs were consistent at the 10-ft and 20-ft standoffs. Again, noise and curve shifts present in the histories were likely due to fragment impact on the pressure-gauge stands.

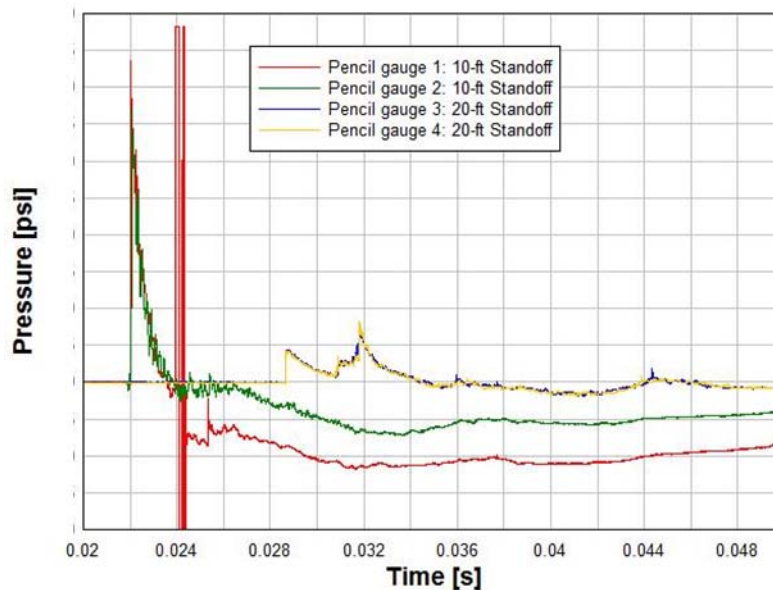


Figure 136. Pressure-Time Histories, xx-lb C4 Charge at 12-in Standoff from Nitrogen-Filled Bare Pipe (Test 17)

7.9 Test 18: Nitrogen-Filled Pipe, xx-lb C4 Contact Charge

7.9.1 Test Details

In Test 18, a nitrogen-filled pipe specimen was tested with xx-lb C4 in contact with the pipe. The test was identical to Test 12 (Section 7.3) except the pipe was filled with nitrogen instead of water.

7.9.2 Post-Test Condition

As shown in Figure 137 through Figure 139, the charge caused breach of both the top and bottom of the pipe. A plug comparable to the one shown in Figure 119 was sheared from the top of the pipe and then penetrated the bottom. Crack propagation was less evident than for the comparable water-filled specimen (results discussed in Section 7.3.2). In addition, the nitrogen-filled specimen depressurized faster than the water-filled specimen (approximately 0.720-s vs. 1.093-s, from high-speed video review). The shorter vent time for the nitrogen-filled specimen was likely due to the lower density of the compressed nitrogen and the fact that two vent holes were formed, which permitted an increased flow rate. Figure 140 and Figure 141 illustrate the relatively quick depressurization of the nitrogen-filled specimen.



Figure 137. Top Hole in Pipe (Test 18)



Figure 138. Bottom Hole in Pipe (Test 18)



Figure 139. Detail of Bottom Hole in Pipe (Test 18)

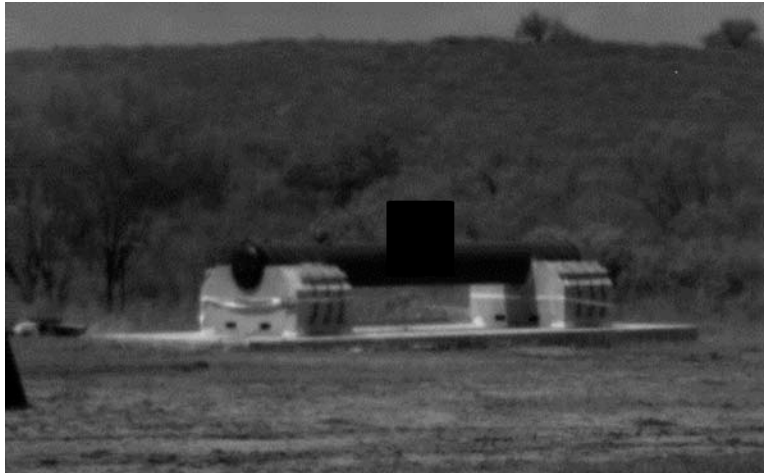


Figure 140. Nitrogen-Filled Pipe, xx-lb C4 Contact Charge (Test 18) at Time = 0 s



Figure 141. Nitrogen-Filled Pipe, xx-lb C4 Contact Charge (Test 18) at Time = 0.2150 s

7.9.3 Pressure-Time Histories

The pressure-time histories for Test 18, which were consistent at the two standoffs, are shown in Figure 142.

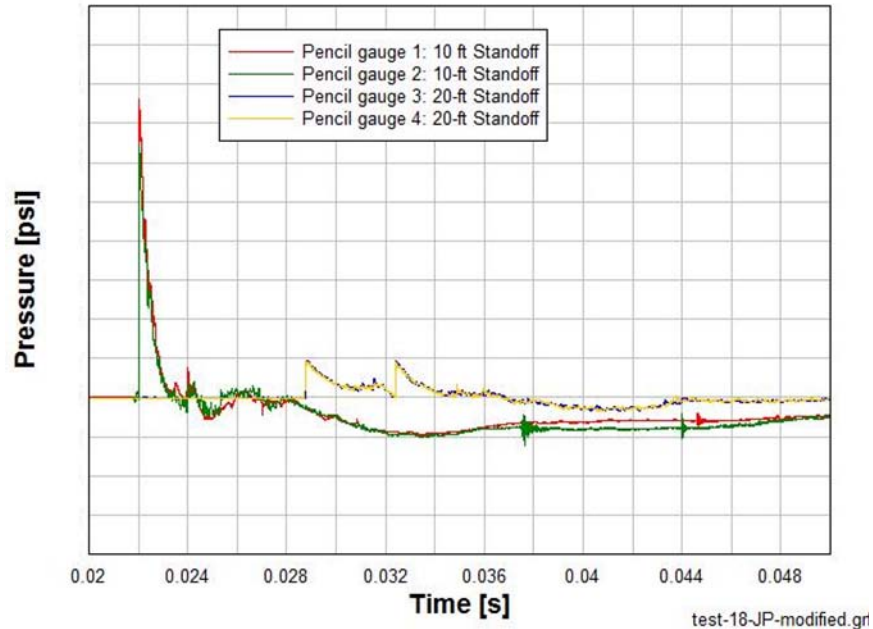


Figure 142. Pressure-Time Histories, xx-lb C4 Contact Charge on Nitrogen-Filled Bare Pipe (Test 18)

7.10 Test 19: Nitrogen-Filled Pipe with SEFRC Cover, xx-lb C4 Contact Charge

7.10.1 Test Details

The test details for Test 19 were identical to Test 13, discussed in Section 7.4.1, except that the pipe specimen was filled with nitrogen rather than water.

7.10.2 Post-Test Condition

As shown in Figure 143 and Figure 144, the SEFRC cover was breached, but the nitrogen-filled pipe did not breach or crack. The pipe remained intact after detonation and retained its pre-detonation internal pressure.



Figure 143. Width of Hole in SEFRC Cover, No Breach of Pipe (Test 19)



Figure 144. Depth of Hole in SEFRC Cover, No Breach of Pipe (Test 19)

7.10.3 Pressure-Time Histories

The pressure-time histories for Test 19 are shown in Figure 145. The pairs of gauges were consistent at the 10-ft and 20-ft standoffs, though the negative phase of gauge 2 had less impulse than the negative phase of gauge 1.

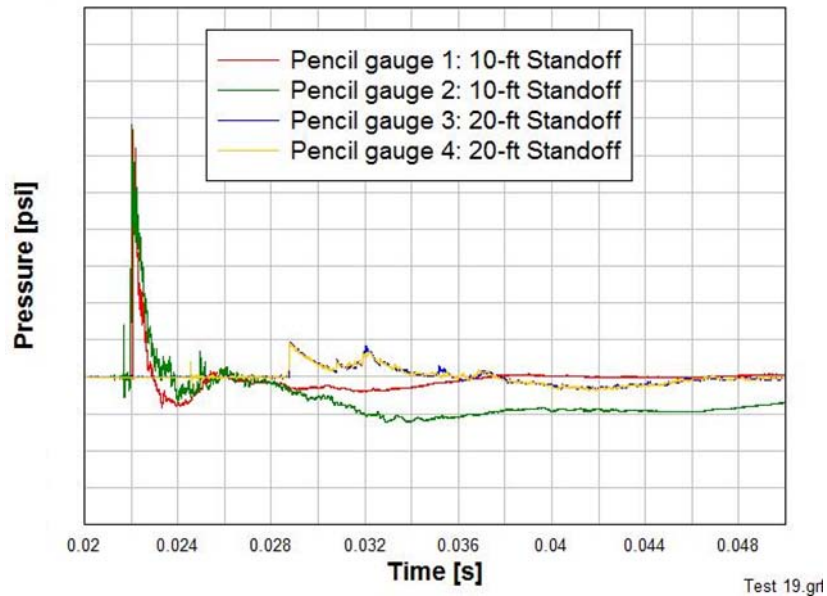


Figure 145. Pressure-Time Histories, xx-lb C4 Contact Charge on SEFRC Pipe Cover (Test 19)

7.11 Test 20: Nitrogen-Filled Pipe with Pipe Jacket, xx-lb C4 Contact Charge

7.11.1 Test Details

The test details for Test 20 were identical to Test 14, discussed in Section 7.5.1, except that the pipe specimen was filled with nitrogen rather than water.

7.11.2 Post-Test Condition

As shown in Figure 146 through Figure 148, the charge breached both the pipe jacket and the pipe. The jacket was found approximately 50-ft from the test pad, as shown in Figure 149. Crack propagation in Test 20 was greater than in the baseline case (Test 18, Section 7.9).



Figure 146. Length of Hole in Jacket-Covered Pipe (Test 20)



Figure 147. Width of Hole in Jacket-Covered Pipe (Test 20)



Figure 148. Bottom of Hole in Jacket-Covered Pipe (Test 20)



Figure 149. Post-Detonation Condition and Location of Pipe Jacket (Test 20)

7.11.3 Pressure-Time Histories

The pressure-time histories for Test 20 are shown in Figure 150. They were consistent with one another at the two standoffs.

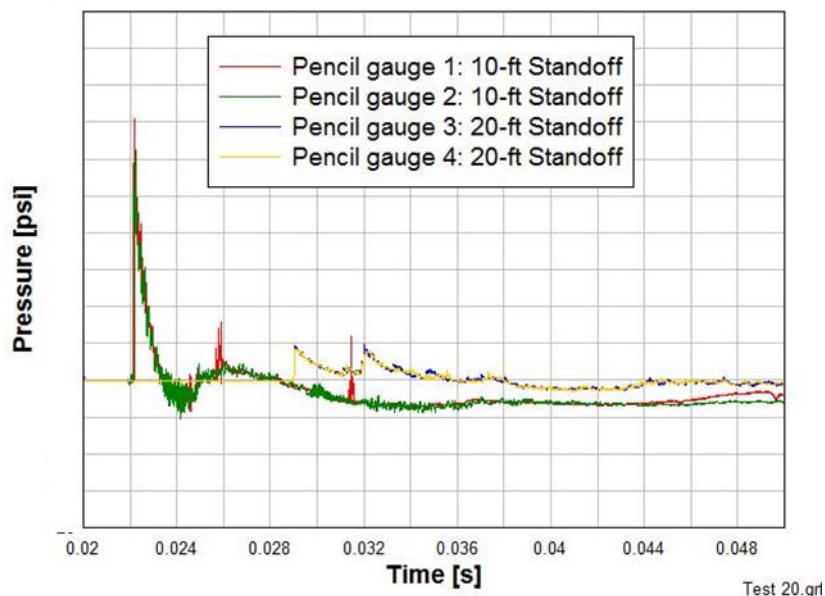


Figure 150. Pressure-Time Histories, xx-lb C4 Contact Charge on Pipe Jacket (Test 20)

7.12 Pipe Tests: Summary of Results

The results from the pressurized pipe tests are summarized in Table 22. Both the water and nitrogen-filled specimens with a 12-in standoff (Tests 11 and 17) remained intact. However, with the exception of the SEFRC covered specimens, all pipe specimens failed when the xx-lb charge was placed in contact with the bare pipe or BMT. The SEFRC covers were breached during the tests, but the pipes remained intact and retained their pre-detonation internal pressures. As noted above, the FRP composite wrap and polymer coating were not tested on nitrogen-filled specimens because the water-filled specimens protected by those BMTs failed. Water adds both inertial and mechanical resistance to failure, a fact which implies that nitrogen-filled specimens protected by FRP or polymer would have failed as well.

Table 22. Summary of Pipe Contact Charge Tests

Test	Component	Fill	Blast Protection	Charge Weight [lb]	Standoff [in]	Post-Test Pipe Condition
11	24-in pipe, 0.375-in wall, X52	Water	None	xx	12	Intact
12	24-in pipe, 0.375-in wall, X52	Water	None	xx	0	Failed
13	24-in pipe, 0.375-in wall, X52	Water	Steel encased FRC	xx	0	Intact
14	24-in pipe, 0.375-in wall, X52	Water	Protective sleeve	xx	0	Failed
15	24-in pipe, 0.375-in wall, X52	Water	Composite wrap	xx	0	Failed
16	24-in pipe, 0.375-in wall, X52	Water	Polymer coating	xx	0	Failed
17	24-in pipe, 0.375-in wall, X52	Nitrogen	None	xx	12	Intact
18	24-in pipe, 0.375-in wall, X52	Nitrogen	None	xx	0	Failed
19	24-in pipe, 0.375-in wall, X52	Nitrogen	Steel encased FRC	xx	0	Intact
20	24-in pipe, 0.375-in wall, X52	Nitrogen	Protective sleeve	xx	0	Failed

8 Valve Tests

8.1 Test Overview

8.1.1 Test Objectives

The goal of these tests was to determine the resistance of bare (unprotected) and protected valves to a xx-lb C4 contact charge.

8.1.2 Failure Criterion

For the valve specimens, failure was defined as either cracking or breach of the outer casing or by inoperability of the valve mechanism. As with the pipe tests, cracking or breach of the casing was readily determined by whether the specimen maintained its internal pressure after detonation.

8.1.3 Typical Valve Specimen

A typical valve specimen is shown in Figure 151. It consisted of two 10-ft lengths of 24-in diameter, 0.375-in thick API 5L-X52 pipe joined to a 24-in ANSI 300 class valve. For assembly, ANSI 300 flanges were welded to the pipe lengths and bolted to the valve. Elliptical end caps were welded to the end of the pipes to permit pressurization. As with the pipe specimens, reinforced-concrete blocks were used to support the specimen at the ends; the clear distance between the blocks was 14-ft. Specimen details are summarized in Table 23.

Table 23. Typical Capped Pipe Segment Properties

Property	Magnitude/Description
Pipe Diameter [in]	24
Pipe Wall Thickness [in]	0.375
Pipe Steel Grade	API 5L X52
Pipe Lengths [ft]	10
Clear Span [ft]	14
Approx. Valve Length [ft]	4
Valve Type	ANSI 300
Flange Type	ANSI 300

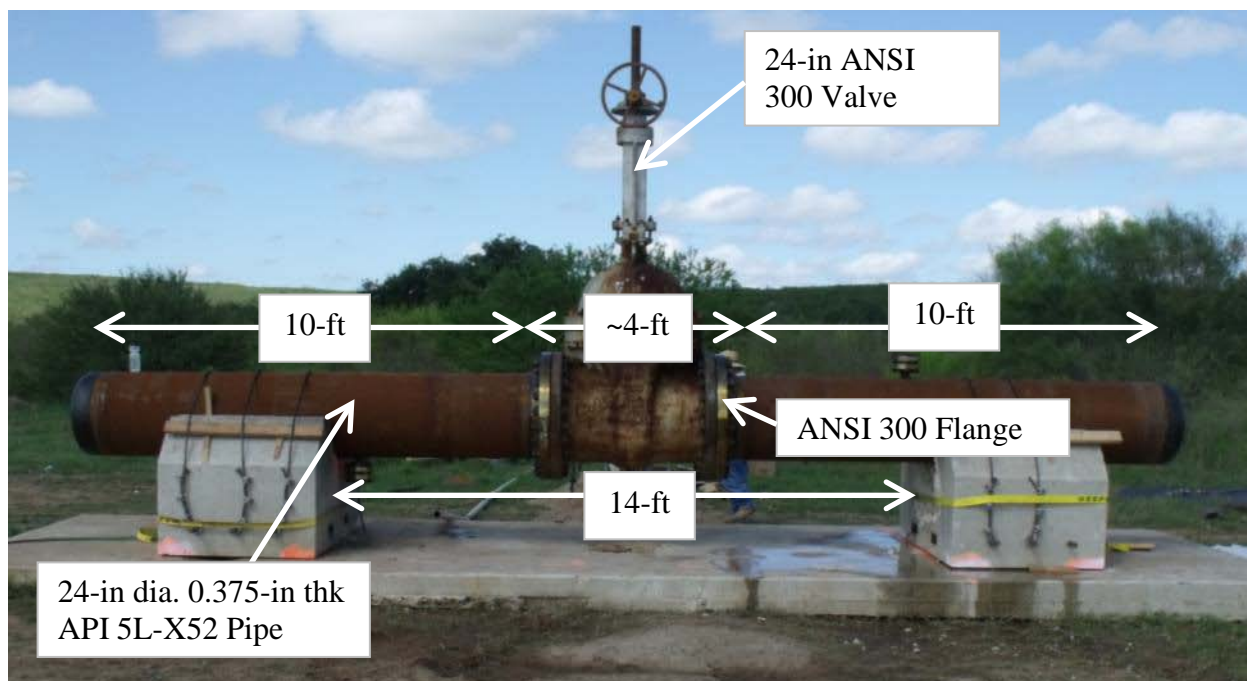


Figure 151. Typical Valve Specimen (Side Elevation View)

The valve specimens nominally were distinguished only by the blast mitigation technologies (BMTs) used to protect them. Because the valves were obtained in decommissioned condition rather than new, it was not possible to obtain identical valves. As a result, there were slight differences in the geometry of the valves, but these were deemed to have negligible effect on the resistance of the valves to the contact-charge threat. Finally, due to the nature of the test site and

differences in the BMTs, layout of instrumentation was distinct for each valve test and consequently will be discussed separately by test.

8.1.4 Explosive Threat

With the exception of Test 22B, the explosive threat for the valve tests was xx-lb C4 in contact with the valve or BMT, nominally identical to the threat in the source characterization tests (Section 6.1.4). Details of placement of the charge in each valve test will be discussed in the appropriate sections below because each test was unique.

8.1.5 Test Matrix

The four valve tests are summarized in Table 24. Test 21 was a baseline test, and Test 22 and 23 tested two distinct BMTs. A follow-on test to Test 22 (Test 22B) was performed under a separate contract between Composite Technologies and SwRI, and Composite Technologies made results from that test available for this report. Test 22B was identical to Test 22 except that the threat was increased to xx-lb C4 in contact.

All three valve specimens were filled with water and pressurized using nitrogen bottles. The specimens in Test 21 and 23 were pressurized to 720 ± 1 psi. However, the specimen used in Tests 22 and 22B could only be pressurized to 690 psi and 683 psi, respectively, due to a leak between the pipe and valve flanges. The pre-detonation pressurizations were at least 95% of the target 720 psi and were deemed sufficient.

Table 24. Valve Contact Charge Tests

Test	Component	Blast Mitigation Technology	Charge Weight [lb]	Purpose
21	24-in valve, 24-in pipe, 0.375-in wall, X52	None	xx	Baseline
22	24-in valve, 24-in pipe, 0.375-in wall, X52	SEFRC Cover	xx	Effect of protection on valve
22B	24-in valve, 24-in pipe, 0.375-in wall, X52	SEFRC Cover	xx	Effect of protection on valve
23	24-in valve, 24-in pipe, 0.375-in wall, X52	Protective Structure	xx	Effect of protection on valve

8.2 Test 21: Bare Valve, xx-lb C4 Contact Charge

8.2.1 Test Details

For Test 21, the C4 charge was placed directly on the surface of the valve, as shown in Figure 152 and Figure 153. This location was selected because it was deemed to be the most vulnerable location on the valve based on inspection of the specimen.



Figure 152. Location of C4 Charge for Bare Valve Test (Test 21)



Figure 153. Detail of Location of C4 Charge for Bare Valve Test (Test 21)

8.2.2 Instrumentation

The instrumentation layout for Test 21 was equivalent to the layout for the pipe tests, as discussed in Section 7.1.6, except for the location of the pressure gauges. As illustrated in Figure 154 and pictured above, the charge was placed on the side of the valve and the position of the pressure gauges was adjusted to maintain standoffs of 10-ft and 20-ft from the center of the charge. The elevations of the instrumentation and pipe supporting the valve were identical to the pipe tests, as illustrated in Figure 93.

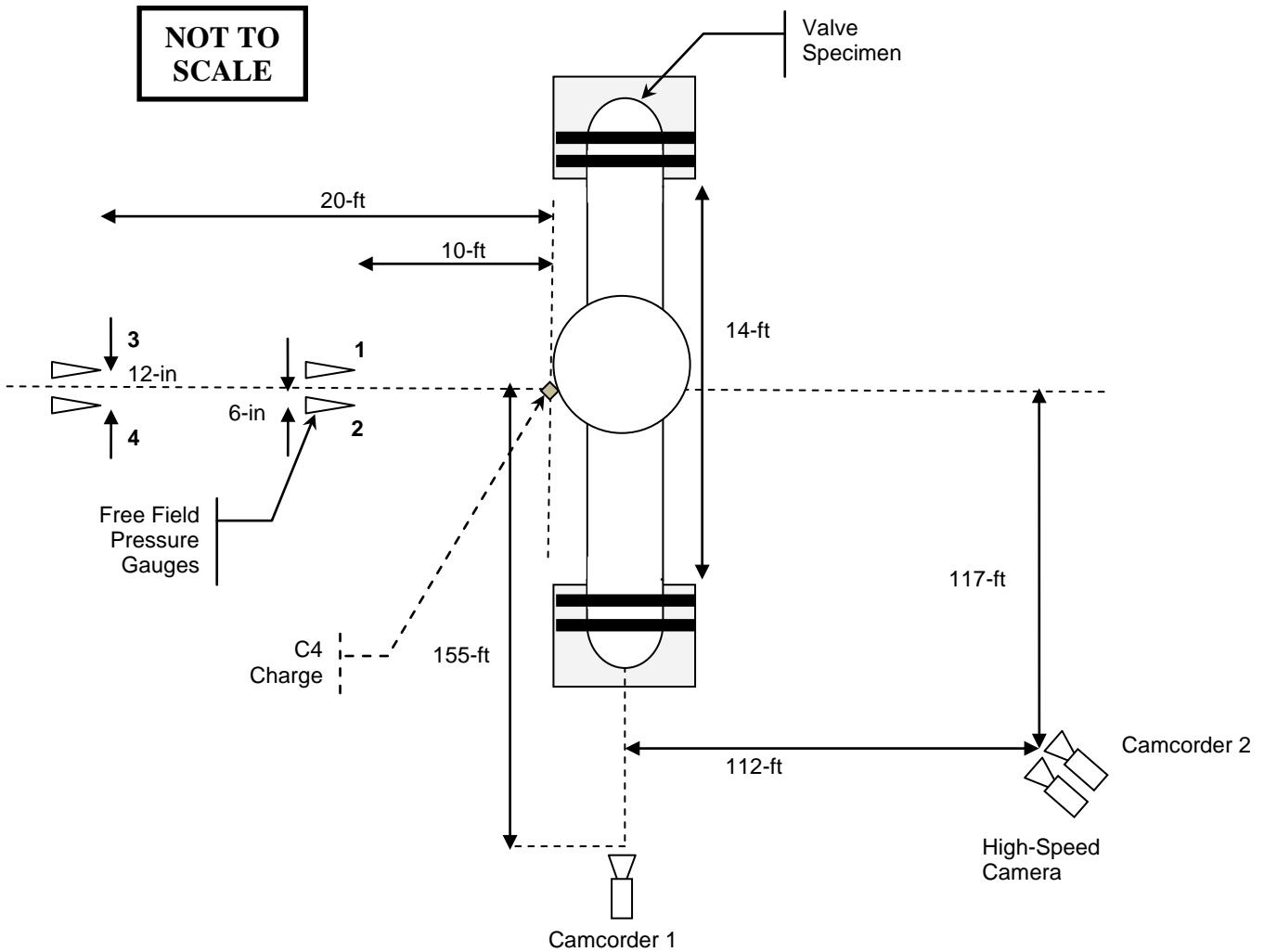


Figure 154. Location of Instrumentation in Valve Test 21 (Plan View)

8.2.3 Post-Test Condition

As shown in Figure 155 through Figure 157, the charge breached the valve in two locations: immediately beneath the charge and adjacent to the charge, on the vertical wall of the casing. The valve before and during rupture is shown in Figure 158 and Figure 159, respectively, which are frames from the high-speed camera used to document the test.



Figure 155. Holes in Bare Valve (Test 21)



Figure 156. Hole Detail in Bare Valve (Test 21)



Figure 157. Hole Detail in Bare Valve (Test 21)



Figure 158. Water-Filled Bare Valve, xx-lb C4 Contact Charge (Test 21) at Time = 0 s



Figure 159. Water-Filled Bare Valve, xx-lb C4 Contact Charge (Test 21) at Time = 0.123 s

8.2.4 Pressure-Time Histories

The pressure-time histories for Test 21 are shown in Figure 160. Peak pressures at both the 10-ft and 20-ft standoff were larger than those observed during the pipe tests due to reflective pressure build-up on the multiple surfaces of the valve.

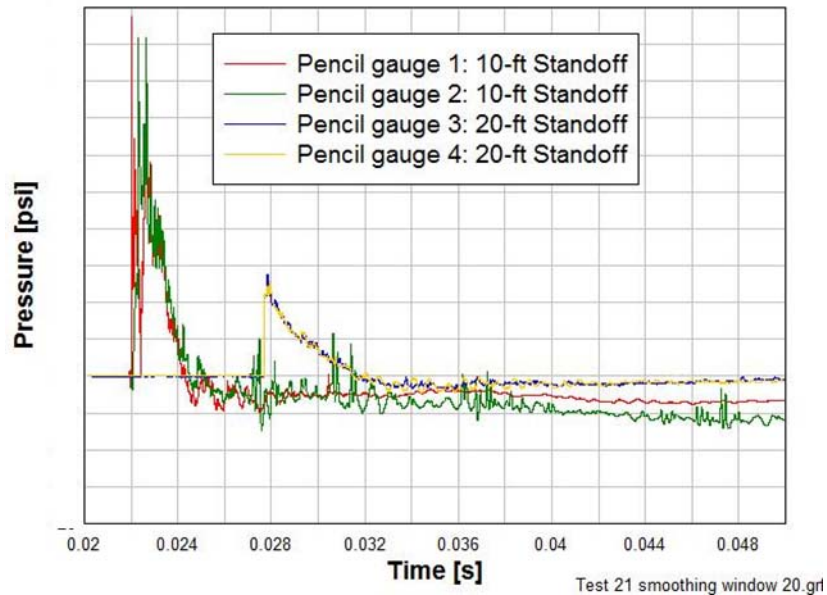


Figure 160. Pressure-Time Histories, xx-lb C4 Contact Charge on Bare Valve (Test 21)

8.3 Test 22: SEFRC-Covered Valve, xx-lb C4 Contact Charge

8.3.1 Test Details

The BMT used to protect the valve in Test 22 was designed, fabricated, and installed by Composite Technologies, in association with BAE Systems and W Industries. This BMT, shown in Figure 161, was an assembly of SEFRC panels bolted together to cover the valve. The assembly was designed to be efficiently installed and removed in the field. As with the pipe specimens, Composite Technologies requested the bare valve specimen be sent to their fabricator, W Industries, where the SEFRC cover was fabricated and installed on the valve. The SEFRC-covered specimen was then shipped to the test site.

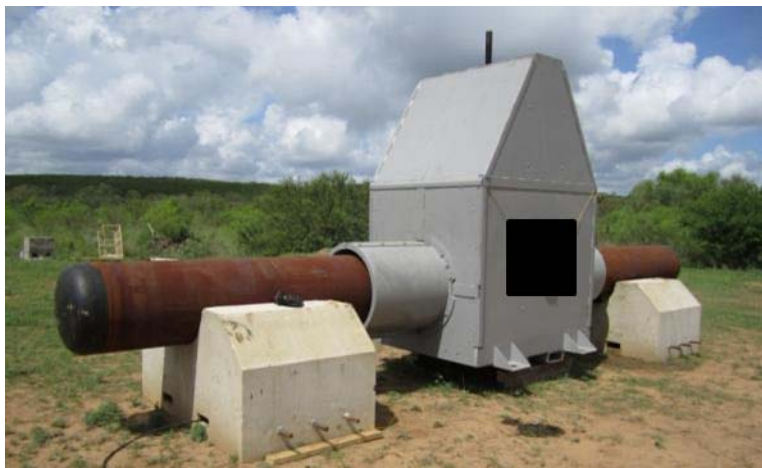


Figure 161. Pre-Test Condition of Valve SEFRC BMT, xx-lb Charge (Test 22)

As shown in Figure 161, the charge was placed in the middle of the bottom square panel. PEC engineers deemed this location to be the most vulnerable because the SEFRC panel had its least support there and secondary debris from the BMT would likely strike the valve, potentially breaching it.

8.3.2 Instrumentation

A plan view of the Test 22 specimen is shown in Figure 162. The elevations of the instrumentation and pipe were identical to the pipe tests, as illustrated in Figure 93.

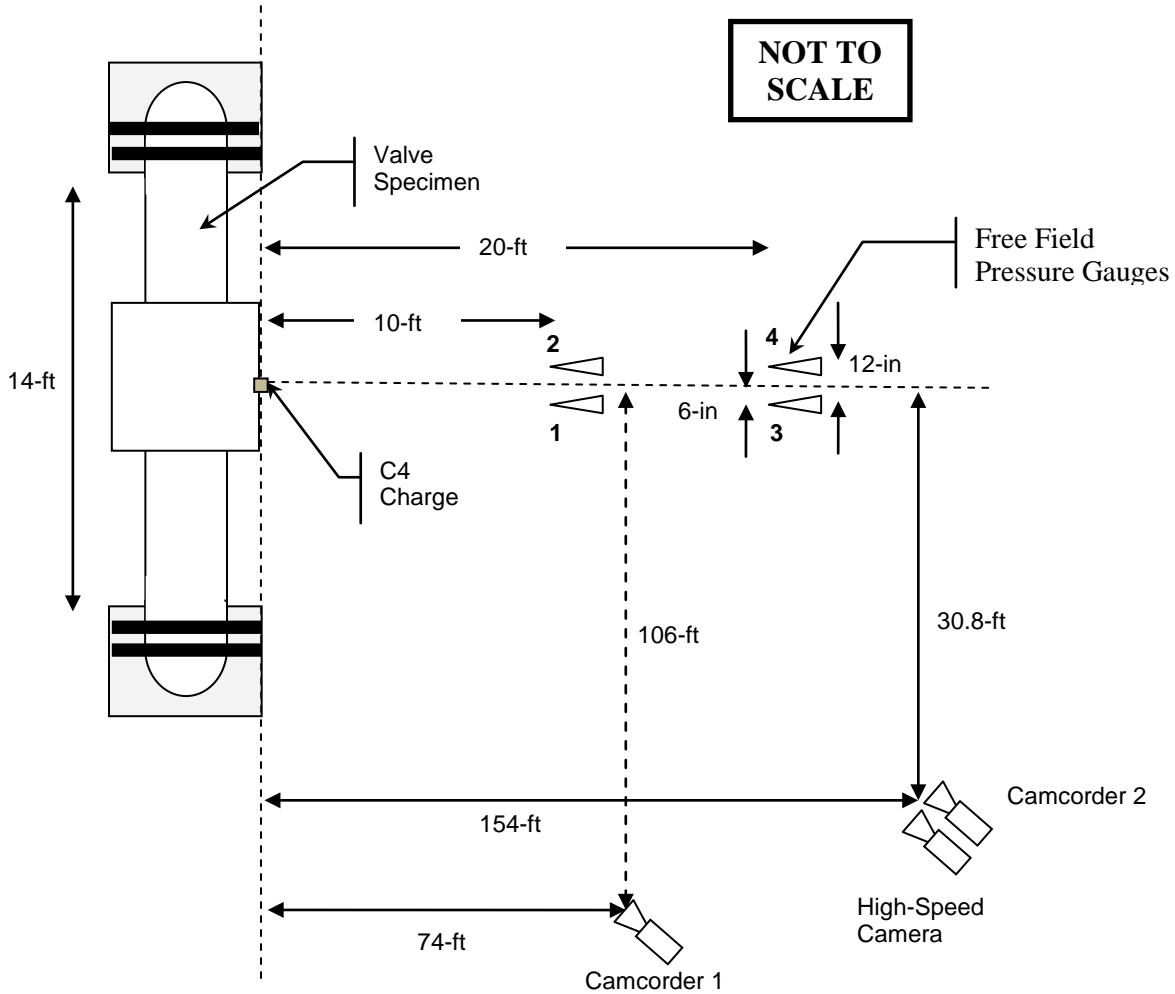


Figure 162. Location of Instrumentation in Valve Test 22 (Plan View)

8.3.3 Post-Test Condition

As shown in Figure 163 through Figure 165, the C4 charge breached the wall of the BMT. However, as shown in Figure 166, debris from the BMT struck the casing of the valve but did not breach the valve. In fact, no deformation of the valve was observed, and the debris from the

BMT left only a superficial mark on the valve face. Also, the specimen maintained its pre-detonation pressurization. Therefore, the BMT successfully prevented failure of the valve as the valve was not breached and remained operable.



Figure 163. Post-Detonation Condition of Valve SEFRC BMT (Test 22)



Figure 164. Width of Hole in SEFRC BMT, No Breach of Valve (Test 22)



Figure 165. Height of Hole in SEFRC BMT, No Breach of Valve (Test 22)



Figure 166. Post-Detonation Mark on Face of Valve,
No Breach (Test 22)

8.3.4 Pressure-Time Histories

Data for this test was not recorded because of a problem with the data acquisition system.

8.4 Test 22B: SEFRC-Covered Valve, ww-lb C4 Contact Charge

8.4.1 Test Details

The set-up for Test 22B, shown in Figure 167, was identical to Test 22 except that a ww-lb charge was placed on the undamaged side opposite the side tested with the xx-lb charge. The shape and aspect ratios for the ww-lb charge were identical to those of the xx-lb charge, discussed in Section 6.1.4. The center of the charge was positioned on the side panel exactly as in Test 22.



Figure 167. Pre-Test Condition of Valve SEFRC BMT, ww-lb Charge (Test 22B)

8.4.2 Instrumentation

Changing the position of the charge required adjustment of the instrumentation layout from Test 22, and the result is shown in Figure 168.

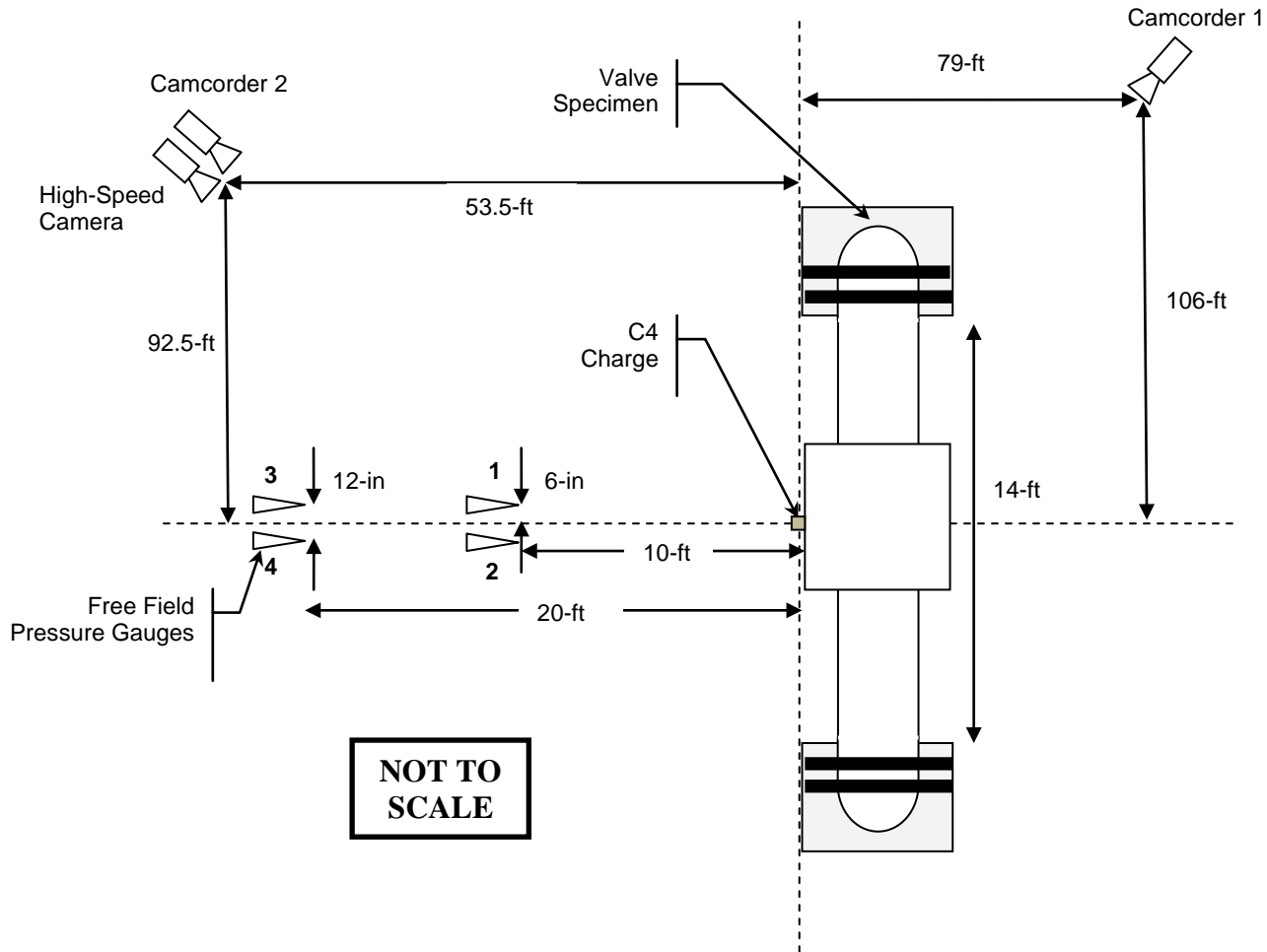


Figure 168. Location of Instrumentation in Valve Test 22B (Plan View)

8.4.3 Post-Test Condition

The post-test condition of the SEFRC cover and valve are shown in Figure 169 through Figure 172. From the figures, the SEFRC cover failed, but, like Test 22, there was no breach of the valve, which was confirmed by the fact that the specimen maintained its pre-detonation pressurization. Debris from the cover left a mark on the face of the valve, but the valve remained operable.



Figure 169. Post-Detonation Condition of Valve SEFRC BMT (Test 22B)



Figure 170. Width of Hole in SEFRC BMT, No Breach of Valve (Test 22B)



Figure 171. Height of Hole in SEFRC BMT, No Breach of Valve (Test 22B)



Figure 172. Post-Detonation Mark on Face of Valve, No Breach (Test 22B)

8.4.4 Pressure-Time Histories

The pressure-time histories for Test 22B are shown in Figure 173. Data from pencil gauge 1 was corrupt and is not included in the figure.

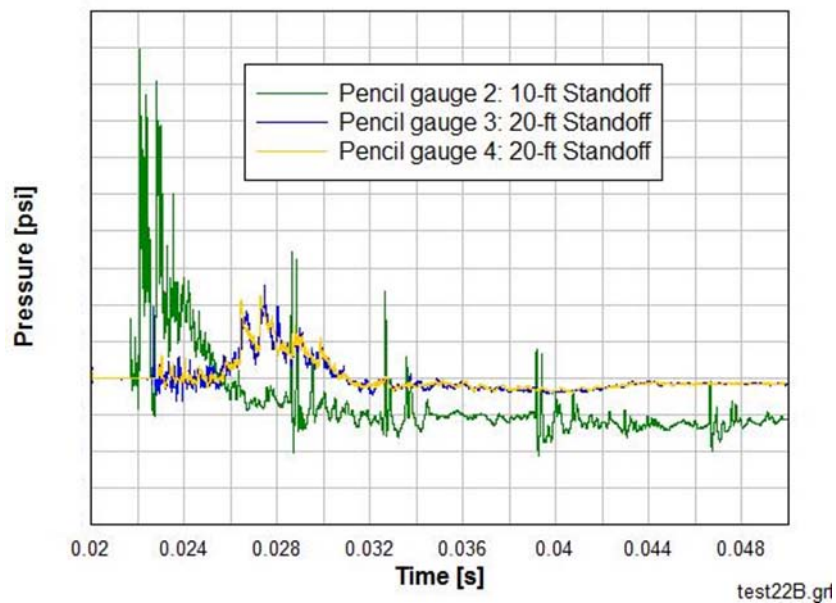


Figure 173. Pressure-Time Histories, ww-lb C4 Charge in Contact with SEFRC Valve Cover (Test 22B)

8.5 Test 23: Steel Protective Structure, xx-lb C4 Contact Charge

8.5.1 Test Details

The valve BMT shown in Figure 174 was provided by WinTec Security. It was composed of four high-strength steel panels bolted together to a square base. The BMT was installed at the test site. The charge was placed as shown in Figure 174 as a worst-case threat. At that location, the charge was centered on the valve at an elevation where debris from the BMT would likely strike the valve mechanism.



Figure 174. Pre-Test Condition of Valve BMT (Test 23)

8.5.2 Instrumentation

A plan view of the instrumentation layout is shown in Figure 175. The elevations of the instrumentation were identical to elevations shown in Figure 93.

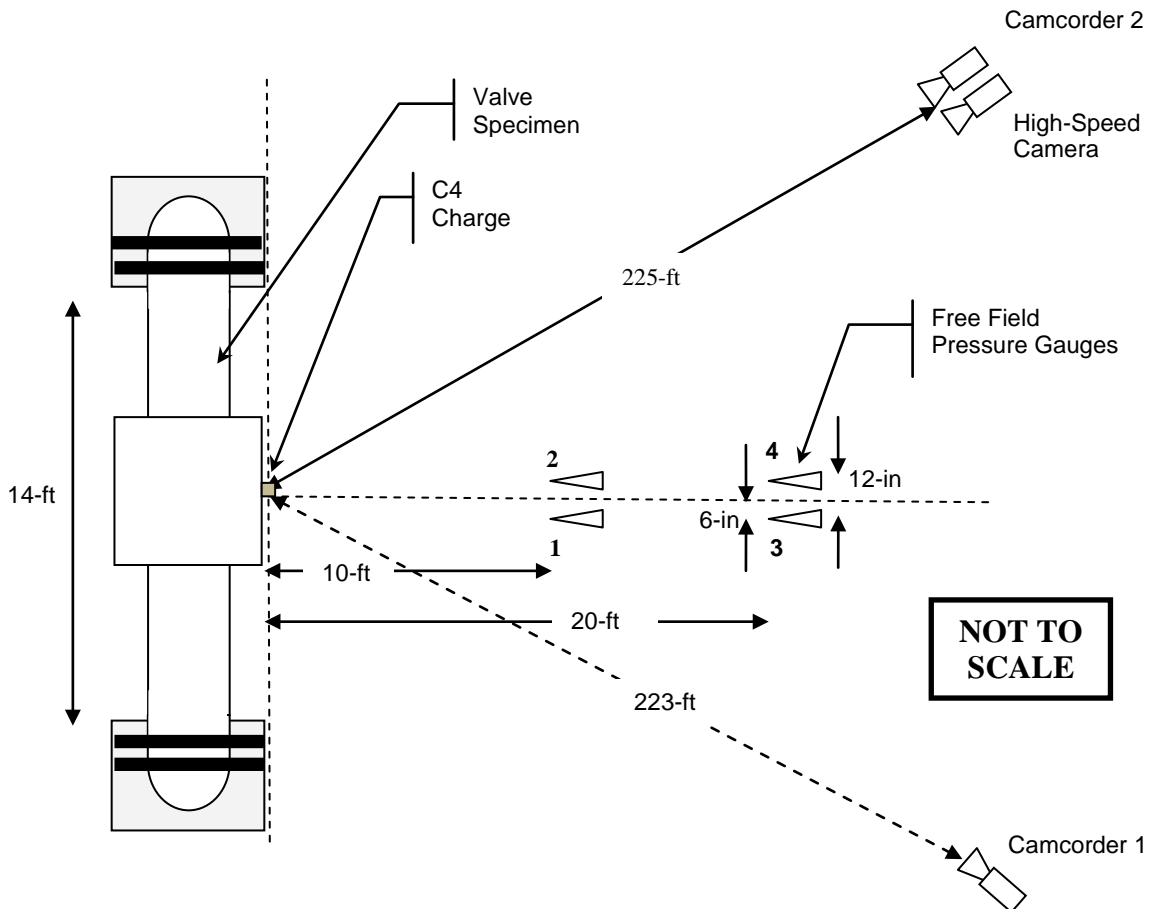


Figure 175. Location of Instrumentation in Valve Test 23 (Plan View)

8.5.3 Post-Test Condition

As shown in Figure 176 through Figure 179, the charge breached both the steel panel of the BMT and the casing of the valve. Therefore, the BMT hardware did not protect the valve. The detail in Figure 179 shows what is likely the plug from the BMT panel fused to the edges of the hole in the casing of the valve.



Figure 176. Post-Detonation Condition of Valve BMT (Test 23)



Figure 177. Width of Hole in BMT (Test 23)



Figure 178. Height of Hole in BMT (Test 23)



Figure 179. Detail of Valve Breach (Test 23)

8.5.4 Pressure-Time Histories

The pressure-time histories for Test 23 are shown in Figure 180. The gauges at each standoff were consistent with each other.

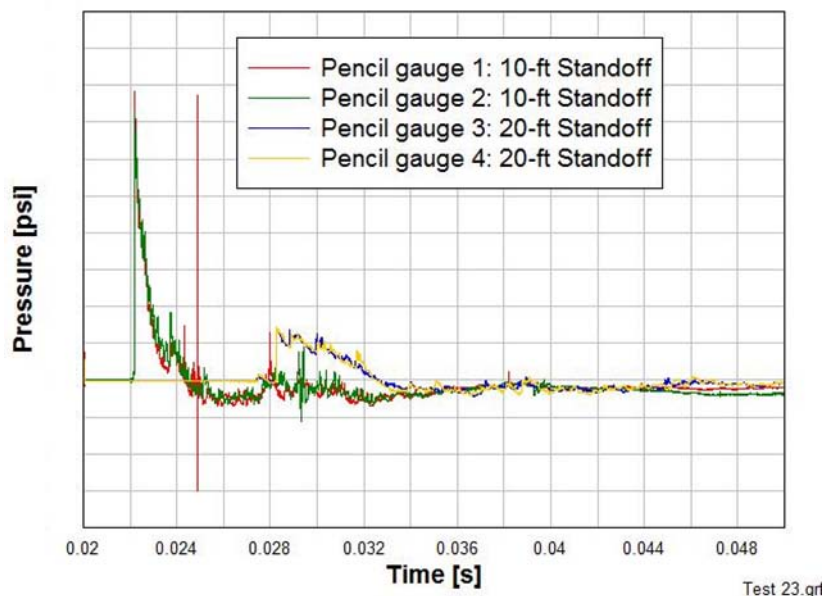


Figure 180. Pressure-Time Histories, xx-lb C4 Charge in Contact with WinTec Protective Structure (Test 23)

8.6 Valve Tests: Summary of Results

The results from the valve tests are summarized in Table 25. Only the SEFRC BMT prevented breach of the valve for the xx-lb C4 contact threat; it was further able to resist the xx-lb threat. As in the pipe tests, the wall of the SEFRC BMT was breached, but this breaching did not result in damage to the protected valve.

Table 25. Summary of Valve Tests

Test	Component	Blast Mitigation Technology	Charge Weight [lb]	Post-Test Valve Condition
21	24-in valve, 24-in pipe, 0.375-in wall, X52	None	xx	Failed
22	24-in valve, 24-in pipe, 0.375-in wall, X52	SEFRC Cover	xx	Intact
22B	24-in valve, 24-in pipe, 0.375-in wall, X52	SEFRC Cover	xx	Intact
23	24-in valve, 24-in pipe, 0.375-in wall, X52	Protective Structure	xx	Failed

9 Protective Structure Contact Charge Tests

9.1 Test Overview

9.1.1 Test Objectives

The purpose of the protective structure is to prevent damage to critical pipeline components such as pumps or compressors. Field tests were performed on two distinct protective structure concepts, and the threats were yy-lb and zz-lb C4 contact charges. The goal was to determine the resistance of the structures to these threats. Ideally, for the yy-lb charge, the protective structures would not breach, and if there were breach for the zz-lb charge, the secondary debris would not be hazardous to the main mechanical components of a pump or compressor.

9.1.2 Failure Criterion

A witness element, shown in Figure 181, was placed behind each protective structure prior to detonation. The element was a decommissioned compressor cylinder from a transmission line for natural gas, selected to represent a critical pipeline component. For the test, breach of any structural component of that witness element was defined as failure. Because the component was not internally pressurized for the test, breach was determined through post-test visual inspection of the cylinder.



Figure 181. Decommissioned Compressor Cylinder as Witness Element

9.1.3 Explosive Threat

Two threats were used: a yy-lb C4 charge and a zz-lb C4 charge. The yy-lb charge was used to determine the breach resistance of the protective structure. The zz-lb charge was an overload case used to assess the effect of secondary debris from the structure on the witness element.

The two charges were rectangular, with the same nominal aspect ratio as the xx-lb charges, 2:1 (base to height). The charge was hand-packed into a plywood box composed of 0.75-in thick

plywood on all sides except the side placed against the structure, which was 0.125-in masonite. The charge was detonated in this plywood case for the test.

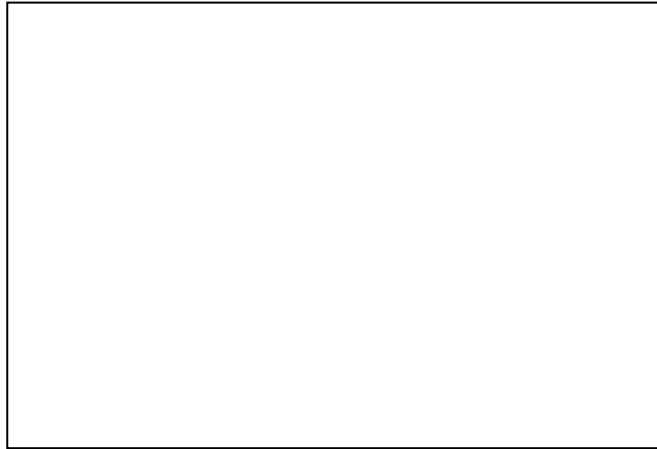


Figure 182. yy-lb C4 Charge

Holes at the 1/3 points on the diagonal were pre-drilled in the top plywood panel to serve as guides for two EBWs, which were pressed into the C4 surface until flush. The installed EBWs immediately before detonation are shown in Figure 183.



Figure 183. yy-lb C4 Charge Placed Prior to Detonation

The zz-lb charge had the same aspect ratio. Figure 184 shows the typical zz-lb charge used in testing.



Figure 184. zz-lb C4 Charge

9.1.4 Test Matrix

The test matrix from the Phase 2 Test Plan is shown in Table 26. Three tests (Test 31 through 33) were performed, and results for each are presented below. Test 34 was not performed for the reasons discussed in Section 9.5. All tests included a witness element behind the structure to assess performance.

Table 26. Protective Structure Contact Charge Tests

Test	Blast Protection	C4 Charge Weight [lb]	Purpose
31	Metalith™	yy	Determine if breach occurs
32	Metalith™	zz	Assess secondary debris risk
33	ICB Panel Structure	yy	Determine if breach occurs
34	ICB Panel Structure	zz	Assess secondary debris risk

9.2 Test 31: Metalith™, yy-lb C4 Contact Charge

9.2.1 Test Details

For both the yy-lb charge (Test 31) and zz-lb charge (Test 32) Metalith™ tests, units 5-ft thick x 10-ft high x 20-ft long were erected. Infrastructure Defense Technologies (IDT) recommended these dimensions to resist the yy-lb threat, and the same dimensions were used for the zz-lb case to assess the effect of secondary debris.

The corrugated steel of the Metalith™ was erected onsite by a local construction company and filled with locally-supplied clean bank sand. Construction of the first course of the Metalith™ is shown in Figure 185 and Figure 186. This process was continued until the structure was completed, as shown in Figure 187.



Figure 185. Corrugated-Steel Retaining Structure



Figure 186. First Course of Structure Filled with Sand

The charge was placed atop a hollow cardboard tube at mid-length of the structure, as shown in Figure 187. The witness element was located nominally 5-ft from the back face of the structure, as shown in Figure 188. It was placed upright on a pile of sand and was supported only by its self-weight. The elevation of the bottom of the charge was 26.5-in above the ground surface (Figure 189). This elevation was selected so that the center of the yy-lb charge was at the same elevation as the center of the zz-lb charge. As noted below, the elevation of the bottom of the zz-lb charge was 24-in.



Figure 187. Pre-Test Metalith™, Blast-Loaded Side (Test 31)



Figure 188. Pre-Test Metalith™, Back Side (Test 31)



Figure 189. Elevation of yy-lb Charge (Test 31)

9.2.2 Instrumentation

The instrumentation layout for Test 31 is shown in Figure 190. Two pressure gauges were located 30-ft from the face of the structure, and two were located 50-ft from the structure. The sampling rate on the pressure gauges was 1,000,000 data points per second, as in all other tests.

Four cameras were used, two high-speed and two regular-speed camcorders. A high-speed camera and a camcorder were located 127-ft from the center of the witness element. These cameras were intended to capture deformation of the structure due to the blast loading and permit tracking of any secondary debris. A fiducial grid was placed 10-ft from the corner of the structure to provide a frame of reference for any debris tracking. The other pair of cameras was located 273-ft from the lower corner of the structure to record the overall event. The elevation of the instrumentation was equal to the elevations shown in Figure 93.

The plywood screen discussed in the Phase 2 Test Plan was not included in the instrumentation set-up. Its intended purpose was to prevent the flash from the detonation from obscuring the cameras' field of view. Examination of site conditions by onsite engineers indicated that the screen would not shield the flash, and the screen was therefore not installed.

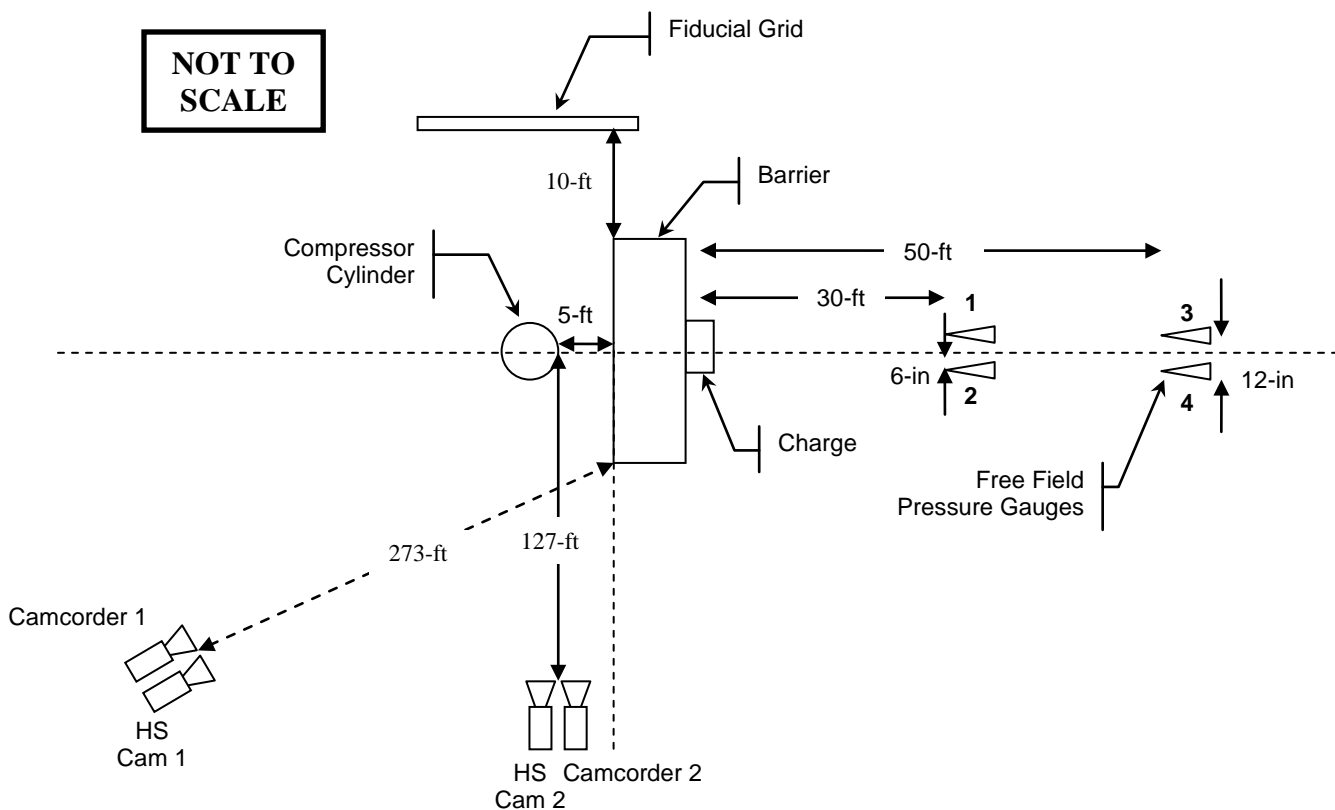


Figure 190. Location of Instrumentation in Protective Structure Test 31 (Plan View)

9.2.3 Post-Test Condition

The post-test condition of the Metalith™ structure is shown in Figure 191 through Figure 193. The 75-lb C4 contact charge caused significant damage to the structure. Corrugated steel from the nearest course separated and protruded from the front and back, and a substantial volume of sand flowed out of the structure. However, secondary debris from the structure was minimal, and the witness element remained undamaged and in its original position as shown in Figure 188 and Figure 193. In Test 31 and the other protective structure tests, tracking of the debris on the high-speed video to determine velocity was not possible because the fireball from the explosive obscured it.



Figure 191. Post-Detonation Blast-Loaded Side (Test 31)



Figure 192. Post-Detonation Blast-Loaded Side Detail (Test 31)



Figure 193. Post-Detonation Back Side (Test 31)



Figure 194. Post-Detonation Witness Element (Test 31)

9.2.4 Pressure-Time Histories

The pressure-time histories for Test 31 are shown in Figure 195. They were consistent at both the 30-ft and 50-ft standoffs except for a difference in the negative phase at the 30-ft standoff.

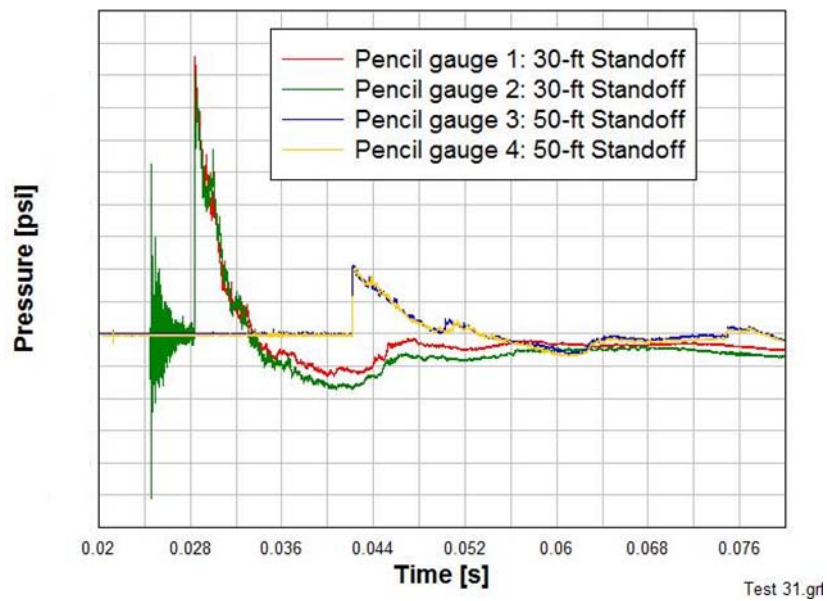


Figure 195. Pressure-Time Histories, yy-lb C4 Contact Charge on Metalith™ Protective Structure (Test 31)

9.3 Test 32: Metalith™, zz-lb C4 Contact Charge

9.3.1 Test Details

The construction of the Test 31 and Test 32 Metalith™ structures was identical; the only difference between the two tests was the charge weight. The completed structure and hollow cardboard tube location for Test 32 are shown in Figure 196. The bottom of the charge was located at an elevation of 24-in (Figure 197) so that the center of the yy-lb (Test 31) and zz-lb charge (Test 32) were nominally at the same elevation.



Figure 196. Pre-Test Metalith™, Blast-Loaded Side (Test 32)



Figure 197. Elevation of zz-lb Charge (Test 32)

9.3.2 Instrumentation

The instrumentation set-up for Test 32 is shown in Figure 198.

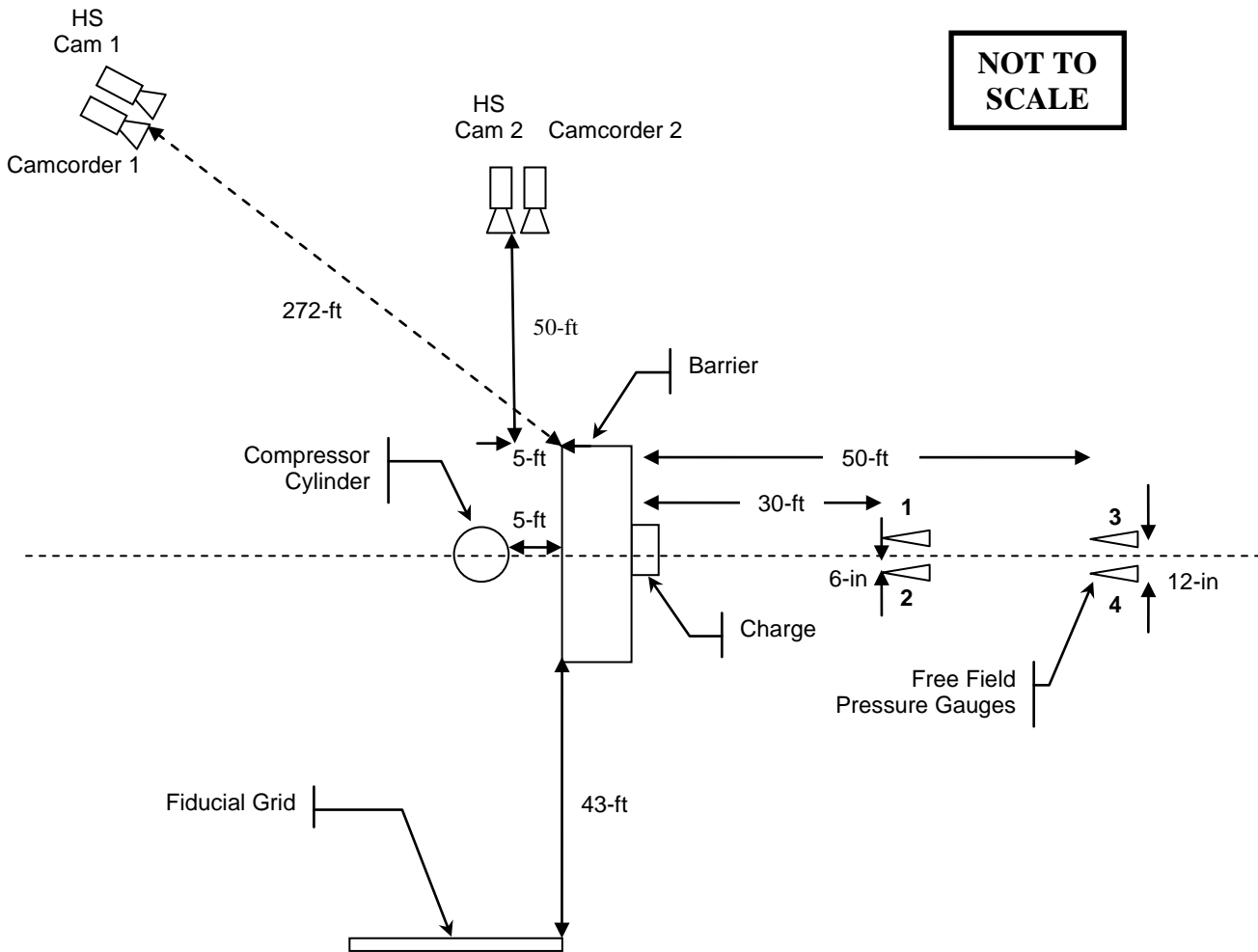


Figure 198. Location of Instrumentation in Protective Structure Test 32 (Plan View)

9.3.3 Post-Test Condition

As shown in Figure 199 and Figure 200, the structure was heavily damaged by the zz-lb charge. The steel of the different courses were offset from each other, and a large volume of sand was expelled from the structure. The witness element was overturned but was not damaged structurally, as shown in Figure 201. Therefore, secondary debris from an overload threat was not a significant hazard for the witness element.



Figure 199. Post-Detonation Blast-Loaded Side (Test 32)



Figure 200. Post-Detonation Back Side (Test 32)



Figure 201. Post-Detonation Witness Element (Test 32)

9.3.4 Pressure-Time Histories

The pressure-time histories for Test 32 are shown in Figure 202. Large peak pressures were measured (some beyond the range of the pressure gauges) due to the large size of the charge and reflections on the face of the protective structure.

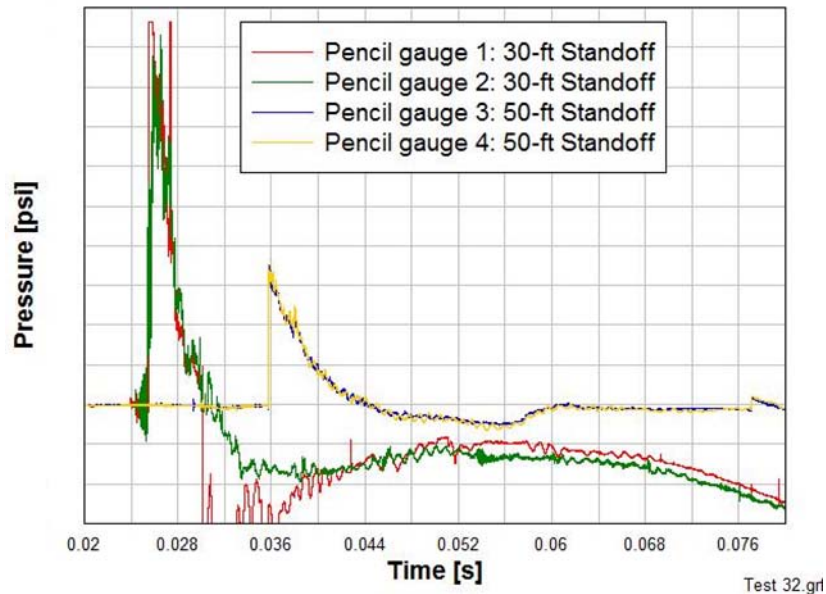


Figure 202. Pressure-Time Histories, zz-lb C4 Contact Charge on Metalith™ Protective Structure (Test 32)

9.4 Test 33: ICB, yy-lb C4 Contact Charge

9.4.1 Test Details

The second concept for a protective structure employed Inorganic Ceramic Binder (ICB) Blast Panels. The ICB panel is a technology developed by PPG Industries for protection against blast and fragments created by IEDs or military ordnance. The ICB panel is a composite material composed of fiberglass reinforced fabrics in the binder. For some applications, a hard granite aggregate layer is used on the strike face, and for others, polyurea coating is placed on the back side to contain spalled materials.

For this application, a spaced panel system was used where the outer and inner panels were 3.5-in thick with a 9.1-in air gap between the panels. A sketch of the panel and support frame design is shown in Figure 203; Figure 204 and Figure 205 are photographs of the installed structure. As shown in Figure 204, the charge was centered on the structure, and the elevation of the bottom of the charge was 26.5-in. The witness element in Figure 205 was placed 5-ft from the back face of the structure, as in the Metalith™ tests.

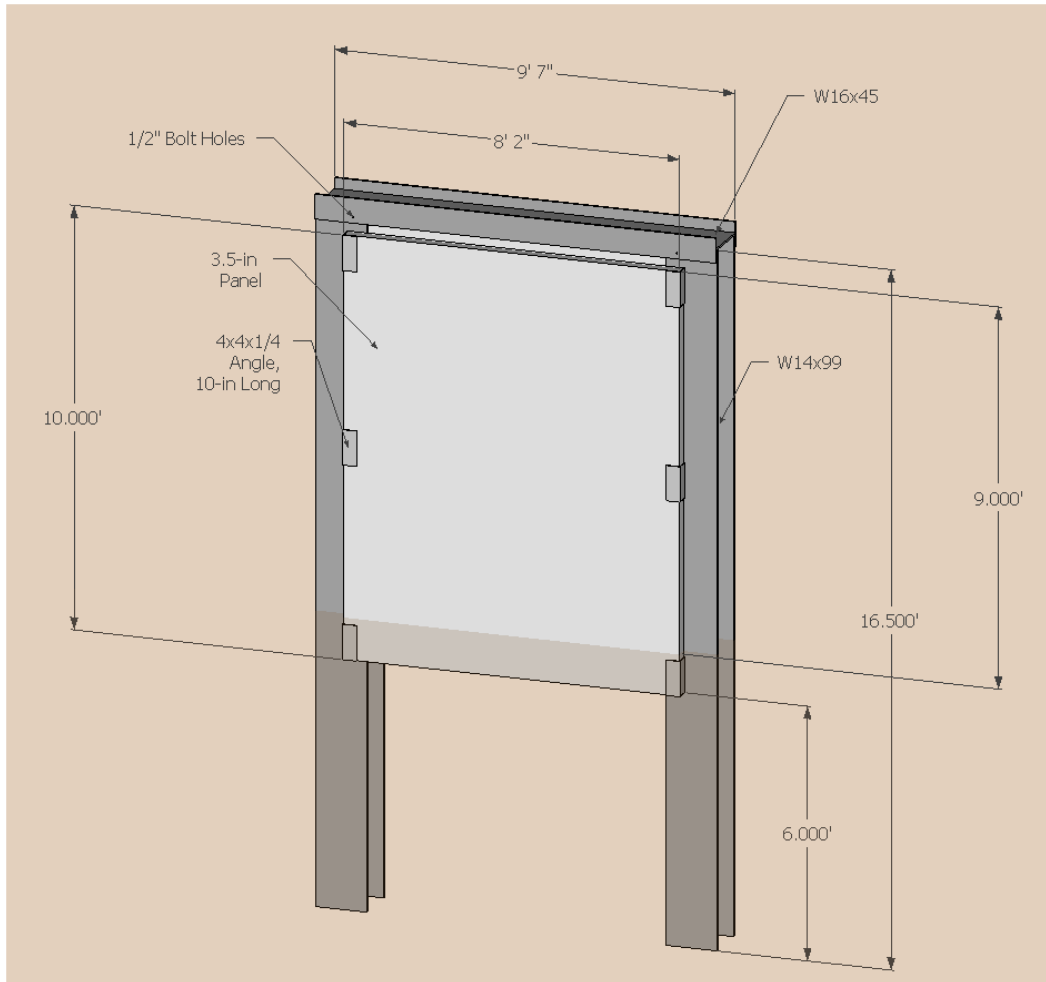


Figure 203. ICB Protective Structure Panel Configuration



Figure 204. Blast-Loaded Side of ICB Panel Structure (Test 33)



Figure 205. Back Side of ICB Panel Structure (Test 33)

9.4.2 Instrumentation

The instrumentation layout for Test 33 is shown in Figure 206. No fiducial grid was included in the test. Instead, a single camera frame of the test was recorded and could be overlaid on the high-speed video as needed, to serve as a grid for determining debris velocities if possible.

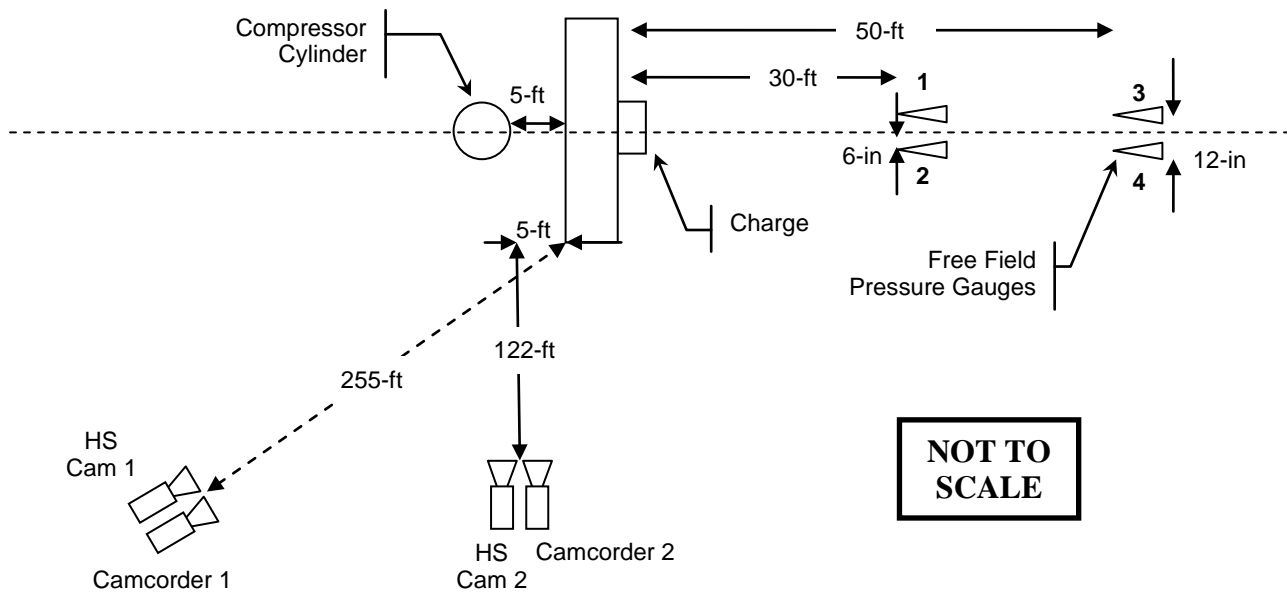


Figure 206. Location of Instrumentation in Protective Structure Test 33 (Plan View)

9.4.3 Post-Test Condition

The condition of the ICB panel structure after the test is shown in Figure 207 and Figure 208. On the blast-loaded side, the charge failed the bottom panel, splitting it in half, and the top panel, which was supported by the bottom, fell to the ground. Debris from the failure of the bottom panel breached the back bottom panel and partially damaged the back top panel. In addition, debris from the structure breached a plate on the witness element, as shown in Figure 209. Therefore, the panel failed due to the blast load, and secondary debris from the structure failed the witness element.



Figure 207. Post-Detonation Blast-Loaded Side (Test 33)



Figure 208. Post-Detonation Back Side (Test 33)



Figure 209. Breach of Witness Element Plate (Test 33)

9.4.4 Pressure-Time Histories

The pressure-time histories for Test 33 are shown in Figure 210. The histories were consistent at the 30-ft and 50-ft standoffs.

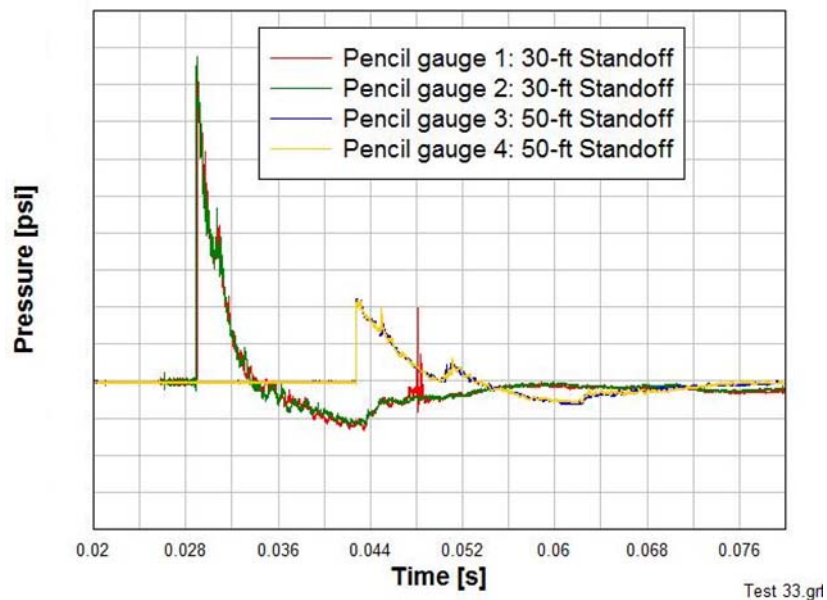


Figure 210. Pressure-Time Histories, yy-lb C4 Contact Charge on ICB Protective Structure (Test 33)

9.5 Test 34: ICB, zz-lb C4 Contact Charge

Test 34, where the threat was a zz-lb charge, was not performed because the ICB structure and witness element failed for the yy-lb threat. Significant failure of the ICB structure at the yy-lb was unexpected because ICB panels have performed well against close-in charges of comparable

charge weight. Therefore, the Test 34 structure was disassembled, and an ICB panel from it was sent to the manufacturer for testing.

Static compression tests performed on the material showed its ultimate strength was lower than assumed for analysis. Post-test examination of the damaged panels in Test 33 revealed irregular spacing of the fiberglass fabric through the ICB thickness. Additional testing would be required to determine how these anomalies affected the performance of the ICB BMT.

9.6 Protective Structure Tests: Summary of Results

The results from the protective structure test are summarized in Table 27. As noted in Section 9.1.2, the failure criterion was failure of any structural component of the witness element. For the Metalith™ barriers, the witness element was intact for the yy-lb and zz-lb threats. In the case of the ICB panel structure, the debris from the yy-lb threat failed the witness element, and the zz-lb test was not performed.

Table 27. Summary of Protective Structure Tests

Test	Blast Mitigation Technology	C4 Charge Weight [lb]	Post-Test Witness Element Condition
31	Metalith™	yy	Intact
32	Metalith™	zz	Intact
33	ICB Panel Structure	yy	Failed
34	ICB Panel Structure	zz	Not Tested

10 Anti-Tamper Tests

10.1 Test Overview

10.1.1 Test Objective

The goal of these tests was to determine the resistance of blast mitigation technologies (BMT) to tampering and removal by an aggressor.

10.1.2 Test Matrix

Per the Phase 2 Test Plan, seven anti-tamper tests were proposed. However, both WinTec Security protective jackets were destroyed in the blast tests, as discussed in Section 7.5 and Section 7.11. As a result, Test 42 could not be performed. Also, as discussed in Section 9.5, static tests of the ICB panels revealed that the material had a low compressive strength. Their low compressive strength would likely prevent them from accurately representing ICB resistance to tamper, and consequently, Test 46 was not performed. Therefore, five of the seven originally proposed anti-tamper tests were performed, as summarized in Table 28. Details of each of the specimens are discussed in the appropriate sections below.

Table 28. Test Matrix for Anti-Tamper Tests

Test No.	Test Specimen	Test Performed
41	Pipe with Steel-Encased FRC	Yes
42	Pipe with Protective Jacket	No
43	Pipe with Composite Wrap	Yes
44	Pipe with Polymer Coating	Yes
45	Metalith™ Protective Structure: w/ Red Oak	Yes
45B	Metalith™ Protective Structure: no Red Oak	Yes
46	ICB Protective Structure	No

10.1.3 Test Procedure

A modified version of the test procedure in ASTM Standard WK10816 *Standard Test Method for Time Evaluation of Forced Entry Resistant Assemblies* (currently in draft form) was used. For the pipe specimens, the goal was to create a minimum 6-in x 6-in clear space on the surface of the pipe. This area was selected because its removal would permit placement of the xx-lb C4 charge directly on the surface of the pipe. For the protective structure specimens, the goal was to create a man-passable opening such that a 12-in x 12-in x 8-in object could be passed through the opening. A man-passable hole would permit the aggressor to clear the barrier and place a charge directly on the pipeline component that the barrier is installed to protect.

The tools used in this assessment were those listed for the Very Low threat level in the draft ASTM standard WK10816 but with the addition of three battery-powered tools, an extra shovel, an oxyacetylene torch, and the removal of the two fire axes as defined below. The entire list of tools is below:

- Hand Tools (ASTM WK10816 Very Low Threat):
 - *Sledgehammer*- Double-face, drop-forged steel head with 36" handle. 2 each
 - *Wood Splitting Maul* – Heat-treated steel head with 3" cutting edge. 2 each
 - *Pry bar* - Forged steel, 60-in. length. 2 each
 - *Cold Chisel* - Conforming to Federal Specifications GGG-313B, 7/8" edge, 8-in. long, 1 each
 - *Screwdriver*- Steel, flathead, 12" long, 1/2" blade. 2 each
 - *Nail Puller*-11" long, steel. 2 each
 - *Axe* - 36" handle length, single-bit axe, steel head. 2 each
 - *Hammer* - Claw hammer, heat-treated, drop-forged steel. 2 each
 - *Pick*-Double-ended, steel 36" handle.
 - *Steel Pipe*, 3-in. diameter, ASTM-A53, 90 degree cut-off, 24-in. long, (10-pounds). 1 each

- *Pin Punch* – 4" and 8" long and 1/16"-3/8" thick, alloy steel, heat-treated. 1- 13 piece set each
 - *Shovel* - Round-point, 60" handle, steel blade. 2 each
 - *Rope* - 20' length of 1/2" diameter manila rope. 1 each
 - *Wire* - 36" of .125" diameter, 11 gauge steel alloy. 1 each
 - *Bolt Cutter* - Alloy steel with compound cutting action, 42" length. 1 each
 - *Diagonal Cutting Pliers* - Alloy steel jaws, hand-type, heavy duty, 7". 1 each
 - *Lineman Pliers* - Alloy steel, beveled nose with side cutting jaws, 8-1/2". 1 each
 - *Tin Snips* – Forged-steel blades with tempered cutting edges, heavy duty, 12". 1 each
 - *Vice Grip* - Straight jaws, 10", cold-forged steel with adjustable jaw lock capacity. 1 each
 - *Wrecking Bar* – 30" steel, 1.5" pry-blade width. 1 each
- Limited Battery-powered Tools (Added for these tests)
 - *Drill* - 1/2" drill motor, 18 VDC and assorted drill bits and hole saws.
 - *Circular Saw* - 6-1/2", 18 VDC and assorted blades.
 - *Reciprocating Saw* - 1" stroke, 18 VDC and assorted blades.
 - Thermal Tool (Added for these tests)
 - *Oxyacetylene Torch* - With 80 cubic feet oxygen tank, 40 cubic feet acetylene tank and 20' of hose.

WK10816 divides testing into two periods: structured and unstructured. In the structured period, which lasts the first five minutes, aggressors are restricted to using one of four tools. If at the end of five minutes the target area has not been entirely removed, the test passes into the unstructured period, where any of the above tools can be used. The test continues until either the target area of BMT has been removed or the total test duration reaches 1 hour (5 minutes structured, 55 minutes unstructured). For these tests, the unstructured period was extended to 1 hour, and the structured period was not performed. WK10816 was used for guidance, and this modification was deemed acceptable.

For all tests except Test 41, the aggressor team consisted of six males, between 18 and 35 years old, in good health, and between 150 and 220-lb body weight. While WK10816 specifies at least two members to be left-handed, all the team members were right handed. This was also considered an acceptable modification from WK10816. For the test, two team members worked at any one time, and new members were substituted as needed to prevent fatigue. The team consisted of employees of PEC and SwRI.

Test 41 was performed on a separate day from the other tests. Therefore, not all six team members were needed to prevent fatigue. Consequently, the team was reduced to four members with the same characteristics (150 to 220-lb body weight, etc.) as above.

10.1.4 Test Documentation

Two digital camcorders were used to record each test, and photographs were taken as appropriate. A stopwatch was used to measure the time that a tool was used and which of the team members used it. These tool-use durations are summarized for each test in a Gantt chart, in the respective sections for each test.

10.2 Test 41: Steel-Encased Fiber-Reinforced Concrete (SEFRC) Cover

10.2.1 Test Details

The specimen from Test 13, discussed in Section 7.4, was placed on level ground and subjected to the anti-tamper test. Prior to test initiation, an 8-in x 8-in target was scribed on an undamaged region of the SEFRC cover, as shown in Figure 211. The target was made 8-in x 8-in because edge irregularities were expected in the removed region. Making the target region 8-in x 8-in helped ensure that the minimum 6-in x 6-in region would be removed. The location of the target was selected to minimize the amount of high-strength fiber-reinforced concrete that needed to be cut through, which was anticipated to be the most difficult to remove.



Figure 211. Target Region on Surface of SEFRC Layer (Test 41)

10.2.2 Test Results

The Gantt chart for Test 41 is shown in Figure 212. The torch was used to cut the exterior layers of steel, as shown in Figure 213. The circular saw with abrasive masonry blade was then applied to the concrete, but it was relatively ineffective. The more effective means of removing the concrete was torching it to melt the steel fibers embedded in the concrete as shown in Figure 214 and then chipping the dross away with hammer and chisel, as shown in Figure 215. After the concrete was removed, the bottom layer of steel was torched (Figure 216) to expose a minimum 6-in x 6-in hole in the SEFRC cover (Figure 217). The clock time for the test was xx min. Per WK10816, 30 sec were added to the clock time to account for set-up of the battery-powered tools, and 30 sec were added for the set-up of the oxyacetylene torch. Therefore, the total time was xx min, which corresponds to a forced entry resistance rating of VLxx.

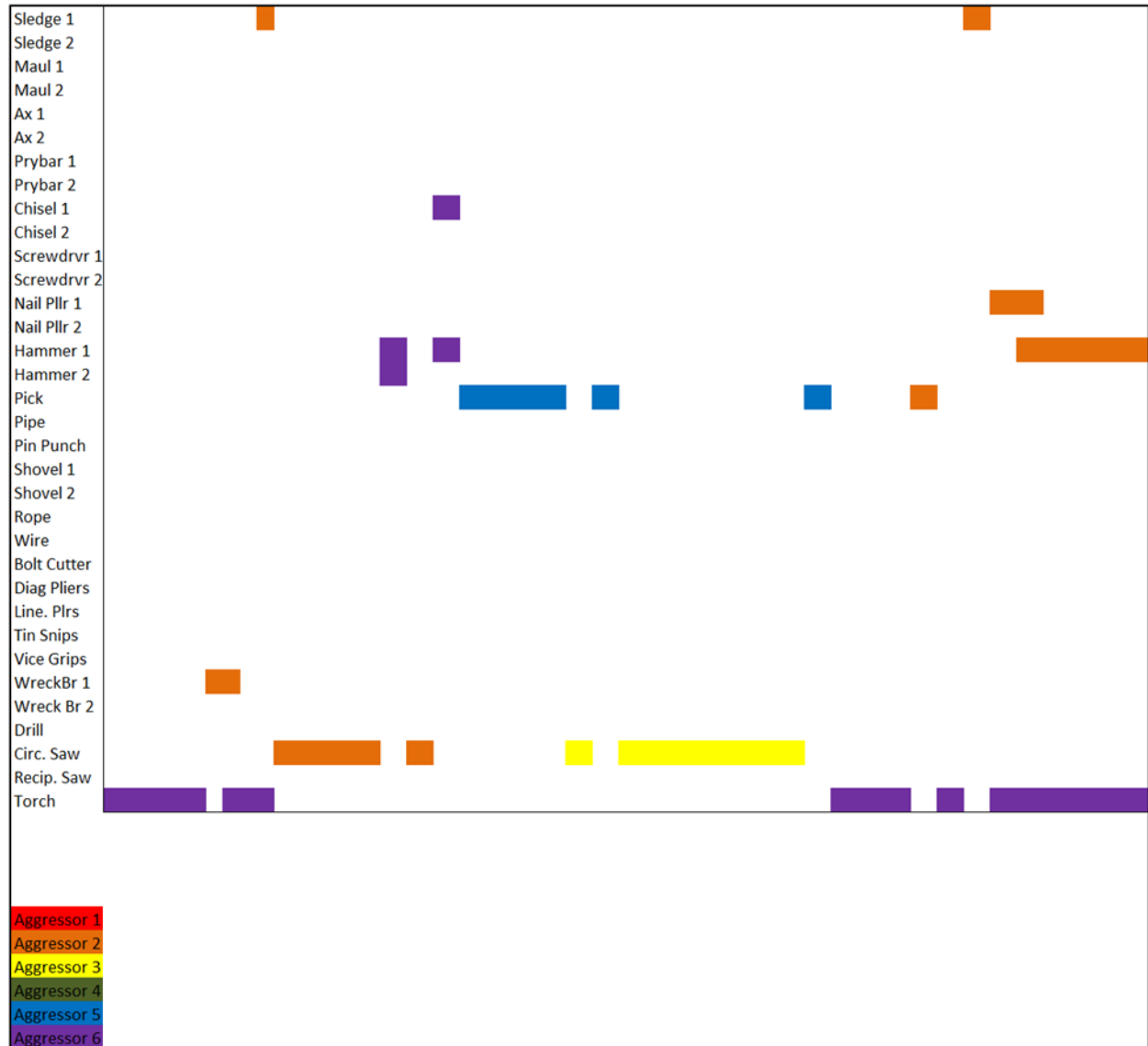


Figure 212. Gantt Chart for SEFRC Cover (Test 41)



Figure 213. Torching of Exterior Steel Layers (Test 41)



Figure 214. Torching of Fiber-Reinforced Concrete Layer (Test 41)



Figure 215. Chipping Cross away with Hammer and Chisel (Test 41)



Figure 216. Torching of Bottom Steel Layer (Test 41)



Figure 217. Minimum 6-in x 6-in Hole in SEFRC Cover (Test 41)

10.3 Test 42: Protective Jacket

Test 42 was not performed because both pipe jackets were destroyed in the blast tests, as discussed in Section 7.5 and Section 7.11.

10.4 Test 43: Fiber-Reinforced Polymer (FRP) Cover

10.4.1 Test Details

After Test 15, as discussed in Section 7.6, the blast-damaged specimen was placed on level ground and subjected to the anti-tamper test. As in Test 41, an 8-in x 8-in target was scribed on an undamaged region of the FRP cover, as shown in Figure 218.

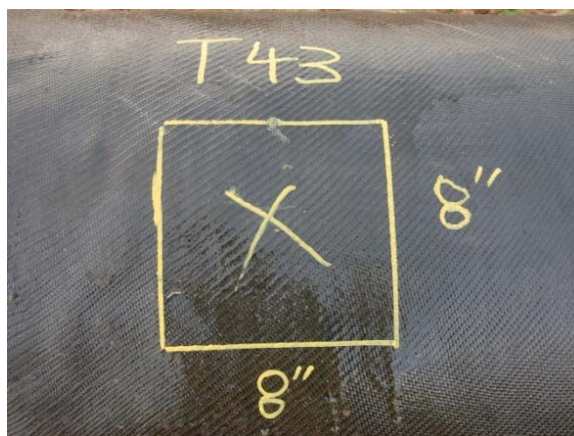


Figure 218. Target Region on Surface of FRP Layer (Test 43)

10.4.2 Test Results

The Gantt chart for the FRP cover is shown in Figure 219. For the first xx min of testing, the FRP layer was weakened and removed by ax blows, as shown in Figure 220. The rest of the test was spent using a combination of either the circular saw with wrecking bar or reciprocating saw with wrecking bar to remove the remaining layers of composite wrap. This approach is pictured in Figure 221. The clock time spent on the test was xx-min. Per WK10816, 30 sec were added to the clock time to account for set-up of the battery-powered tools. This increased the total chargeable time to xx-min, which corresponds to a forced entry resistance rating of VLxx.

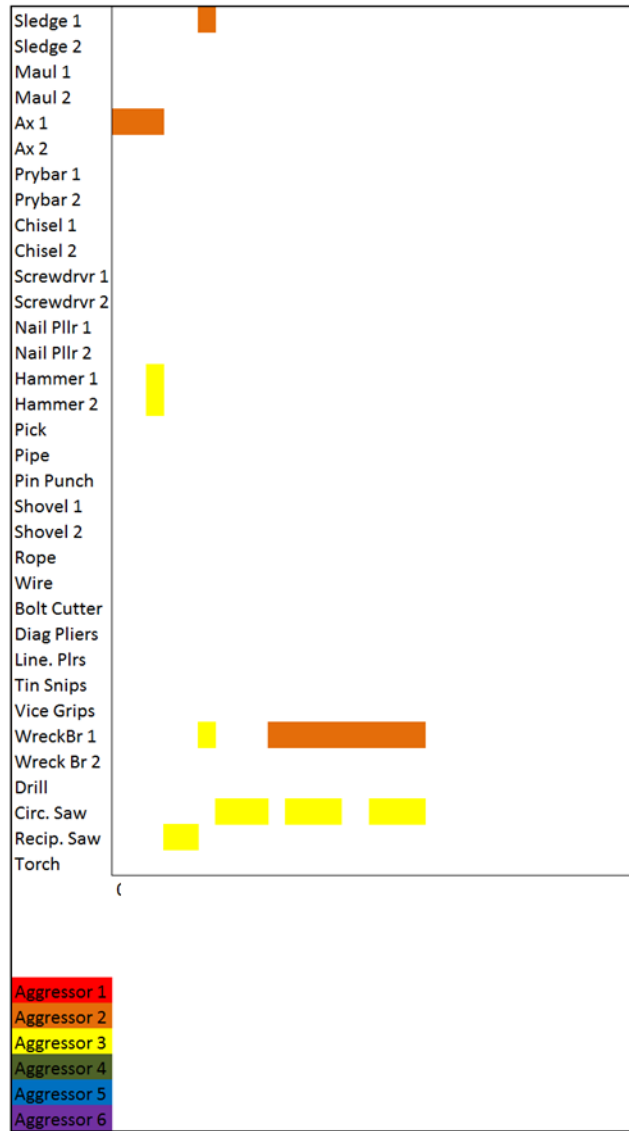


Figure 219. Gantt Chart for FRP Cover (Test 43)



Figure 220. Removal of FRP Layer with Axe (Test 43)

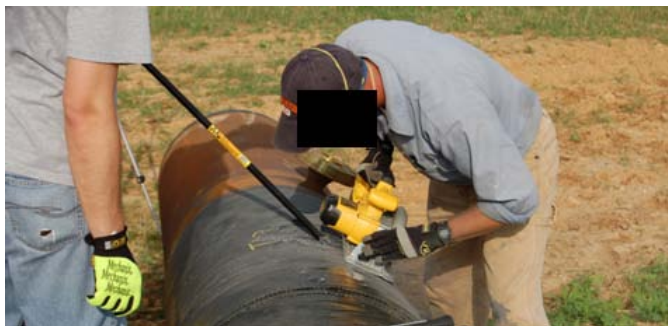


Figure 221. Removal of FRP Layer with Circular Saw and Wrecking Bar (Test 43)



Figure 222. Minimum 6-in x 6-in Hole in FRP Layer (Test 43)

10.5 Test 44: Polyurea Coating

10.5.1 Test Details

The test specimen from Test 16, discussed in Section 7.7, was placed on level ground after the blast test. The anti-tamper Test 44 was then performed. As in Test 41 and 43, the target area was an 8-in x 8-in square scribed on an undamaged portion of the specimen.

10.5.2 Test Results

The Gantt chart for Test 44 is shown in Figure 223. A circular saw was used to score the polyurea coating as shown in Figure 224. Hammer and chisel were used to remove the strips of coating that resulted from the scoring, as shown in Figure 225. The clock time spent on the test was xx-min. Per WK10816, 30 sec were added to the clock time to account for set-up of the battery-powered tools, increasing the total to xx-min. This corresponds to a forced entry resistance rating of VLxx.

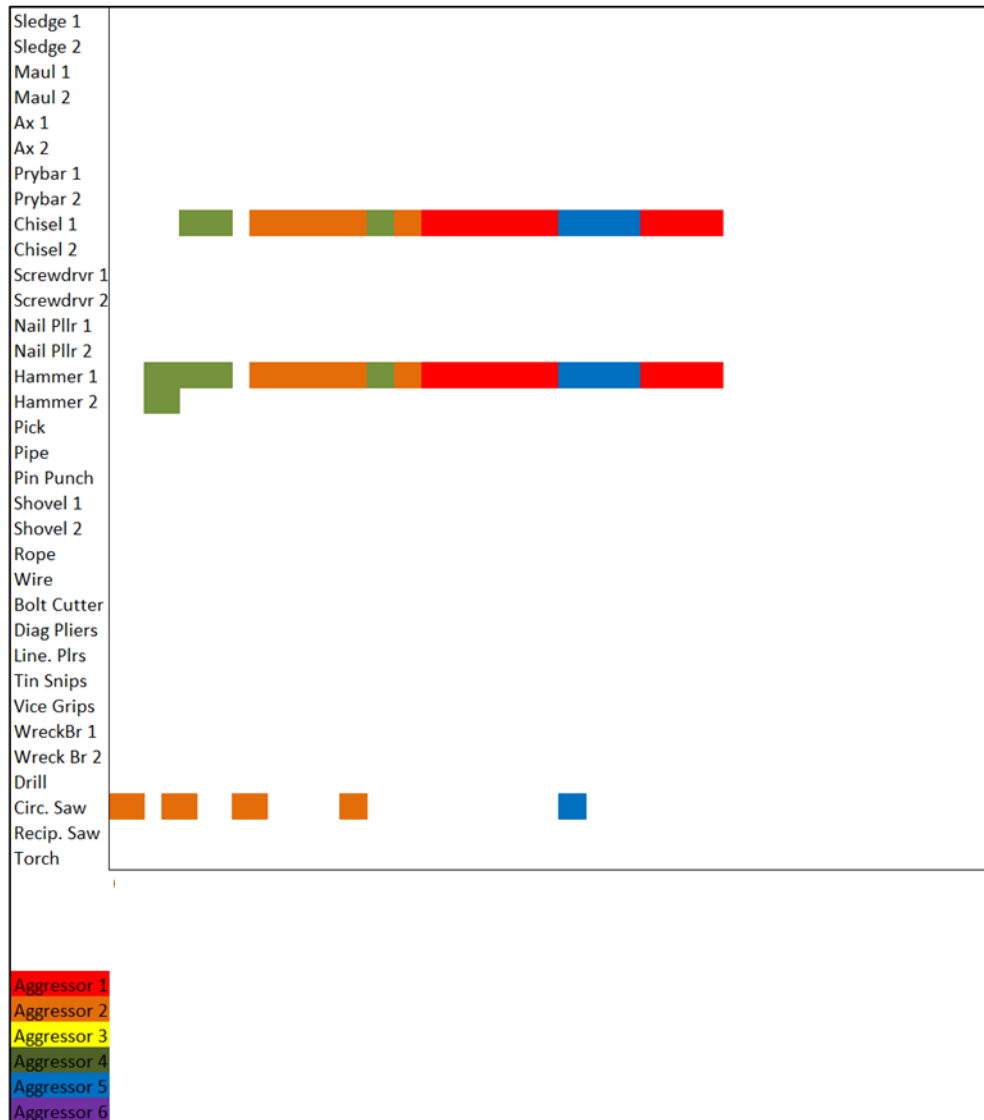


Figure 223. Gantt Chart for Polyurea Coating (Test 44)



Figure 224. Scoring of the Polyurea Coating (Test 44)



Figure 225. Removal of Polyurea Coating with Chisel and Hammer (Test 44)

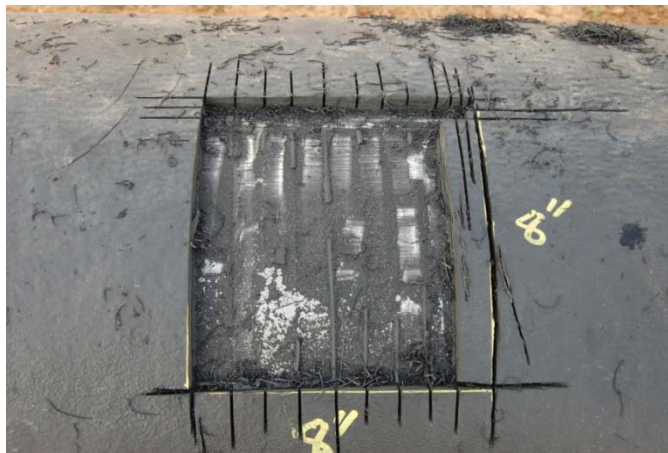


Figure 226. Minimum 6-in x 6-in Hole in Polyurea Coating (Test 44)

10.6 Test 45: Metalith™ Protective Structure, with Red Oak

10.6.1 Test Details

A single Metalith™ barrier was erected for two separate anti-tamper tests. The erection steps were identical to those discussed in Section 9.2 except a layer of red oak was included in one cavity to increase tamper resistance. The layer was composed of red oak planks 0.81-in x 5.5-in located 6-in from the corrugated steel wall, as shown in Figure 227 and Figure 228, respectively. The layer was offset from the corrugated panel by 6-in to permit sand to settle between the wood and steel layers. By filling the corrugations in the steel wall, the sand serves to reinforce the steel.

The cavity containing the red oak was tested in Test 45. Again, the objective of the test was to make a man-passable opening, one that permitted passage of a 12-in x 12-in x 8-in object, in the back steel wall of the barrier.



Figure 227. Erection of Red Oak Planks in Metalith™ Cavity (Test 45)



Figure 228. Gap of 6-in between Red Oak and Corrugated Steel Layer (Test 45)

10.6.2 Test Results

The Gantt chart for Test 45 is shown in Figure 229. Approximately the first xx-min of the test were spent using a torch to cut a 4-ft x 4-ft area from the front wall of the barrier, as shown in Figure 230. The circular and reciprocating saws were then used to remove the red oak behind the front steel wall, as shown in Figure 231. Shoveling the sand out of the cavity (Figure 232) required an additional xx-min. As shown in Figure 233, the sand removed was only what was necessary to permit torch access to the back steel wall. The resulting man-passable hole is shown in Figure 234. The clock time spent on the test was xx-min. Per WK10816, 30 sec were added to the clock time to account for set-up time of the battery-powered tools, and 30 sec were added for the set-up of the oxyacetylene torch. Therefore, the total time was xx-min, which corresponds to a forced entry resistance rating of VLxx.

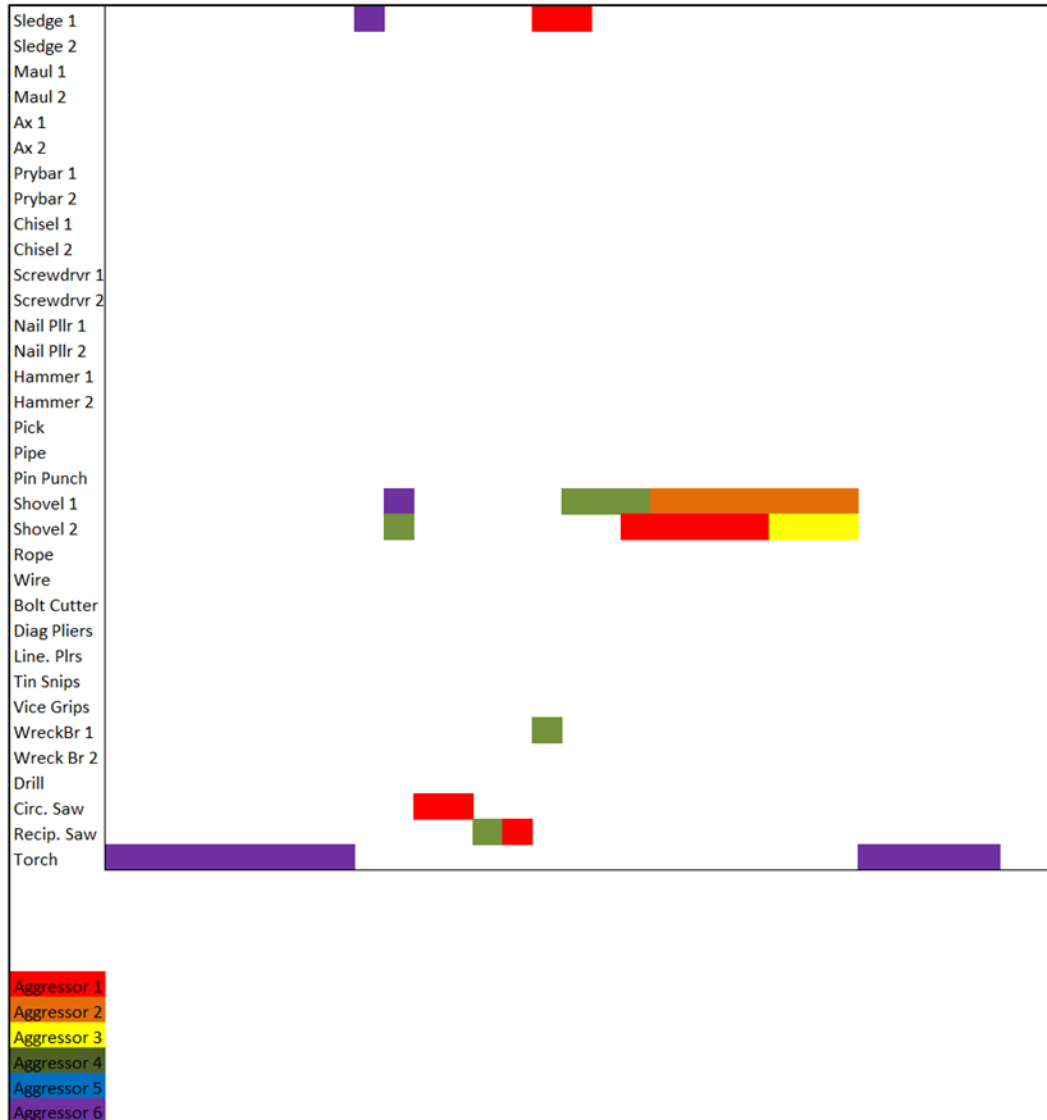


Figure 229. Gantt Chart for Metalith™ with Red Oak (Test 45)



Figure 230. Torch Burning Front Wall (Test 45)



Figure 231. Circular Saw Cutting the Panel (Test 45)



Figure 232. Removal of Sand from Cavity (Test 45)



Figure 233. Torching Back Panel (Test 45)



Figure 234. Man-Passable Hole in Back Wall (Test 45)

10.7 Test 45B: Metalith™ Protective Structure, No Red Oak

10.7.1 Test Details

The cavity in the Metalith™ barrier without red oak immediately adjacent to the one containing the layer of red oak was tested in Test 45B. The segment of barrier tested was identical to Test 45, as discussed in Section 10.6, except the cavity did not contain a layer of red oak.

10.7.2 Test Results

The Gantt chart for Test 45B is shown in Figure 235. This test followed a similar sequence as Test 45, as shown in Figure 236 through Figure 238, but there was no time spent removing the red oak panel. The clock time spent on the test was xx-min. Per WK10816, 30 sec were added to the clock time to account for set-up of the battery-powered tools, and 30 sec were added for the set-up of the oxyacetylene torch. These additions result in a total chargeable time of xx-min which corresponds to a forced entry resistance rating of VLxx.

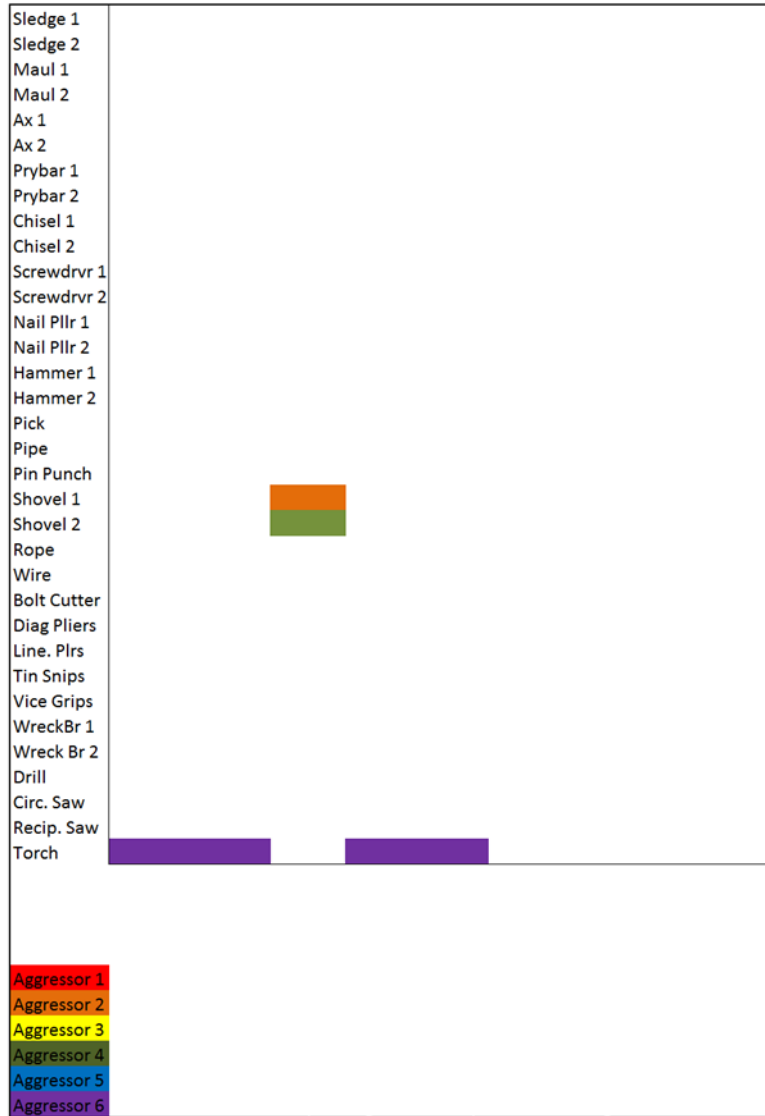


Figure 235. Gantt Chart for Metalith™ with No Red Oak (Test 45B)



Figure 236. Removal of Sand from Barrier Cavity (Test 45B)



Figure 237. Ingress into Barrier Cavity (Test 45B)



Figure 238. Man-Passable Hole in Back Wall (Test 45B)

10.8 Test 46: ICB Protective Structure

As discussed in Section 9.5, the strength of the ICB panels was unrepresentative. Therefore, no anti-tamper test was performed on the panels.

10.9 Anti-Tamper Tests: Summary of Results

The results from the anti-tamper tests are summarized in Table 29. Tests 42 and 46 were not performed as discussed in Section 10.1.2. As shown in the table, the SEFRC cover and Metalith™ with red oak had the highest forced entry resistance rating of VLxx. The polyurea coating and Metalith™ with no red oak had a lower rating of VLxx. Finally, the FRP had the lowest rating of VLxx.

Table 29. Anti-Tamper Test Results

Blast Mitigation Technology	Test No.	Forced Entry Resistance Rating
Steel-Encased Fiber-Reinforced Concrete (SEFRC) Cover	41	VLxx
Protective Jacket	42	Not performed
Fiber-Reinforced Polymer	43	VLxx
Polyurea Coating	44	VLxx
Metalith™ Protective Structure: w/ Red Oak	45	VLxx
Metalith™ Protective Structure: no Red Oak	45B	VLxx
ICB Protective Structure	46	Not performed

11 Conclusions

A summary of all tests for the pipe contact charge, valve contact charge, protective structure, and anti-tamper evaluation is provided in Table 30. Several of the blast mitigation technologies (BMTs) considered in the explosives tests were not evaluated to determine their forced entry resistance rating either because no test was planned, the technology was destroyed in the blast test, or the material provided by the supplier was unrepresentative.

Table 30. Summary of Test Results

Blast Mitigation Technology	Test No.	Installation	Protected Component	Component Contents	Post-Test Component Condition	Forced Entry Resistance Rating
Steel-Encased Fiber-Reinforced Concrete (SEFRC)	13, 41	Pipe Cover	Pipe	Nitrogen	Intact	VLxx
	19, 41	Pipe Cover	Pipe	Water	Intact	VLxx
	22, 22B	Valve Structure	Valve	Water	Intact	No test planned
Protective Jacket/Structure	14	Pipe Jacket	Pipe	Nitrogen	Failed	Jacket destroyed in blast test
	20	Pipe Jacket	Pipe	Water	Failed	Jacket destroyed in blast test
	23	Valve Structure	Valve	Water	Failed	No test planned
Fiber-Reinforced Polymer	15, 43	Reinforcing Layer	Pipe	Water	Failed	VLxx
Polyurea	16, 44	Protective Coating	Pipe	Water	Failed	VLxx
IDT Metalith™	31, 32, 45	Steel-Clad Earthen Barrier	Compressor Cylinder	NA	Intact	VLxx*
ICB Panel Structure	33	Panel Barrier	Compressor Cylinder	NA	Failed	Unrep. material

*Forced-entry resistance rating based on Metalith™ without red oak layer.

The steel-encased fiber-reinforced concrete (SEFRC) cover prevented failure of pipe and valve specimens for xx-lb C4 in contact with the BMT. In addition, the valve remained intact when the charge weight was increased to xx-lb. The pipe cover composed of SEFRC was the most tamper-resistant, with a forced entry resistance rating of VLxx. Therefore, SEFRC is a viable technology for mitigating blast damage and providing anti-tamper protection to pipeline components.

No other BMT prevented failure of the pipe or valve. The WinTec protective jacket did not prevent failure of the pipe, whether the contents were nitrogen or water; the WinTec protective structure did not prevent failure of the valve. Also, the fiber-reinforced polymer (FRP) layer and polyurea coating did not prevent failure of the water-filled pipe. Water-filled pipe was the best case for survival of the protective layer because water provides more inertial and mechanical resistance than pressurized nitrogen. Therefore, it can be inferred that the FRP and polyurea coating would have failed as well if they covered nitrogen-filled pipe.

The steel-enclosed soil barrier, developed by IDT Metalith™, is the other viable technology for protecting pipeline components. It resisted a yy-lb C4 contact charge and thereby protected a compressor cylinder for that threat. In addition, the secondary debris created by the zz-lb C4 threat did not damage the compressor cylinder. The conventional design for the Metalith™ had a moderate forced entry resistance rating of VLxx, and this is the value reported in Table 30. However, the addition of a layer of red oak to the barrier increased the rating to VLxx.

The ICB panel structure failed to protect the compressor cylinder for the yy-lb C4 threat; secondary debris from the ICB structure breached a structural plate on the compressor cylinder. The zz-lb C4 contact charge and anti-tamper tests were not performed.

To conclude, this test series has shown that there are two viable BMTs for protecting pipeline components: SEFRC covers and Metalith™ barriers. SEFRC covers are particularly appropriate for installations where there is minimal clearance around the component to be protected. Metalith™ barriers are more appropriate for hardening the perimeter around large pipeline components.

¹*Pipeline Modal Annex to the Transportation Sector Specific Plan*, Department of Homeland Security, 2010 (Draft Only), Washington, DC, www.dhs.gov

²*Transportation Systems: Critical Infrastructure and Key Resources Sector-Specific Plan as input to the National Infrastructure Protection Plan*, Department of Homeland Security, May 2007, Washington, DC, www.dhs.gov

³*The Latest Innovation in Pipe & Culvert Repair using Carbon FRP*, Mo Ehsani, Ph.D, P.E., S.E., Webinar September 16, 2009

⁴<http://www.armedforces-int.com/companies/fiber-reinforced-polymer-frp.asp>

⁵<http://www.armedforces-int.com/companies/fiber-reinforced-polymer-frp.asp>

⁶<http://www.hardwirellc.com/>

⁷<http://www.hardwirellc.com/solutions/reinforcements.html>

⁸ Courtesy of Infrastructure Defense Technologies, Belvidere, IL

⁹ *ibid*

¹⁰ Courtesy of the Technical Support Working Group (TSWG), Washington, DC

¹¹<http://www.armordesigns.com/products-energy.html>

¹²<http://www.composite-technologies.com/blast.html>

¹³http://www.wintecusa.com/pipeline_protection.html

¹⁴http://www.wintecusa.com/pipeline_protection.html

¹⁵<http://www.blastgardintl.com>

¹⁶<http://www.popsci.com/scitech/article/2005-11/blastgard-international-blastwrap>

¹⁷ Sharpe, Kevin J., "Protection of Oil Pipe Lines from Explosive Attack," BlastGard® International, October, 2004

¹⁸http://www2.basf.us/urethanechemicals/Specialty_Systems/sm_index.html

¹⁹ Courtesy of Berry Plastics™, Evansville, IN

²⁰ *ibid*

²¹*Characteristics and Common Vulnerabilities Infrastructure Category: Natural Gas Pipelines*, Department of

-
- Homeland Security, 22 April 2005, Washington DC, <http://www.dhs.gov/index.shtm>, p. 5
- ²² Discussion with Ed Bowles, Southwest Research Institute, San Antonio, TX
- ²³ US Department of Transportation, Pipeline and Hazardous Materials Safety Administration (PHMSA), <http://www.phmsa.dot.gov/pipeline/library/data-stats>
- ²⁴ www.qtrinc.biz/index.htm
- ²⁵ *ibid*
- ²⁶ *ibid*
- ²⁷ *ibid*
- ²⁸ Courtesy of Ed Bowles, Southwest Research Institute, San Antonio, TX
- ²⁹ *ibid*
- ³⁰ *ibid*
- ³¹ Courtesy of Ariel Corporation, Mount Vernon, OH
- ³² *Characteristics and Common Vulnerabilities Infrastructure Category: Natural Gas Pipelines*, Department of Homeland Security, 22 April 2005, Washington DC, <http://www.dhs.gov/index.shtm>, p. 5
- ³³ Courtesy of Ed Bowles, Southwest Research Institute, San Antonio, TX
- ³⁴ *ibid*
- ³⁵ *ibid*
- ³⁶ Email correspondence with Ed Bowles, Southwest Research Institute, San Antonio, TX
- ³⁷ *ibid*
- ³⁸ <http://www.scadalink.com/support/scada.html>
- ³⁹ *Characteristics and Common Vulnerabilities Infrastructure Category: Petroleum Pipelines*, Department of Homeland Security, 22 April 2005, Washington DC, <http://www.dhs.gov/index.shtm>, p. 8
- ⁴⁰ *ibid*, p.3ff
- ⁴¹ US Department of Transportation, Pipeline and Hazardous Materials Safety Administration (PHMSA), <http://www.phmsa.dot.gov/pipeline/library/data-stats>
- ⁴² Courtesy of Henry Oliver, Odessa Pumps, Boerne, TX
- ⁴³ *ibid*
- ⁴⁴ *ibid*
- ⁴⁵ *Characteristics and Common Vulnerabilities Infrastructure Category: Petroleum Pipelines*, Department of Homeland Security, 22 April 2005, Washington DC, <http://www.dhs.gov/index.shtm>, p. 6
- ⁴⁶ *ibid*
- ⁴⁷ *ibid*
- ⁴⁸ *Characteristics and Common Vulnerabilities Infrastructure Category: Petroleum Pipelines*, Department of Homeland Security, 22 April 2005, Washington DC, <http://www.dhs.gov/index.shtm>, p. 8
- ⁴⁹ *ibid*
- ⁵⁰ *Characteristics and Common Vulnerabilities Infrastructure Category: Petroleum Pipelines*, Department of Homeland Security, 22 April 2005, Washington DC, <http://www.dhs.gov/index.shtm>, p. 7
- ⁵¹ <http://www.energyindustryphotos.com>
- ⁵² *Pipeline Modal Annex to the Transportation Sector Specific Plan*, Department of Homeland Security, 2010 (Draft Only), Washington, DC, www.dhs.gov
- ⁵³ *Characteristics and Common Vulnerabilities Infrastructure Category: Petroleum Pipelines*, Department of

-
- Homeland Security, 22 April 2005, Washington DC, <http://www.dhs.gov/index.shtm>, p. 12
- ⁵⁴ibid, p. 11
- ⁵⁵UFC3-340-01 *Design and Analysis of Hardened Structures to Conventional Weapons Effects*, Department of Defense, 1 June 2002, Washington DC
- ⁵⁶*Pipeline Threat Assessment*, Transportation Security Administration, Office of Intelligence, 23 October 2008, Washington DC, <http://www.tsa.gov/>
- ⁵⁷*Vulnerability of Large Diameter Natural Gas Pipelines to Attack with Commercial Explosives*, Bert von Rosen, Canadian Explosives Research Laboratory, presented at the International Pipeline Security Forum, 23-25 October 2007
- ⁵⁸ibid
- ⁵⁹*Characteristics and Common Vulnerabilities Infrastructure Category: Petroleum Pipelines*, Department of Homeland Security, 22 April 2005, Washington DC, <http://www.dhs.gov/index.shtm>, p. 3
- ⁶⁰Correspondence with Phil Lightfoot and Bert von Rosen, Natural Resources Canada, Ottawa, ON
- ⁶¹<http://www.alyeska-pipe.com>
- ⁶²*Vulnerability of Large Diameter Natural Gas Pipelines to Attack with Commercial Explosives*, Bert von Rosen, Canadian Explosives Research Laboratory, presented at the International Pipeline Security Forum, 23-25 October 2007
- ⁶³Holland, Carrie, *Blast-Resistant Design of Highway Bridge Columns*, University of Texas at Austin, August 2008, p. 95
- ⁶⁴*Technical Study of Rapid Restoration of Pipeline Service*, US Department of Transportation, Research and Special Programs Administration, Office of Pipeline Safety, 15 April 2003, p. 39
- ⁶⁵Correspondence with Terry Boss, Senior Vice President, Safety and Environment, Interstate Natural Gas Association of American (INGAA)
- ⁶⁶*Pipeline Threat Assessment*, Transportation Security Administration, Office of Intelligence, 23 October 2008, Washington DC, <http://www.tsa.gov/>
- ⁶⁷http://www.woodcousa.com/line_pipe_properties.htm
- ⁶⁸UFC3-340-01 *Design and Analysis of Hardened Structures to Conventional Weapons Effects*, Department of Defense, 1 June 2002, Washington DC
- ⁶⁹ibid
- ⁷⁰Kingery, C.N., and G. Bulmash, *Airblast Parameters from TNT Spherical Air Burst and Hemispherical Surface Burst*, ARBRL-TR-02555, Ballistic Research Laboratory, April 1984.
- ⁷¹Jones, N., "Plastic Failure of Ductile Beams Loaded Dynamically," *Journal of Engineering for Industry*, February 1986, pp. 131-136.
- ⁷²<http://www.blastgardintl.com/>
- ⁷³UFC3-340-01 *Design and Analysis of Hardened Structures to Conventional Weapons Effects*, Department of Defense, 1 June 2002, Washington DC, p. 6-17
- ⁷⁴ibid
- ⁷⁵ibid
- ⁷⁶http://www.dynawell.de/products_specialty_products.html, www.mcelph.com/lfe.htm
- ⁷⁷Jones, N., "Plastic Failure of Ductile Beams Loaded Dynamically," *Journal of Engineering for Industry*, February 1986, pp. 131-136.
- ⁷⁸Vigil, Manuel G., *A Scaling Law Describing the Penetration of Reinforced Concrete Barriers by Explosively Driven Flyer Plates*, Sandia Laboratories Report SAND79-1253, August 1979.

⁷⁹ *ibid*

⁸⁰ *Characteristics and Common Vulnerabilities Infrastructure Category: Petroleum Pipelines*, Department of Homeland Security, 22 April 2005, Washington DC, <http://www.dhs.gov/index.shtm>, p. 11ff

⁸¹ Correspondence with Terry Boss, Senior Vice President, Safety and Environment, Interstate Natural Gas Association of American (INGAA)

⁸² *Technical Study of Rapid Restoration of Pipeline Service*, US Department of Transportation, Research and Special Programs Administration, Office of Pipeline Safety, 15 April 2003, p. 40

⁸³ US Department of Transportation, Pipeline and Hazardous Materials Safety Administration (PHMSA), <http://www.phmsa.dot.gov/pipeline/library/data-stats>

⁸⁴ Correspondence with Terry Boss, Senior Vice President, Safety and Environment, Interstate Natural Gas Association of American (INGAA)

⁸⁵ Correspondence with Terry Boss, Senior Vice President, Safety and Environment, Interstate Natural Gas Association of American (INGAA)

⁸⁶ *Characteristics and Common Vulnerabilities Infrastructure Category: Natural Gas Pipelines*, Department of Homeland Security, 22 April 2005, Washington DC, <http://www.dhs.gov/index.shtm>, p. 16

⁸⁷ *Technical Study of Rapid Restoration of Pipeline Service*, US Department of Transportation, Research and Special Programs Administration, Office of Pipeline Safety, 15 April 2003, p. 14

⁸⁸ *Characteristics and Common Vulnerabilities Infrastructure Category: Petroleum Pipelines*, Department of Homeland Security, 22 April 2005, Washington DC, <http://www.dhs.gov/index.shtm>, p. 11ff

⁸⁹ *ibid*, p. 4

⁹⁰ <http://www.composite-technologies.com/blast.html>

⁹¹ http://www.wintecusa.com/pipeline_protection.html